PhD degree in Systems Medicine

(curriculum in Human Genetics)

European School of Molecular Medicine (SEMM),

University of Milan and University of Naples "Federico II"

Settore disciplinare: MED03

THE UBIQUITIN-SPECIFIC PROTEASE USP14 CONTROLS CILIOGENESIS AND THE HEDGEHOG PATHWAY

Filomena Massa

TIGEM, Pozzuoli

Matricola n. R10725

Supervisor:

Prof. Brunella Franco

TIGEM, Pozzuoli

Internal Co-supervisor:

Prof. Antonella De Matteis

TIGEM, Pozzuoli

Coordinator:

Prof. Andrea Ballabio

TIGEM, Pozzuoli

External Co-supervisor:

Prof. Emilio Hirsch

Università degli Studi di Torino

Academic Year 2016/2017

Table of Contents

List of abbreviations

ADPKD	Autosomal Dominant Polycystic Kidney Disease
ALP	Autophagy-Lysosome Pathway
A/P	AnteroPosterior
APC	Anaphase-Promoting Complex
ARPKD	Autosomal Recessive Polycystic Kidney Disease
AurA	Aurora A
axJ	spontaneous ataxia mutation
BBS	Bardet-Biedl Syndrome
BCC	Basal Cell Carcinomas
CCCI	Cilia/Centrosome Complex Interactome
CE	Convergent Extension
CEP290	Centrosomal Protein 290
CK1	Casein Kinase 1
CNS	Central Nervous System
CP	20S Core Particle
CV	Ciliary Vesicle
DAV	Distal Appendages Vesicle
Dhh	Desert Hh
DMSO	DiMethyl SulfOxide
DUBs	Deubiquitinases/Deubiquitinating enzymes
ESs	Embryonic stem cells
EV	Empty Vector
E1	**E1** Ubiquitin Activating Enzymes
E2	**E2** Ubiquitin Conjugating Enzymes
E3/E4	**E3/E4** Ubiquitin Ligases

FL	Full-Length
Gli1/2/3	Glioma-associated oncogene1/2 /3
GSK-3	Glicogen Synthase Kinase-3
HEK293	Human Embryonic Kidney cells 293
Hh	Hedgehog
HIF-1α	Hypoxia-Inducible Factor-1α
hTERT-RPE1	human Telomerase-Retinal Pigment Epithelium1
IF	ImmunoFluorescence
IFT	IntraFlagellar Transport
Ihh	Indian Hh
INPP5E	Inositol polyphosphate-5-phosphatase E
IP	Immuno-Precipitation
IU1	1-[1-(4-fluorophenyl)-2,5-dimethylpyrrol-3-yl]-2-pyrrolidin-1-ylethanone
JBTS	Joubert Syndrome
KIF 7	Kinesin family member 7
KO	Knockout
LCA	Leber Congenital Amaurosis
LIF	Leukemia-Inhibiting Factor
Lys	Lysine
MCPIP	Monocyte Chemotactic Protein-Induced Protein
MDCK	Madin-Darby Canine Kidney
MEFs	Mouse Embryonic Fibroblasts
MIB1	MindBomb 1
MJD	Machado–Joseph Disease protein domain protease
MKS	Meckel Grouber Syndrome
NPHP	Nephronophthisis

NT	Unstimulated Conditions
OFDI	Oral-Facial-Digital type 1 syndrome
OTU	Ovarian-Tumour Protease
PBS	Phosphate-Buffered Saline
PCD	Primary Ciliary Dyskinesia
PCM-1	PeriCentriolar Material-1
PCP	Planar Cell Polarity
Pc1/Pc2	Polycystin1/Polycystin2
PDGF	Platelet-Derived Growth Factor
PKA	Protein Kinase A
PKD	Polycystic Kidney Disease
PM	Plasma Membrane
PT	Permeability Transition
Ptch1/PTC	Patched1
PVDF	PolyVinylidene DiFluoride
qPCR	quantitative Real-Time PCR
R	Repressor
RP	19S Regulatory Particles
RPT	Regulatory Particle Triple-A
RPN	Regulatory Particle Non-ATPase
SAG	Smoothened AGonist
SEM	Standard Error of the Mean
SFN	SulForaphaNe
Shh	Sonic hedgehog
shRNA	short hairpin RNA
siRNA	small interfering RNA
Smo	Smoothened

Sufu	Suppressor of Fused
TL	Total Lysate
TZ	Transition Zone
Ub	Ubiquitin
UBA	Ubiquitin Associated domains
UBD	Ubiquitin-Binding domain
UBL	Ubiquitin-Like domain
UCH	Ubiquitin Carboxy-terminal Hydrolase
UPS	Ubiquitin-Proteasome System
USP14	Ubiquitin-Specific Protease14
VHL	Von Hippel-Lindau
WB	Western blot
WT	Wild Type

Table of figures

Abstract

Primary cilia are microtubule-based organelles on the apical surface of mammalian cells, and play a crucial role in vertebrate development and tissue homeostasis. Consequently, ciliary defects are associated with human disorders called ciliopathies. This organelle represents an organizing center for signaling pathways. In particular, in vertebrates, the Hedgehog (Hh) pathway controls embryonic development and adult homeostasis using the primary cilium to transduce its signal. Hh components localize to cilia and Kif7, a key player in cilia structure and length, controls the ciliary localization of Hh signaling molecules. Phenotypes associated to Hh signaling impairment are often observed in ciliopathies. Recent studies established a link between ciliary proteins and the Ubiquitin proteasome system (UPS) pathway, however much remains to be understood. The main role of the UPS is to mark proteins for degradation although it also functions in a wide variety of cellular processes. The aim of my PhD project was to investigate the association between cilioproteins and proteasomal functions, with particular emphasis on the cilia-associated OFD1 protein, which is responsible for the rare OFD type I syndrome. The results obtained demonstrate that OFD1 controls proteasomal complex composition through direct binding with proteasomal components (see Liu et al. in appendix). Our results also demonstrate a role for Usp14, a deubiquitinating enzyme, in the control of ciliogenesis, cilia length and proper activation of the Hh pathway**.** We propose a new mechanism by which cilia maintenance and the Hh pathway are regulated by Usp14 via modulation of Kif7 proteasomal degradation (manuscript in preparation). This mechanism may be relevant not only in ciliopathies but also in other pathological conditions associated to Hedgehog signaling defects. Overall our results provide new insight into the spectrum of action of the UPS and may provide novel opportunities for therapeutic intervention in pathological conditions associated to cilia dysfunction.

Introduction

1. The Primary Cilium

1.1. Structure and functions of primary cilia

Cilia are evolutionarily-conserved microtubule-based organelles that protrude from the cell surface of almost all mammalian cells and although exceptions have been described, can be classified into two main functional groups: motile (also called flagella) and non-motile cilia (also called sensory or primary cilia). Motile and non-motile cilia are structurally related (see below) and have developed different functions (Keeling, Tsiokas et al. 2016).

Numerous motile cilia are present on epithelial cells in various tissues, such as trachea, oviducts, and epididymis of the reproductive tracts. These cilia are used for cell locomotion or for the generation of fluid flow over the cell surface. One example is the beating on tracheal cells, which is important for pulmonary clearance (Stannard and O'Callaghan 2006, Roy 2009). In contrast to motile cilia, primary cilia are non-motile solitary organelles (Singla and Reiter 2006). They were long believed to be vestigial organelles without relevant biological functions. However, experimental evidence collected over the past twenty years revealed that primary cilia are essential sensory organelles functioning as cells' antenna in many different instances: e.g. in signal transduction (Brown and Witman 2014); in mouse embryo patterning (Huangfu, Liu et al. 2003, Goetz and Anderson 2010); for chemosensing in olfactory neurons (e.g. for detecting odorants), photo-sensing in rods and cones (e.g. for receiving and transducing the stimuli of light on the retina), and as mechanosensors in renal epithelia (e.g. for sensing fluid flow in kidney tubules) (Satir and Christensen 2007).

Primary cilia consist of a microtubule-based core-skeleton, called axoneme, which is surrounded by a ciliary membrane (Breslow, Koslover et al. 2013).

The **ciliary membrane** (Figure 1), a specialized subdomain of the cell membrane, although continuous with the plasma membrane at the basal portion of the primary cilium, exhibits a distinct lipid and protein composition. Particularly, a specific portion of the ciliary membrane that extends from the axoneme (the ciliary tip) appears to have important roles for signals transduction (Rohatgi and Snell 2010) and in constrain of ciliary length.

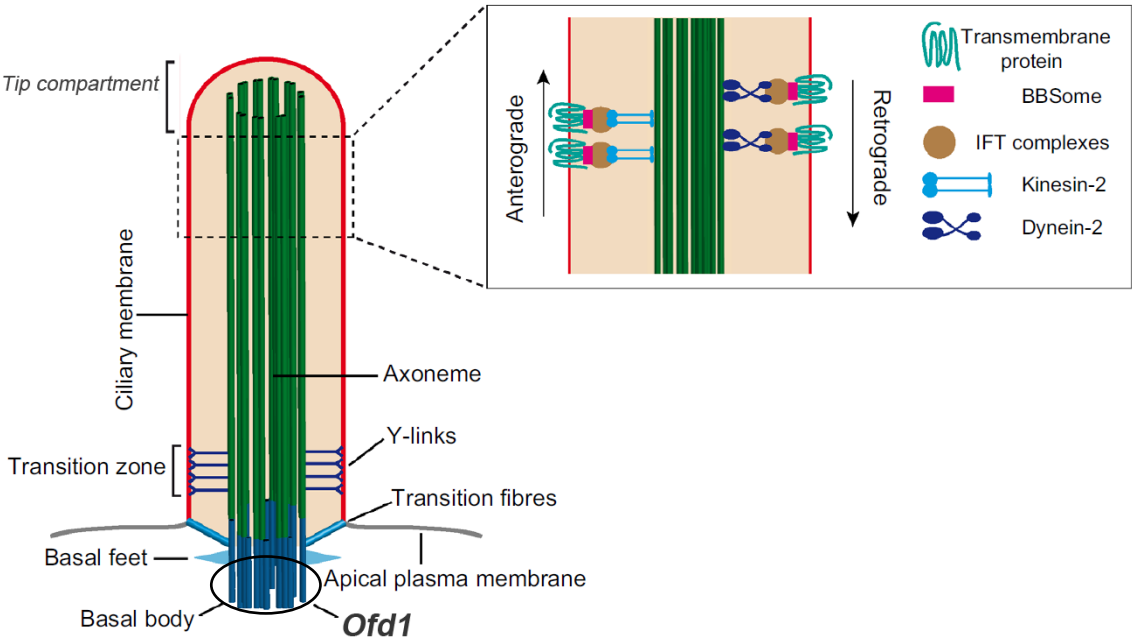

Figure 1. Structure of the primary cilium
The primary cilium consists of a microtubule-based core-skeleton, called axoneme, which is surrounded by a ciliary membrane, which is continuous with the plasma membrane. The basal body is attached to the ciliary membrane by the transition fibers. Between the basal body and the axoneme of the primary cilia there is a substructural zone, named transition zone (TZ). IFT is carried out by the IFT-A and IFT-B complexes powered by dynein-2 and kinesin-2 motors, respectively (modified from (Bernabe-Rubio and Alonso 2017)). The localization of the Ofd1 protein at the basal body is also indicated.

The core of cilia is the **axoneme,** which emanates from the basal portion of the cilium (the basal body) (Figure 1). It consists of nine outer microtubule doublets, termed 9+0 pattern, and lacks the central pair of microtubules typical of motile cilia (9+2 pattern) (Figure 2). Cilia localized at the embryonic node (nodal cilia) are an exception given that they are motile but lack a central pair of microtubules. The absence of the central microtubule doublet and of the accessory motility machinery (e.g., dynein arms, radical spokes, central pair projections) makes primary cilia non-motile. In place of this pair of microtubules, an electron-dense material, which varies from cell to cell, occupies the central portion of

primary cilia (Gluenz, Hoog et al. 2010). The outer axonemal microtubules doublets consist of a complete tubule (A microtubule) connected to an adjacent incomplete tubule (B microtubule), and lacking the third microtubule (C microtubule), which on the other hand, is present into the triplet microtubule pattern of the basal body of cilia (Gerdes, Davis et al. 2009) (Figure 2).

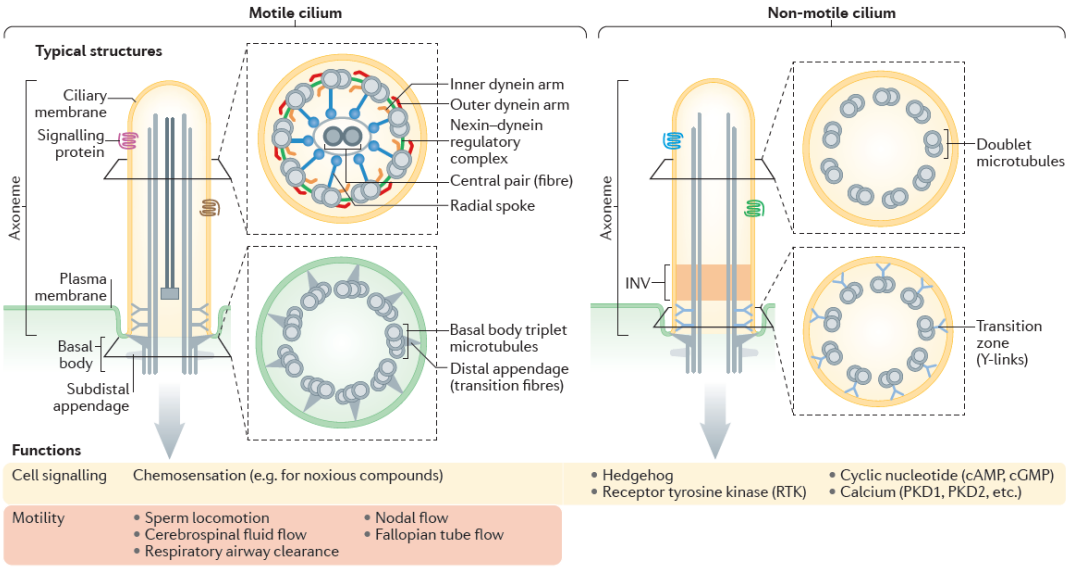

Figure 2. Structures of motile and non-motile cilia.
All cilia extend from a basal body that typically consists of triplet microtubules, and sub distal and distal appendages. Distal appendages (also known as transition fibers) tether the basal body to the base of the ciliary membrane. The axoneme is composed of doublet of microtubules. The transition zone, which contains doublet microtubules that are connected to the ciliary membrane via Y-shaped structures is localized between the basal body and the axoneme. In motile cilia, axonemes usually contain associated accessory proteins and structures (for example, the central pair and axonemal dyneins) that are required for cilia motility. Cilia may contain additional subdomains, including singlet microtubules at the distal end, and regions with specific protein composition or functions. Ciliary signaling functions, and roles in motility are summarized. PKD, polycystin (modified from (Reiter and Leroux 2017))

The microtubule subunits undergo post-translational modification for the establishment of functional microtubules (Janke and Kneussel 2010), such as acetylation (Piperno, LeDizet et al. 1987), detyrosination (Gundersen and Bulinski 1986), or glutamylation (Lee, Silhavy et al. 2012). These modifications are thought to be important for stability, motility, and formation, and function of primary cilia (Janke and Bulinski 2011, Konno, Setou et al. 2012). Cilia are devoided of protein synthesis. The intraflagellar transport (IFT) machinery, a multiprotein complex responsible for transporting cargoes into the cilia (anterograde

transport) and out of the cilia (retrograde transport) runs along axonemal microtubules. It mediates both the assembly and resorption of the cilium, and the trafficking of key intermediates of signaling cascades. The anterograde transport is regulated by the IFT-B complex and the kinesin2 motor, whereas the retrograde transport is mediated by the IFT-A complex and the dynein motor (Scholey 2008, Sasai and Briscoe 2012).

At the base of the axoneme, under the cell surface, is located the **basal body** (Figure 1). It derives from the mother centriole, anchors the microtubules, and connects the axoneme to the rest of the cell (Dirksen 1991).

Between the basal body and the axoneme of the primary cilia there is also another substructural zone, named **transition zone** (TZ) (Figure 1). Recent work has further defined this compartment near the base of the cilium as an important region for trafficking and ciliary gating, involved in the formation of a physical barrier that prevents free mixing of proteins between the plasma and the ciliary membranes (Czarnecki and Shah 2012). Several protein complexes, responsible for cilia formation as well as for selectively loading ciliary proteins to the IFT cargoes, localize at the transition zone (Nozawa, Lin et al. 2013).

1.1.1. Cilia mediated signaling pathways

Cilia act as complex sensory machines involved in transducing extracellular stimuli into cellular responses as they sense extracellular signals and transmit them from the cilium to the cytoplasm and nucleus in order to control gene expression and cell behavior, thereby playing several important roles in cell and developmental biology (Yuan, Serra et al. 2015). The extracellular sensory function of cilia is mediated by different signaling pathway receptors, ion channels, transporter proteins, and their downstream molecules located in the axoneme or in the basal body. A variety of signaling pathways are coordinated through this organelle during development, tissue homeostasis, cell migration, cellular differentiation, cell cycle, and apoptosis (Eggenschwiler and Anderson 2007, Satir, Pedersen et al. 2010).

Examples of signaling pathways that need intact cilia to properly transduce their signals include: the Hedgehog (Hh) pathway), involved in regulation of cell proliferation, cell fate determination, in the epithelial-to-mesenchymal transition and maintenance of homeostasis in adult cells (Simpson, Kerr et al. 2009, Briscoe and Therond 2013)(see also section 2); the PDGF pathway, which regulates cell proliferation, cell survival, and migration during embryogenesis and tissue homeostasis (Clement, Mally et al. 2013); the Wnt pathway, which is crucial during development and important for controlling cell proliferation, apoptosis, cell fate determination, microtubule stabilization, and cell polarization (Angers and Moon 2009), and the Ca2+ signaling cascade, which plays a key role in proper development of kidneys, by regulating the intracellular Ca2+ concentration (Kestler and Kuhl 2008, Angers and Moon 2009).

1.2. Primary cilia biogenesis

The formation of primary cilia is a process tightly linked to the cell cycle: as a matter of fact, the formation of the primary cilium is inversely correlated with cell cycle progression. The primary cilium assembles only when cells exit the cell cycle from mitosis, and for this reason it is considered an organelle of cells in quiescent or differentiated state. Therefore, when cells re-enter the cell cycle, cilium resorption occurs (Quarmby and Parker 2005).

It has been proposed that formation of primary cilia proceeds by two distinct pathways (intracellular and extracellular/alternative pathways) (Sorokin 1962, Sorokin 1968). In the **intracellular pathway** the initiation of ciliogenesis is a well-orchestrated process where distal appendages vesicles (DAVs) originated from the Golgi attach to the distal ends of the mother centriole, which differentiates into a basal body. Ciliogenesis continues with fusion of DAVs to form the ciliary vesicle (CV), the basal body acquires positive regulators of ciliogenesis, as the Intraflagellar transport protein 20 (Ift20), and removes negative regulators, allowing docking and formation of the TZ. Once the basal body docks

at the plasma membrane (PM), the axoneme extends into the extracellular space. Thus, in this case, the basal body associates with a vesicle "en route" to the plasma membrane, and additional vesicles support the growing axoneme until the vesicular structure comes in contact and fuses with the plasma membrane (Sorokin 1962, Bernabe-Rubio and Alonso 2017) (Figure 3).

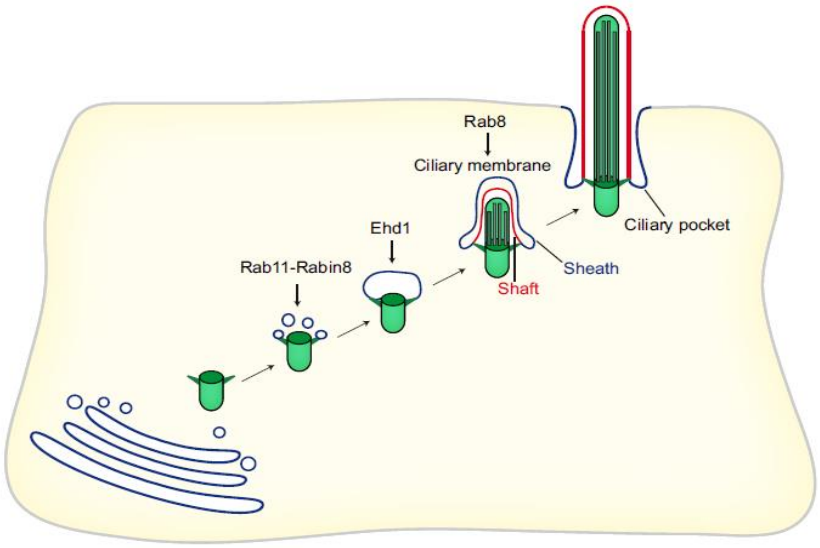

Figure 3. The intracellular pathway.
Ciliogenesis initiates intracellularly with the formation of a large ciliary vesicle (CV) at the distal end of the appendages of the mother centriole by fusion of smaller distal appendages vesicles (DAVs). The axoneme starts forming intracellularly and, as it grows, deforms the CV and establishes an inner membrane (shaft) and an outer membrane (sheath). The incipient cilium is finally exocytosed and the cilium becomes exposed in the plasma membrane. The sheath gives rise to the ciliary pocket, and the shaft forms the ciliary membrane (modified from (Bernabe-Rubio and Alonso 2017))

Conversely, in the **extracellular pathway,** the basal body fuses with the apical surface of the plasma membrane and the cilium protrudes directly into the extracellular space where it elongates (Kobayashi and Dynlacht 2011).

The use of a pathway rather than the other depends on the cell type and the position of the centrosome in the cell (Bernabe-Rubio and Alonso 2017). In non-polarized cells of connective tissues, as in the case of fibroblasts, where the centrosome is near the nucleus, ciliogenesis starts intracellularly and finishes at the plasma membrane, generating an invagination, known as the ciliary pocket; whereas, in polarized epithelial cells, the centrosome is close to the plasma membrane and the process takes place entirely at the

plasma membrane and no pocket appears (Rohatgi and Snell 2010, Benmerah 2013, Bernabe-Rubio and Alonso 2017) (Figure 4).

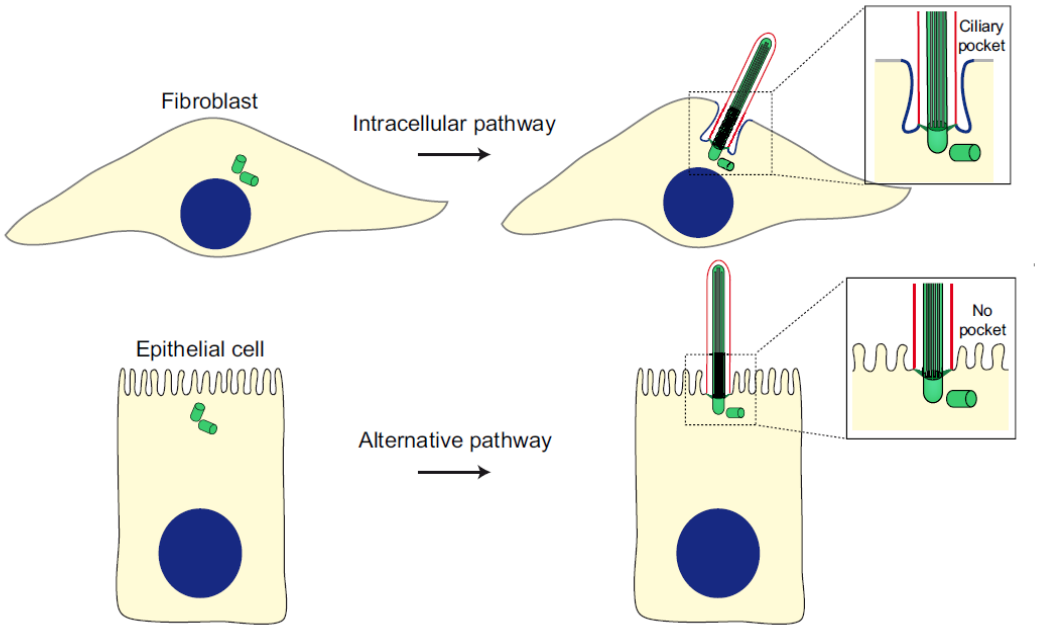

Figure 4. Routes of primary ciliogenesis.
The position of the centrosome, near the nucleus or close to the plasma membrane, and the presence or absence of a ciliary pocket predicts the type of pathway used for primary ciliogenesis. Fibroblasts and polarized epithelial cells are cells that use the intracellular and alternative routes, respectively (modified from (Bernabe-Rubio and Alonso 2017)).

The formation of the primary cilium is also induced by other conditions, such as starvation by using serum-free media and by cell confluency (Kiprilov, Awan et al. 2008), which forces the cell into a non-mitotic state.

1.3 Control of ciliary length

The primary cilium remains a highly dynamic organelle not only because it is assembled during specific phases of the cell life, but also because a dynamic turnover continually occurs at the distal tip of the axoneme (Satir and Christensen 2007, Pedersen and Rosenbaum 2008, Kobayashi and Dynlacht 2011). The ciliary axoneme is only ~0.25 µm in diameter, but it can reach up to 20 µm in length depending on the cell type. A precise balance between assembly and disassembly of the primary cilium is crucial for determining its length (Sanchez and Dynlacht 2016). When this balance is disrupted, cilia growth or

resorption will occur (Kozminski, Johnson et al. 1993, Marshall and Rosenbaum 2001, Marshall, Qin et al. 2005). It is believed that in all ciliated cells the regulation of the ciliary growth is mediated by IFT, which provides the necessary components, such as tubulins and other axonemal precursors, at the tips of the cilia and recycles ciliary turnover products at the base. Thus, a change in cilia length is considered to be indicative of a change in anterograde or retrograde IFT (Engel, Ludington et al. 2009). Moreover, there are emerging evidences that some kinesin motor proteins, well known for their roles in intracellular transport, can regulate the dynamics of tubulin polymerization. For example, KIF4A, a kinesin-4 protein, controls microtubule length during cell division (Hu, Coughlin et al. 2011) and another kinesin-4 protein, KIF21A, inhibits microtubule growth at the cell cortex (van der Vaart, van Riel et al. 2013). In K. Anderson's laboratory it has been demonstrated that the Kinesin family member 7 (Kif7), a conserved regulator of Hh signaling (Tay, Ingham et al. 2005, Cheung, Zhang et al. 2009, Endoh-Yamagami, Evangelista et al. 2009, Liem, He et al. 2009), binds to microtubule plus ends at cilia tips to control cilia length, architecture, and stability, thus it organizes a specialized compartment that mediates Hh signaling (He, Subramanian et al. 2014). Recent genetic studies have also identified *KIF7* mutations in patients with typical ciliopathy phenotypes (see below) (Dafinger, Liebau et al. 2011, Putoux, Thomas et al. 2011, Putoux, Nampoothiri et al. 2012, Walsh, Shalev et al. 2013).

1.4. Ciliopathies

Dysfunctions and malformations of motile or immotile cilia, due to mutations in genes encoding defective cilioproteins belonging to the different ciliary structures (primary cilium/basal body, axoneme, transition zone and fibers), are associated with a wide range of human diseases called ciliopathies (Badano, Mitsuma et al. 2006, D'Angelo and Franco 2009) (Figure 5). These disorders show a broad spectrum of shared and overlapping

phenotypes involving various organ systems (Quinlan, Tobin et al. 2008), such as retinal degeneration, renal, hepatic and pancreatic cysts, skeletal defects, *situs inversus*, obesity, ciliary dyskinesia, mental retardation, and Central Nervous System (CNS) malformations (Davis and Katsanis 2012). These symptoms display different degrees of severity which also depend on whether ciliogenesis is affected or not and the disease is more severe if cilia architecture is compromised.

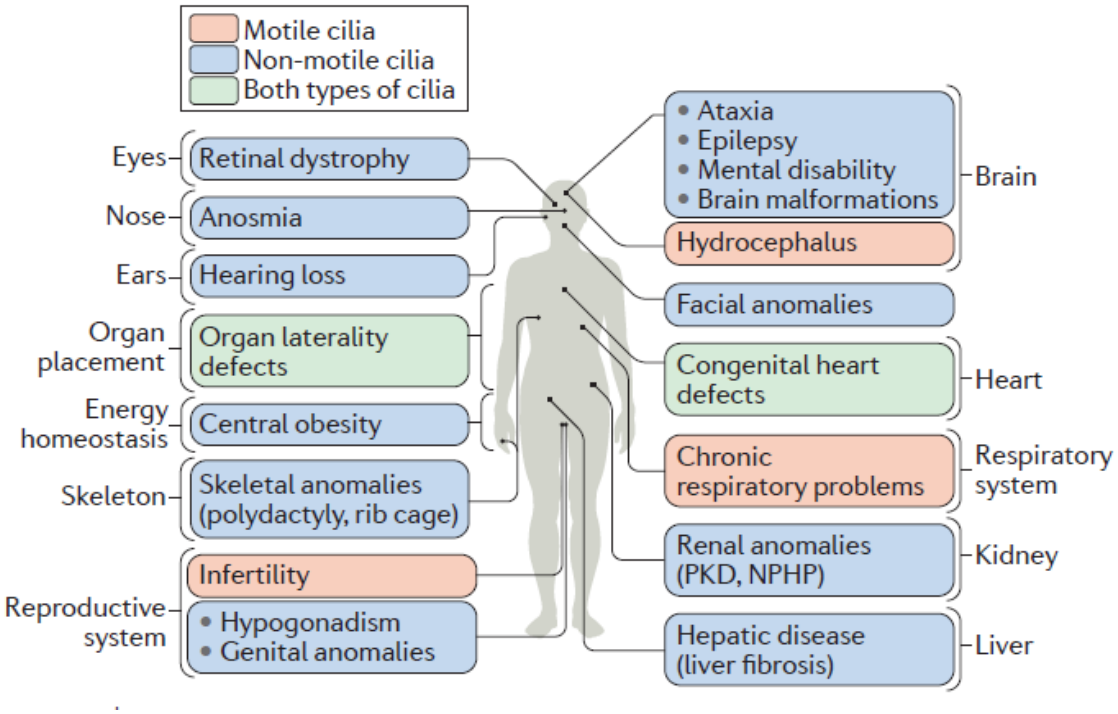

Figure 5. Dysfunctions in motile and/or non-motile cilia affect most human organ systems and cause ciliopathies.
Different organ systems or tissues affected in ciliopathies, and principle phenotypes in each organ are depicted. Ciliopathies caused primarily by defects in motile cilia (orange), those resulting from defects in non-motile primary cilia (blue) and those associated with defects in both types of cilia (green) are illustrated in the scheme. NPHP, nephronophthisis; PKD, polycystic kidney disease (modified from (Reiter and Leroux 2017)).

The number of reported ciliopathies is increasing, as well as the number of established and candidate ciliopathy associated genes. Moreover, ciliopathies that result from the disruption of proteins, which neither localize at, nor take part in cilia formation (non-ciliary proteins), but which are required for ciliary functions, are occurring more frequently. Consequently, the range and the overlap between ciliopathy phenotypes is also increasing. Indeed, the relationship between a ciliary gene and a ciliopathy is often more complex than

a one-gene-to-one-phenotype relationship. Mutations in different cilia-associated transcripts result in defined ciliopathies (Novarino, Akizu et al. 2011, Waters and Beales 2011), however multiple ciliopathies with no, or limited, phenotypic overlap are also caused by mutations in the same gene. A single gene can be linked to multiple phenotypes if the alleles differ in strength. In addition, different mutations in one gene can also result in ciliopathies that are associated with distinct phenotypes (for example: mutations in one gene encoding protein isoforms with different functions). Additionally, genetic modifiers present in different backgrounds can influence the clinical manifestation of mutations in ciliopathy-associated genes, partially explaining the pleiotropy of ciliopathies (Reiter and Leroux 2017). Therefore, although ciliopathies can be recognized as distinct clinical entities, it is becoming apparent that these are determined not only by the specific gene that is mutated, its biological role and pattern of expression, but also by the type and effect of the mutation on the function of the protein and by the total mutational load across different ciliary genes and ciliopathy-associated genes (Adams, Smith et al. 2008, Cardenas-Rodriguez and Badano 2009, Deltas and Papagregoriou 2010).

We can distinguish between ciliopathies caused by dysfunction of ciliary proteins of motile cilia (motile ciliopathies) and ciliopathies that result from the disruption of proteins that affect immotile cilia (sensory ciliopathies) (Figure 5). In addition, non-ciliary proteins can also contribute to ciliopathies influencing ciliary functions, and ciliary proteins can have extra-ciliary roles causing phenotypes that are unrelated to ciliopathies when they are impaired (Reiter and Leroux 2017). However, altered formation or function of motile cilia that doesn't normally affect ciliary signaling almost exclusively results in **motile ciliopathies. The most common of which** is known as **Primary Ciliary Dyskinesia (PCD)**. PCD is an inherited autosomal recessive disease characterized by chronic respiratory tract infections (attributable to defective clearance of lung mucus), abnormally positioned internal organs (different degrees of *situs inversus*), and male infertility (due to defective sperm locomotion) (Horani, Ferkol et al. 2016). On the other hand, **sensory**

ciliopathies result specifically from defects in the sensory and/or signaling functions of cilia, and are primarily caused by defects in non-motile cilia. Examples of ciliopathies caused by mutation in proteins affecting the primary cilium include: **Bardet-Biedl Syndromes (BBS)**, a multisystemic disorder involving developmental abnormalities (polydactyly, mental retardation, and developmental delay) and degenerative phenotypes (retinal degeneration and renal cystic disease) (Forsythe and Beales 1993); **Leber Congenital Amaurosis (LCA),** a severe dystrophy of the retina that results in severe vision loss at an early age (McAnany, Genead et al. 2013); **Oral-Facial-Digital type 1 syndrome (OFDI)**, an X-linked dominant developmental disorder lethal to males. Female patients present malformations of the oral cavity, face, digits, renal cysts, and CNS malformations (Toriello, Franco et al. 1993)(see also section 1.4.1); **autosomal dominant (ADPKD)** (Harris and Torres 1993) or **recessive (ARPKD) polycystic kidney disease** (Sweeney and Avner 1993) characterized by the development of fluid filled cysts in the kidney, gradually leading to end-stage renal failure, and by extrarenal manifestations; **Joubert Syndrome (JBTS)** characterized by three primary findings: a distinctive cerebellar and brain stem malformation called the molar tooth sign (MTS), hypotonia, and developmental delays (Parisi and Glass 1993); **Nephronophthisis (NPHP)** associated to reduced renal concentrating ability, chronic tubulointerstitial nephritis, cystic renal disease, and progression to end-stage renal disease (ESRD) before the age of 30 (Stokman, Lilien et al. 1993); **Meckel Grouber Syndrome (MKS)** an autosomal recessive lethal condition characterized by occipital meningoencephalocele, polycystic kidneys, postaxial polydactyly, and ductal plate malformation of the liver (Henkel, Pfeiffer et al. 1993).

Primary cilia have evolved several modes for sensing environmental and intercellular signals respect to motile cilia. Therefore, it is expected that defects in sensory cilia functions cause more varied sensory, physiological, and developmental anomalies compared to defects in motile cilia. Sensory ciliopathies have multiple possible molecular etiologies, including impaired cilium formation or maintenance, abrogation of ciliary

signaling pathway components, or trafficking defects that prevent the signaling machinery from being localized to, or removed from, cilia (Reiter and Leroux 2017)

1.4.1 Oral-Facial-Digital syndrome type 1 (OFD1)

Oral-facial-digital syndromes (OFDs) are a heterogeneous group of developmental disorders that feature malformations of the face, oral cavity, and digits. Other organ systems can also be involved, and the current classification has identified several different forms of OFDs (Franco and Thauvin-Robinet 2016, Bruel, Franco et al. 2017). Orofaciodigital syndrome type 1 (OFDS1, OMIM #311200), the most common type, occurs in 1:50000-1:250000 live births, and can be easily recognized for the typical X-linked dominant male lethal transmission, even though few live males with mutations in OFD1 have been reported (Thauvin-Robinet, Thomas et al. 2013, Tsurusaki, Kosho et al. 2013, Wentzensen, Johnston et al. 2016). OFD type 1 is caused by mutation of the *OFD1* (OMIM #300170) gene, located on the chromosome Xp22.2-Xp22.3 region (Feather, Winyard et al. 1997, Ferrante, Giorgio et al. 2001, Toriello 2009). To date, over 130 different mutations have been identified in *OFD1* with many truncating mutations (Franco and Thauvin-Robinet 2016).

About 75% of cases with OFD1 are sporadic, and different papers exclude a convincing genotype/phenotype correlation (Stoll and Sauvage 2002, Macca and Franco 2009, Bisschoff, Zeschnigk et al. 2013). Mutations in the *OFD1* gene have also been identified in association with four recessive X-linked phenotypes: Joubert syndrome, intellectual disability, type 2 Simpson-Golabi-Behmel syndrome, and retinitis pigmentosa (Budny, Chen et al. 2006, Coene, Roepman et al. 2009, Field, Scheffer et al. 2012, Webb, Parfitt et al. 2012, Tenorio, Arias et al. 2014). The cardinal clinical features of OFD1 syndrome include craniofacial abnormalities (facial asymmetry, hypertelorism, frontal bossing, microretrognathia, broadened nasal bridge, cleft palate, multi-lobulated tongue with

nodules, and abnormal dentition), and digital abnormalities (which affect the hands more often than the feet) including brachydactyly, syndactyly, clinodactyly, and pre- or post-axial polydactyly (Figure 6).

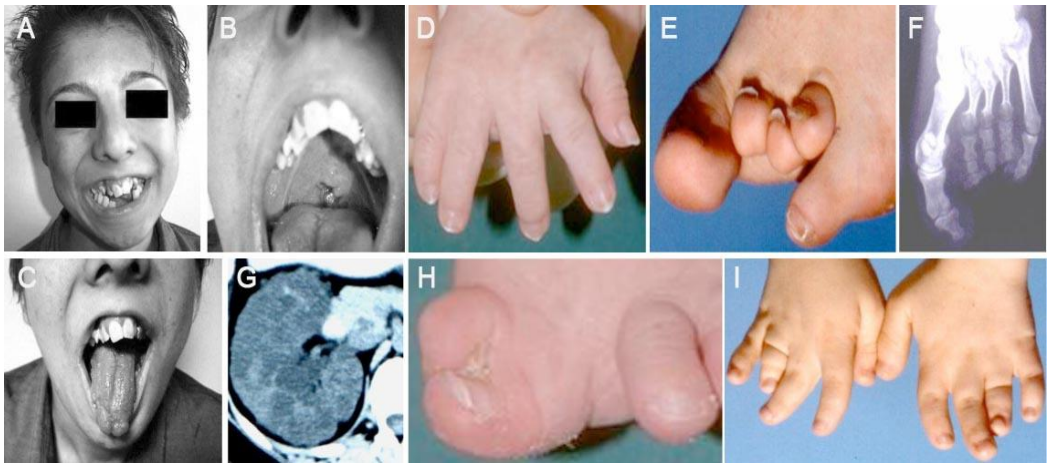

Figure 6. Clinical signs of OFDI syndrome.
(A) Peculiar face of the patient and tooth abnormalities, (B) cleft palate, (C) lobulated tongue, (D) clinodactyly, (E and F) Brachydactyly, (G) Cystic kidney, (H) Hallux duplication, (I) Brachydactyly and syndactyly. (modified from (Toprak, Uzum et al. 2006, Macca and Franco 2009)

About 60% of cases with OFD type 1 show brain structural abnormalities, developmental delay, and intellectual disabilities (Del Giudice, Macca et al. 2014), and most of the patients suffer from renal cystic disease (Feather, Woolf et al. 1997, Ferrante, Giorgio et al. 2001, Prattichizzo, Macca et al. 2008). In addition, about 5% of OFDI affected females develop pancreatic, hepatic, and/or ovarian cysts (Ferrante, Giorgio et al. 2001, Macca and Franco 2009, Toriello 2009, Saal, Faivre et al. 2010).

The *OFD1* gene contains an open reading frame of 3033 base pairs (bp) spanning over 23 coding exons and generates two main splice variants, *OFD1a* and *OFD1b*. *OFD1b* codifies for an unstudied putative protein of 367 aminoacids (aa) derived from exons 1–11 (de Conciliis, Marchitiello et al. 1998, Ferrante, Giorgio et al. 2001, Romio, Wright et al. 2003), while *OFD1a* encodes for a 1012-amino acid protein (hereafter called OFD1) conserved among vertebrates (de Conciliis, Marchitiello et al. 1998, Ferrante, Giorgio et al. 2001, Romio, Wright et al. 2003). This protein contains a Lis1 homology (LisH) motif in

its N-terminal region and six predicted coiled-coil (CC) domains distributed along the C-terminal region (de Conciliis, Marchitiello et al. 1998, Emes and Ponting 2001, Budny, Chen et al. 2006). Interestingly, the *OFD1* gene has been found to escape X-inactivation in humans while the murine counterpart is subjected to X-inactivation (Ferrante, Barra et al. 2003).

The OFD1 transcript is expressed in both human and murine structures, in all tissues affected by the disorder from early stages of development to adulthood. In particular, it is highly expressed during human organogenesis in the metanephros, gonads, brain, tongue, and limbs, and at lower levels in pancreas, kidneys, skeletal muscle, liver, lung, placenta, brain, and heart (de Conciliis, Marchitiello et al. 1998, Ferrante, Giorgio et al. 2001, Romio, Wright et al. 2003).

1.4.1.1 The OFD1 protein: functions and animal models

OFD1 is a centrosome-associated protein (Romio, Wright et al. 2003, Giorgio, Alfieri et al. 2007) and it follows the dynamic distribution of the centrosome throughout the cell cycle (Romio, Fry et al. 2004). In post-mitotic cells, when the mother centriole forms the basal body to allow nucleation of the ciliary axoneme, OFD1 localizes at the basal body of primary cilia (Romio, Wright et al. 2003, Giorgio, Alfieri et al. 2007) (Figure 7A-C). More specifically, OFD1 localizes at the distal regions of centrioles and it appears to be important in the control of centriole length, centriole distal appendage formation, and centriolar recruitment of the Intraflagellar transport protein 88 (Ift88) (Singla, Romaguera-Ros et al. 2010). Furthermore, OFD1, as well as CEP290, (a protein mutated in NPHP and Joubert syndrome), PCM-1 (pericentriolar material 1), and BBS4 (Bardet-Biedl syndrome 4) is an important component of centriolar satellites, the particles surrounding centrosomes and basal bodies, whose integrity depends on each of these proteins (Lopes, Prosser et al. 2011) (Figure 7D-E).

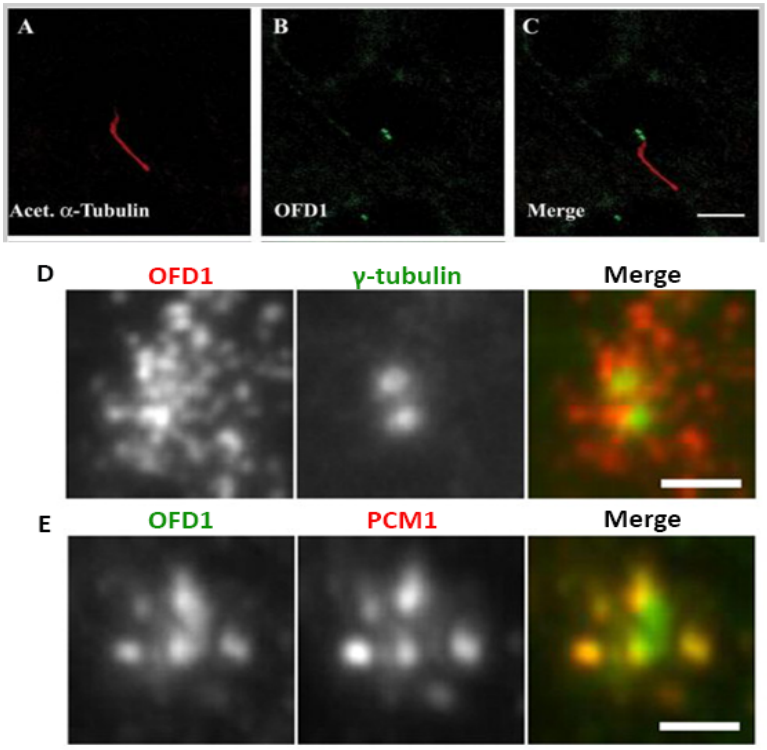

Figure 7. Subcellular localization of the endogenous OFD1 protein.
OFD1 localization at primary cilia in MDCK cells. (A) Staining with the anti-acetylated α-tubulin to detect the primary cilium. (B) Staining with the anti-OFD1 C-ter antibody. (merge in C) OFD1 localizes at the basal body of the primary cilium. (modified from (Giorgio, Alfieri et al. 2007))
OFD1 localization at centriolar satellites in hTERT-RPE1 cells. (D) Staining with the anti-γ-tubulin to detect the centrosome, and with the anti-OFD1. (E) Staining with anti-OFD1, and anti-PCM-1 to identify centriolar satellites. Scale bars: 2 μm. (modified from (Lopes, Prosser et al. 2011))

Recently, it has been demonstrated that OFD1 at centriolar satellites has a crucial role in suppressing primary ciliogenesis: in fact, the selective degradation of OFD1 in this specific location promotes primary cilia biogenesis (Tang, Lin et al. 2013). Thus, while Ofd1 at centrioles is essential for primary cilia formation, the Ofd1 component associated to centriolar satellites inhibits ciliogenesis.

Research with animal models has proved useful for better understanding of the role/s of Ofd1 in health and disease. Thus, to gain initial insight into the molecular role of Ofd1, a null murine model for OFD type I syndrome was generated using a Cre-loxP system (Ferrante, Zullo et al. 2006). The knockout mice displayed ubiquitous inactivation of Ofd1 from early stages of development and reproduced the main features of the human disease, albeit with increased severity, probably due to differences between the X-inactivation

patterns observed in humans and mice (Ferrante, Barra et al. 2003, Morleo and Franco 2008). The heterozygous females ($Ofd1^{\Delta 4\text{-}5/+}$) died at birth. The pups were small, with skeletal abnormalities as polydactyly or polysyndactyly, and craniofacial defects including cleft palate, which probably underlies the perinatal lethality (Ferrante, Zullo et al. 2006). The newborn heterozygous females also showed brain disorganization, reduced lung size, cardiac great vessel defects and cystic kidneys. In female mutants, cilia were missing from the cells within kidney cysts, whereas adjacent cells were ciliated, thus implicating ciliogenesis as a mechanism underlying cyst development in OFD1. It is likely that this is due to the X-inactivation phenomenon with the presence of both cells expressing the mutated X and cells expressing the normal wild-type allele on the X chromosome (Ferrante, Zullo et al. 2006). The majority of hemizygous male embryos ($Ofd1^{\Delta 4\text{-}5}$), completely lacking gene function, died by E12.5 with early developmental defects. The $Ofd1^{\Delta 4\text{-}5}$ embryos are small and a striking pericardial edema is evident, accompanied by randomization or failure of heart looping, observed in about 50% of embryos, suggesting defective L-R patterning mediated by the absence of nodal cilia (Ferrante, Zullo et al. 2006). These results are consistent with the subcellular localization of Ofd1 in the basal body and confirm that this protein is required for primary cilia formation and left right axis specification (Ferrante, Zullo et al. 2006).

Ofd1 plays also a crucial role in forebrain development, and in particular, in the control of dorso-ventral patterning and early corticogenesis (D'Angelo, De Angelis et al. 2012). Due to X inactivation, $Ofd1^{\Delta 4\text{-}5/+}$ heterozygous females at E12.5 show a high degree of variability ranging from a mild to a severe neurological phenotype, characterized by enlarged heads and a disorganization of the brain architecture with affected dorsal-ventral patterning in the telencephalon and an abnormal activation of Sonic hedgehog (Shh) (see also section 2.2) throughout the forebrain (D'Angelo, De Angelis et al. 2012). Ultrastructural studies demonstrated that early Ofd1 inactivation results in the absence of ciliary axonemes, which most likely causes defects in cytoskeletal organization and apical-

basal polarity, despite the mature basal bodies being properly orientated and docked (D'Angelo, De Angelis et al. 2012). To investigate whether Ofd1 has a developmental stage-dependent role in the forebrain, a conditional null mouse model, in which the Ofd1 floxed allele was crossed with an inducible Cre-line expressing the Cre recombinase under the actin promoter (CAGG-creERTM), was generated (Ofd1-indKO). Ofd1 inducible-tamoxifen mediated inactivation at birth does not affect ciliogenesis in the cortex, suggesting that Ofd1 is dispensable for ciliogenesis in post-natal stages. Therefore, Ofd1 is critical for forebrain development and plays a crucial developmental stage-dependent role in ciliogenesis that occur after docking and before axoneme elongation *in vivo* (D'Angelo, De Angelis et al. 2012).

In addition, to bypass the male mortality and better study the possible correlation between the cysts formation in kidney and the dysfunction of primary cilia observed in *Ofd1* null mice, a conditional mouse model with renal specific inactivation of *Ofd1* was generated. Using the *Ksp-Cre* transgenic line in which the Cre recombinase is specifically expressed in renal tubular epithelial cells, a viable model characterized by renal cystic disease and progressive impairment of renal function was obtained (Zullo, Iaconis et al. 2010). In this model, primary cilia are present in all renal tubules of mutant animals ($Ofd1^{fl};cre^{Ksp}$) at precystic stages (P7) and then disappear from cells lining the renal cysts, indicating that cilia form before the development of cysts and suggesting that the absence of primary cilia is a consequence rather than the primary cause of renal cystic disease (Zullo, Iaconis et al. 2010).

Moreover, another conditional model was generated to elucidate the role of the Ofd1 in limb development. The specific inactivation of *Ofd1* in limb mesoderm results in mutant mice displaying polydactyly with loss of digit identity in the presence of shorter and malformed cilia, and shortened long bones accompanied by defects in chondrocytes organization, reduction in mineralization process, and defective Hh signaling (see also section 2.2) (Bimonte, De Angelis et al. 2011). The skeletal phenotype observed in these

Ofd1 mutant animals recapitulates the skeletal abnormalities observed in OFD type I patients, indicating that Ofd1 plays an important role in regulating digit number and identity during limb, and skeletal patterning.

Finally, Ofd1 function was also studied during Zebrafish (Danio rerio) embryonic development (Ferrante, Romio et al. 2009). The Zebrafish homolog, ofd1, encodes a protein with a 29.6% identity with the human OFD1 and the same centrosome/basal body localization previously described in humans and mice (Ferrante, Romio et al. 2009). Injection of antisense morpholinos (MOs) in one-cell stage embryos determines a typical ciliary phenotype with bent body, laterality defects, and edema. In this model, cilia are shorter with altered ultrastructure, which causes alteration of the fluid flow and consequently laterality defects in the brain, heart, and viscera (Ferrante, Romio et al. 2009). Interestingly, ofd1 has also a role in convergent extension (CE) during gastrulation, consistent with other studies linking cilia and non-canonical, PCP, Wnt signaling (May-Simera and Kelley 2012). However, while cystic disease was not observed, the described CE defects could also be responsible for the delayed glomerular fusion observed in ofd1 morphants; the glomerular vascularization is also compromised (Ferrante, Romio et al. 2009). Overall, the phenotype observed in the Zebrafish model together with the phenotype described in the murine models indicate that Ofd1 plays an important role in the pathogenesis of inherited renal cystic disease, and in proper brain and skeletal development.

2. The Hedgehog (Hh) signaling pathway

The Hedgehog (Hh) signaling pathway regulates many developmental processes in both vertebrates and invertebrates. The *Hh* gene was first discovered in a large-scale genetic screen for mutations that disrupt the Drosophila larval body plan. Hh was found to be one of several genes important for body segmentation in flies. The name of the pathway

originates from the short and "spiked" phenotype of the cuticle of the Hh mutant Drosophila larvae, which resembles the hedgehog animal (Ingham, Nakano et al. 2011). Years later, three vertebrate Hedgehog genes, Indian Hh (*Ihh*), Desert Hh (*Dhh*) and Sonic Hh (*Shh*), with conserved role in body organization, were identified (Robbins, Fei et al. 2012). The Hh proteins codified from these genes act as morphogens and form a concentration gradient to direct tissue patterning. Their general physiological functions are the same but they differ in the pattern of expression. Ihh is important for bone and cartilage development, while Dhh is needed for germ cell development in the testis and peripheral nerve sheath formation (Burglin 2008). Shh is the most studied and best characterized component of this family. It is important for the specification of neuronal identities along the dorsal-ventral axis in the neural tube, as well as for the proper patterning of limbs (Briscoe and Therond 2013). The identification of these roles for Hh proteins matches the model of developmental biology, a model in which organizer tissues secrete the Hh morphogens whose cellular responses triggering action is dependent on their concentration.

2.1. Hedgehog signaling and the primary cilium

Overall, the key components of the Hh pathway are highly conserved from fruit flies to humans, although additional pathway mediators and the requirement of primary cilia have added complexity to this pathway in vertebrates (Varjosalo, Li et al. 2006). Underscoring the link between primary cilia and Hh signaling, it has been demonstrated that mutations affecting either formation or functionality of primary cilia prevent cellular responses to Hedgehog ligands. Additionally, most of the proteins required for vertebrate Hh signal transduction localize at the cilium and shift their localization in response to the ligand (Goetz and Anderson 2010), thus emphasizing the importance of primary cilia for proper Hh signaling transduction.

In the absence of the Hh ligand, the pathway is inactive and the 12-transmembrane

receptor Patched1 (Ptch1) localizes within primary cilia where actively represses the accumulation of the 7-transmembrane protein Smoothened (Smo) (Rohatgi, Milenkovic et al. 2007). When Hh ligand binds Ptch1 on the receiving cells, Ptch1 is activated and de-represses Smo, which is free to translocate into the primary cilia and initiates a signal transduction cascade that leads to the activation of Gli (Glioma-associated oncogene) family transcription factors (Corbit, Aanstad et al. 2005) (Figure 8). In this off state, the protein Suppressor of Fused (Sufu) that locates on the primary cilium in a Gli-dependent manner (Haycraft, Banizs et al. 2005, Zeng, Jia et al. 2010), negatively regulates the pathway by directly binding to Gli proteins and anchoring them in the cytoplasm thus preventing the activation of target genes, such as *Gli1* and *Ptch1*(Kogerman, Grimm et al. 1999, Paces-Fessy, Boucher et al. 2004, Chen, Wilson et al. 2009, Li, Wang et al. 2011).

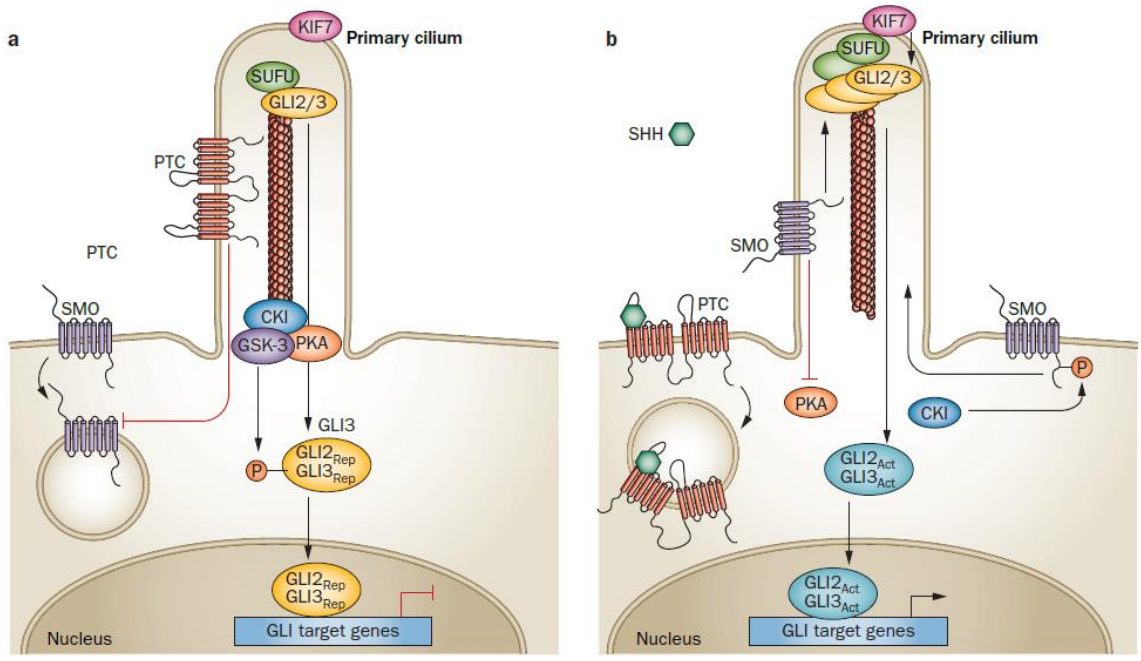

Figure 8. Hedgehog signaling and the primary cilium.
In vertebrates, primary cilia can act as an organizing center for GLI proteins processing. a) In the absence of Hedgehog, PTCH1 (PTC) is localized to the cilium and prevents accumulation of SMO in the cilium through an undetermined mechanism. SUFU directly interacts with GLI2 and GLI3, enabling their phosphorylation by PKA, CKI and GSK-3, which promotes their proteolytic processing to GLI2Rep and GLI3Rep. b) Binding of hedgehog ligands to PTC promotes removal of PTC from the cilium. Enzymes (including CKI) phosphorylate SMO, which is activated thereby and accumulates in the primary cilium, resulting in translocation of SUFU–GLI protein complexes to ciliary tips. KIF7 acts through both SUFU-dependent and SUFU-independent mechanisms to control the ciliary localization and dissociation of SUFU–GLI protein complexes, which results in translocation of GLI2Act and GLI3Act into the nucleus, promoting GLI target

gene transcription. Abbreviations: Act, transcriptional activator; Rep, transcriptional repressor (modified from (Alman 2015)).

As mentioned before, in vertebrates, there are three Gli transcription factors (Gli1, Gli2 and Gli3). Gli1 is the main full-length transcriptional activator, whereas Gli2 and Gli3 act as either positive or negative regulators as determined by post-translational processing through the proteasome (Ruiz i Altaba 1997, Sasaki, Nishizaki et al. 1999). The functions of the three Gli proteins overlap but are also distinct. This is mostly determined by the intrinsic molecular nature of the proteins. In the absence of Hh signaling activation by the ligand, Gli proteins are present in low amount at the ciliary tip and the majority of full-length Gli proteins (Gli2FL and Gli3FL) are proteolytically processed to the N-terminal transcriptional repressor forms (Gli2R and Gli3R) that translocate to the nucleus and inhibit the transcription of target genes (Wang, Fallon et al. 2000) (Figure 8). Cytoplasmic sequestration of Gli proteins by Sufu facilitates their processing to repressor forms and their degradation, thus inhibiting the Hh pathway (Kogerman, Grimm et al. 1999). Gli3 processing depends on consecutive phosphorylation of multiple serine and threonine residues at its C-terminus by Protein Kinase A (PKA), Casein Kinase 1 (CK1), and Glycogen Synthase Kinase 3 (GSK3). The phosphorylated Gli3FL is bound and ubiquitinated by the SCFβTrCP ubiquitin E3 ligase and is consequently processed by the proteasome in a site-specific manner to generate Gli3R (Tempe, Casas et al. 2006, Wang and Li 2006). Hh signaling induction inhibits Gli3 processing and activates the Gli3FL, which leads to upregulation of target genes (Wang, Fallon et al. 2000, Huangfu and Anderson 2005). However, activated Gli3FL presents only a weak activator function (Wang, Ruther et al. 2007), working mainly as an inhibitor of Hh signaling. In contrast to Gli3, Gli1 is a potent transcriptional activator, and its transcription is directly regulated by Hh signaling (Dai, Akimaru et al. 1999, Bai and Joyner 2001). This is mostly due to the absence of the repressor domain and of proteolytic processing (Dai, Akimaru et al. 1999, Sasaki, Nishizaki et al. 1999, Kaesler, Luscher et al. 2000, Bai and Joyner 2001).

Nevertheless, Gli1 is not essential for the initial step of Hh signaling transduction, it appears to enforce the expression of Hh target genes after their initial activation mainly due by Gli2. Indeed, Gli2 acts as the primary transcriptional activator that mediates Hh signaling, and through Gli2FL is also processed to generate a repressor, although the extent of its processing is lower than what observed in Gli3 (Pan, Bai et al. 2006). However, the maintenance of a proper ratio of the Gli2/3FL to the Gli2/3R forms plays an essential role in Hh signaling (Goetz and Anderson 2010, Li, Wang et al. 2011).

In conclusion, Hh pathway activation coincides with the exclusion of Ptch1 from, and concomitant accumulation of Smo, in the primary cilium (Corbit, Aanstad et al. 2005, Rohatgi, Milenkovic et al. 2007), which results in inhibiting of Gli2 and Gli3 proteolytic processing thus allowing their accumulation at the tip of primary cilia. At this point, Gli proteins are converted into transcriptional full-length activators (GliA), by a mechanism still unknown, most likely related to post-translational modifications of Gli2 sequence (Kim, Kato et al. 2009) (Figure 8). Specific regions of the Gli2 protein, that could be subjected to post-translational modifications, regulate the localization to distinct subcellular sites resulting in modulation of its activity. In fact, a domain required for ciliary localization is also essential for Gli2 transcriptional activity, suggesting that the primary cilium is required for its function (Santos and Reiter 2014) and that the ciliary localization is crucial for a cilium dependent activation of Hedgehog signaling (Liu, Zeng et al. 2015). Furthermore, Hh activation promotes the cilium dependent dissociation of Sufu from Gli2FL and Gli3FL (Humke, Dorn et al. 2010, Tukachinsky, Lopez et al. 2010), which migrate to the nucleus and induce the transcriptional outcome of Hh target genes (Figure 8). Hh-mediated dissociation does not occur in cells either lacking cilia or with activated PKA, suggesting that the dissociation of Sufu-Gli complexes is dependent on the cilium in response to PKA inactivation (Chen, Wilson et al. 2009, Jia, Kolterud et al. 2009, Humke, Dorn et al. 2010, Tukachinsky, Lopez et al. 2010).

Another additional important player for regulating Gli activity is the kinesin family

member 7 (Kif7), a human ciliopathy protein (Dafinger, Liebau et al. 2011, Putoux, Thomas et al. 2011) which belongs to the kinesin-4 family. Beyond Sufu and Gli proteins, Kif7 also shows basal level of cilia localization in Mouse Embryonic Fibroblasts (MEFs), which enriches in cilia tips in response to Hh pathway activation (Liem, He et al. 2009). Recently, it has been demonstrated that Kif7 regulates Hh signaling by affecting Gli processing and activity (Liem, He et al. 2009, Maurya, Ben et al. 2013), however, the basic mechanisms of its function are still poorly understood. Solid experimental evidence demonstrates that its function in the Hh pathway depends strictly on the primary cilium (Endoh-Yamagami, Evangelista et al. 2009, Liem, He et al. 2009). In fact, Kif7 modulates the length of microtubules at the tip of primary cilia, and promotes the localization and appropriate regulation of Gli and Sufu in this location by controlling axonemal microtubules directly (He, Subramanian et al. 2014). In agreement, Gli2 and Sufu localize abnormally in puncta along the axoneme when Kif7 is absent or mutated, whereas in wild-type cells they accumulate at ciliary tips, as expected (Briscoe and Therond 2013) (Figura 9). Cilia on *Kif7*-mutant embryonic neural progenitor cells and cultured fibroblasts are longer, unstable and have structural defects at the axonemal tip, similarly to cilia fibroblasts from human patients with *Kif7* mutations (Putoux, Thomas et al. 2011). Kif7 increases the frequency of shrinkage at the distal end of axonemal microtubules, highlighting that it is important for the primary cilia integrity by regulating microtubule growth at the distal tip. This is the reason why *Kif7*-mutant cells have elongated cilia and mislocalization of Gli and Sufu to ectopic tip-like compartments along the axoneme, causing deregulation of Hh signaling (He, Subramanian et al. 2014) (Figura 9). Overall, the precise molecular and biochemical mechanism/s underlying the key role/s of Kif7 in affecting Gli localization, processing, and function to regulate expression of target genes remain unclear, but, researchers agree on the existence of a direct link between microtubule-regulation-dependent morphogenesis of primary cilia and the control of the Hh signaling pathway (Goetz, Ocbina et al. 2009, He, Subramanian et al. 2014, Gerhardt,

Leu et al. 2016).

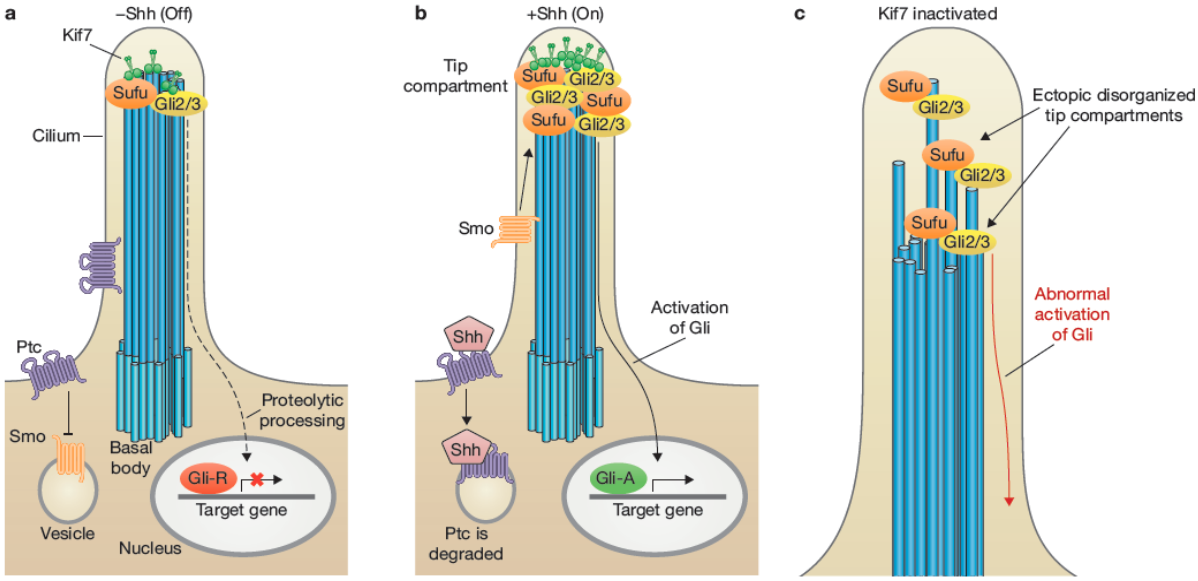

Figure 9. The primary cilium and regulation of Hedgehog signaling by Kif7.
(a) In the absence of Shh, Ptc localizes to the ciliary membrane and inhibits Smo, located in vesicles in the cytoplasm. Kif7, Sufu and the Gli2 and Gli3 transcription factors are present in low amounts at the ciliary tip. Gli2 and Gli3 are processed to their repressor forms (Gli-R) and target gene transcription is turned off. (b) Shh binds to Ptc, causing the receptor to exit the cilium concomitantly with Smo ciliary entry and accumulation of Kif7 and Gli–Sufu complexes at the ciliary tip. Kif7 organizes ciliary tips for appropriate localization and regulation of Gli–Sufu complexes, and Gli2 and Gli3 are converted to their full-length activator forms (Gli-A) for target gene transcription in the nucleus. For simplicity, only the most relevant proteins are shown. For a detailed overview of Hedgehog signaling in cilia, see (Nozawa, Lin et al. 2013). (c) In Kif7-mutant cells, the ciliary tip compartment is disorganized. Axonemal microtubules are longer and of unequal length, leading to the formation of ectopic tip-like compartments where Gli–Sufu complexes become localized and inappropriately activated in the absence of Shh ligand (modified from (Pedersen and Akhmanova 2014)).

Mutations in the *KIF7* gene have recently been identified in patients with ciliopathies, such as hydrolethalus (HLS) and acrocallosal (ACLS) syndromes, characterized by polydactyly, brain abnormalities, and cleft palate (Putoux, Thomas et al. 2011, Putoux, Nampoothiri et al. 2012, Walsh, Shalev et al. 2013); Bardet-Biedl (BBS) (DeLuca, Weed et al. 2015) and Joubert syndromes (Dafinger, Liebau et al. 2011) with brain malformation, cerebellar hypoplasia, ataxia, psychomotor delay, retinal degeneration, renal cyst, and skeletal abnormalities. Thus, the interest in understanding the precise mechanism at the base of Gli regulation by Kif7 is growing more and more.

However, despite recent progress, the mechanisms by which the cilium regulates Hh signaling remain obscure, and still unanswered are many questions about the activation of Gli proteins, including how Glis are trafficked into the cilium, whether other ciliary events are required for their activation, and how they move from the cilium to the nucleus.

2.2 Hedgehog signaling in health and disease

The Hedgehog signaling pathway plays important roles in the embryonic development of multicellular organisms, while, in adults, it is required for tissue homeostasis, repair, and regeneration, and it is often abnormal in diseased states (Beachy, Karhadkar et al. 2004, Lum and Beachy 2004, Petrova and Joyner 2014). It controls the digit pattern in limbs and the organization of neuronal subtype identity in the CNS of vertebrates. Dysregulation of this pathway is responsible for congenital syndromes, such as holoprosencephaly (a rare congenital brain malformation resulting from incomplete separation of the two hemispheres); other developmental malformations (such as, neural tube disorders, axial skeleton and limb malformations) (Hui and Angers 2011); as well as carcinogenesis (Jacob and Briscoe 2003, Motoyama 2006). The Hh signaling cascade is activated in various types of human malignancies including basal cell carcinomas (BCC), the most common type of skin cancer, and the Shh subtype of medulloblastoma, the most common type of brain cancer (Ebrahimi, Larijani et al. 2013).

In the vertebrate embryo, the Hedgehog ligand is initially expressed in the notochord, a mesodermal-derived structure that lies along the anteroposterior (A/P) axis of the body; it guides specification of all ventral cell types such as motor neurons in the developing neural tube, which will later on become the spinal cord (Jessell 2000). After birth, Shh continues to play important roles in the growth of the brain and in the maintenance of neural progenitors (Ruiz i Altaba, Palma et al. 2002). During skeletal development, it is required for limb formation and specification of digit number and identity in developing limb buds

(Johnson, Riddle et al. 1994). To be more precise, Hedgehog ligands are expressed by cells of the posterior portion of the limb bud mesoderm and diffuse across the developing limb bud, producing a concentration gradient that acts as a morphogen to specify digit development (Yang, Guillot et al. 1998). The repressor activity of Gli3 is especially important in embryonic patterning of limbs and also of the neural tube (Jiang and Hui 2008). During limb buds development, Gli3R shows an A/P gradient inversely proportional to Shh levels. In the neural tube, Gli3 is critical to establish a double Gli gradient with opposite polarities of activators (high to low from ventral to dorsal) and repressors (high to low from dorsal to ventral) to regulate the specification of individual neural subtypes (Jiang and Hui 2008, Briscoe and Therond 2013). In addition to limb and neural development (Wang, Ruther et al. 2007), Gli3R is involved in the development of the vertebrate lung, kidneys, ureter, mammary gland, and ears (Lee, Zhao et al. 2016). Also, Gli2R takes part in the development of the brain and the limbs in mice as well as the neural tube in Zebrafish (Ke, Kondrichin et al. 2008, Bowers, Eng et al. 2012). Gli2R, together with Gli3R, controls anterior limb patterning and digit number. Overall, all three vertebrate Hh transcription factors (Gli1, Gli2 and Gli3 proteins) act together to integrate Hh signaling inputs, resulting in the regulation of tissue pattern, size, and shape (Ruiz i Altaba, Mas et al. 2007, Wang, Ruther et al. 2007, Hui and Angers 2011).

Mutations that affect hedgehog signaling cause skeletal defects including polydactyly (the presence of extra digits) and neural tube defects. Similarly, also mutations in cilia genes (e.g. the Ift mutants) associated to defective Hh pathway result in altered Hh-dependent digit development, polydactyly and abnormal dorso-ventral patterning of the neural tube (Goetz and Anderson 2010). In Shh mutants, ventral neural cell types fail to be specified and the limbs lack digits (Goetz and Anderson 2010); in anterograde IFT mutants (e.g. the IFT-B mutants Ift88 or Ift172) that lack cilia, the Hh signaling is reduced, the neural tube is dorsalized and polydactyly occurs, whereas IFT-A mutants (e.g. Ift139) exhibit phenotypes consistent with excessive Hh signaling and ventral cell types expand in the

neural tube (Goetz and Anderson 2010, Reiter and Leroux 2017) (Figure 10).

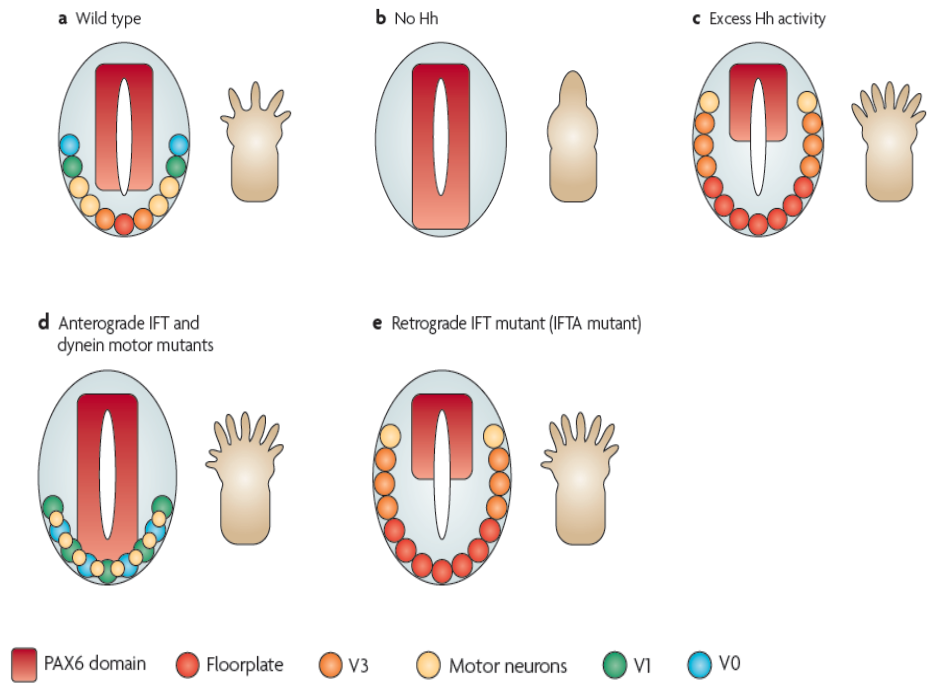

Figure 10. Neural and limb patterning phenotypes in hedgehog pathway and cilia mutants.
a | In wild type embryos, ventral neural cell fates are specified by a gradient of sonic hedgehog (Shh). The number and identity of digits in the limb is established by an Shh gradient from the posterior limb bud to the anterior limb bud, where the repressor form of Gli3 (Gli3R) inhibits Shh. b | In the absence of hedgehog (Hh) (for example, in smoothened (Smo)$^{-/-}$ embryos) ventral neural cell fates are lost. The limbs of Shh$^{-/-}$ mutants lack digits. c | If the pathway is hyperactive (for example, in patched 1 (Ptch1)$^{-/-}$ embryos), ventral cell types expand in the neural tube. Activation of the pathway within the limb, such as in Gli3$^{-/-}$ mutants (which lack Gli3R), causes the formation of extra digits. d | Anterograde intraflagellar transport (Ift) mutants (for example, Ift88$^{-/-}$ or Ift172$^{-/-}$ embryos) lack cilia: Hh signaling is reduced, and the neural tube is dorsalized. This phenotype is milder than in b because cilia are also required for Gli3R processing, and cell types that require low levels of Hh signaling are specified. Reduced Gli3R results in polydactyly. Dynein motor mutants display a similar phenotype; however, they retain motor neurons in the caudal neural tube. e | IftA complex mutants (for example, Ift139$^{-/-}$ embryos) exhibit phenotypes consistent with excess Hh signaling (Modified from (Goetz and Anderson 2010)).

Many clinical features seen in ciliopathies models can be attributed to abnormal Hh signaling. In fact, mouse mutants with *Ofd1* inactivation that reproduces OFD type I syndrome display severe polydactyly with loss of A/P digit patterning and shortened long bones. These models show loss of digit identity associated with a progressive loss of Shh signaling and an impaired processing of Gli3. On the other hand, the defects in limb outgrowth observed in *Ofd1* mutants are due to defective Ihh signaling and abnormal mineralization during endochondral bone formation (Bimonte, De Angelis et al. 2011).

Another important physiological role played by the Hh signaling pathway is the embryonal regulation of the early craniofacial development. Hh is essential for establishing subdivision of the eyefield, for bilateral patterning of the ventral forebrain (Chiang, Litingtung et al. 1996), and for early formation of the upper lip and palate. Many studies indicate that the concentration of ligand and the duration of Hh signaling are also important for the correct development of the face. Collectively, the time-space coordinated function of Hh signaling activity is essential for orchestrating fundamental organization of the craniofacial region (Xavier, Seppala et al. 2016). Mutations in many genes that encode Hh signaling proteins, or that cause impairment of the Hh pathway, are associated with craniofacial anomalies in the human population. Thus, mice with deletion of *Shh* have significant craniofacial defects, including alobar holoprosencephaly, cyclopia (Chiang, Litingtung et al. 1996), failure of the primary mouth opening (Tabler, Bolger et al. 2014), and hypoplasia of the first pharyngeal arch (Washington Smoak, Byrd et al. 2005, Yamagishi, Yamagishi et al. 2006). Moreover, a mouse model for MKS, caused by loss of *Mks1*, shows altered Hh signaling that underlies some of the defects, including craniofacial abnormalities (Weatherbee, Niswander et al. 2009).

Finally, given the implications of the Hh pathway in human diseases, there is an evident interest in identifying small molecules capable to target and modulate this pathway and to develop pharmacologic strategies to apply in conditions where this pathway is impaired.

3. Protein degradation and cilia

Given that the diverse responses of the cell to the Hh pathway in different tissues during development depend on the duration of exposure to Hh ligand and on a proper gradient concentration of secreted Hh protein, several mechanisms that dynamically and tightly regulate the amount of Hh signaling mediators are necessary. A well-established

mechanism for limiting signal duration is the Hh induced ubiquitination and degradation of Gli proteins. The impairment of this process can lead to cell patterning disruption and uncontrolled cell proliferation (Di Marcotullio, Ferretti et al. 2006, Kent, Bush et al. 2006, Di Marcotullio, Ferretti et al. 2007, Ou, Wang et al. 2007). As mentioned before, the UPS also proteolytically processes Gli2 and Gli3 (Wang, Fallon et al. 2000). During this processing event, ubiquitination takes place immediately after phosphorylation of Gli2 and Gli3, but it is still unknown if this event occurs at the basal body. However, considering that the resulting truncated forms of both proteins play decisive roles during development of almost every vertebrate organ (Goetz and Anderson 2010, Waters and Beales 2011, Briscoe and Therond 2013), the correct functionality of the proteasome is really essential. In addition to Gli factors, a growing number of evidence suggests that ubiquitination also plays critical roles in modulating other Hh signaling components including Ptc, Smo, and Sufu, thus demonstrating that ubiquitination is an important mechanism in the regulation of Hh pathway dynamics and in the turnover of its mediators (Hsia, Gui et al. 2015).

In general, intracellular protein turnover is essential for the regulation of cellular functions and maintenance of cellular homeostasis. Their levels within cells are determined not only by rates of synthesis, but also by rates of degradation. The rapid turnover of proteins is necessary to change quickly their levels in response to external stimuli (Lecker, Goldberg et al. 2006). This general mechanism for cellular protein is really important and also shared by ciliary proteins. In addition, also misfolded or damaged proteins are recognized and fast degraded within cells to avoid toxicity. Each protein is degraded at widely differing rates that vary from minutes to days or weeks. Overall, the rates of protein degradation in each cell must be precisely balanced because even a small acceleration of degradation can result in a marked loss of protein storages, with a consequential loss of protein which is not available for performing its cellular functions (Mitch and Goldberg 1996, Lecker, Goldberg et al. 2006).

Cells contain multiple proteolytic systems to carry out degradation processes together with

complex regulatory mechanisms to ensure that the proteolytic processes are highly selective. Cells use two major protein degradation systems: the **ubiquitin-proteasome system (UPS)**, which usually degrades the majority of proteins, and the **autophagy-lysosome pathway (ALP),** primarily responsible for the degradation of most long-lived or aggregated proteins and cellular organelles (Lilienbaum 2013).

3.1 The Ubiquitin-Proteasome System (UPS)

The **Ubiquitin Proteasome System (UPS)** is a highly regulated mechanism responsible for degrading 80-90% of proteins. Considering that cells are permanently subjected to external and internal changes as well as stressful insults, a constant remodeling and repair or elimination of many regulated, short-lived, denatured, or damaged proteins is required (Dikic 2017). Ubiquitin-dependent degradation by the proteasomal machinery is involved in the regulation of several processes including maintenance of different aspects of cellular homeostasis (ATP balance, amino acid recycling, control of protein quality), regulation of gene transcription, antigen presentation, cell cycle progression, DNA repair, receptor-mediated endocytosis, cell stress response, apoptosis, cell differentiation, and proper activity of pathways (Dikic 2017, Varshavsky 2017). The proteasome is a machine for efficient and automatic destruction of ubiquitin protein conjugates into oligopeptides and ubiquitin releasing and recycling, but it is also important for determining whether an ubiquitinated protein should undergo degradation or should survive intact (Collins and Goldberg 2017). Defects in UPS can result in the pathogenesis of relevant and common human conditions, such as neurodegenerative disorders and cancer. More recently, impaired UPS has also been associated to ciliopathies (Ciechanover, Orian et al. 2000, Gerhardt, Leu et al. 2016).

UPS controls the activity of various cellular processes by covalently attaching ubiquitin to protein substrates. Proteins are initially tagged by a covalently linked poly-ubiquitin chain,

which is recognized as a degradation signal by the proteasome. As a result, the ubiquitin chain is removed and the protein is unfolded in an ATP dependent manner and translocated into the center of the proteasome complex, where it is degraded into small peptides (Kisselev and Goldberg 2001). The key factor in this process is the ubiquitin (Ub), which is an highly conserved, small (8.5kDa), regulatory, globular protein composed of 76 amino acids (Callis 2014). Ubiquitin is encoded by four different genes (*UBB, UBC, UBA52,* and *UBA80* (*RPS27A*)) and is produced as a precursor that must be proteolytically processed to release mature ubiquitin (Bianchi, Giacomini et al. 2015). It is strongly expressed in cells and can be covalently coupled to the ε-amino group of a lysine (Lys) within a substrate protein. Ubiquitination is both an inducible and reversible signaling cascade used in all eukaryotic cells and requires the orchestration of three different classes of enzymes: ubiquitin activating enzymes (E1), ubiquitin-conjugating enzymes (E2), and ubiquitin ligases (E3), but a new class of ubiquitin elongation factors called ubiquitin ligases (E4) has been found (Callis 2014) (Figure 11). Each of these enzymes plays a different role in activating free ubiquitin and catalyzing its covalent addition for ubiquitin modification of protein substrates. Although ubiquitination can have many effects on the modified protein (such as in regulating the stability, function, and/or localization), its role as a signal for regulated protein degradation by proteasomal degradation is well established and characterized. Ubiquitination is mediated by an enzymatic cascade of three reactions. In the first step, the E1 catalyzes the ATP-dependent activation of ubiquitin resulting in the formation of a thioester bond between the C-terminus of ubiquitin and a cysteine residue in the E1 active site. Subsequently, activated Ub is transferred to an active cysteine residue of the E2 to generate again a new thiol ester intermediate. At the end, the E3, with cooperation of E2, attaches Ub to a Lys residue of a substrate protein. In some cases, the extension of short ubiquitin chains requires the action of additional elongation factors, the E4 enzymes (Callis 2014). (Figure 11).

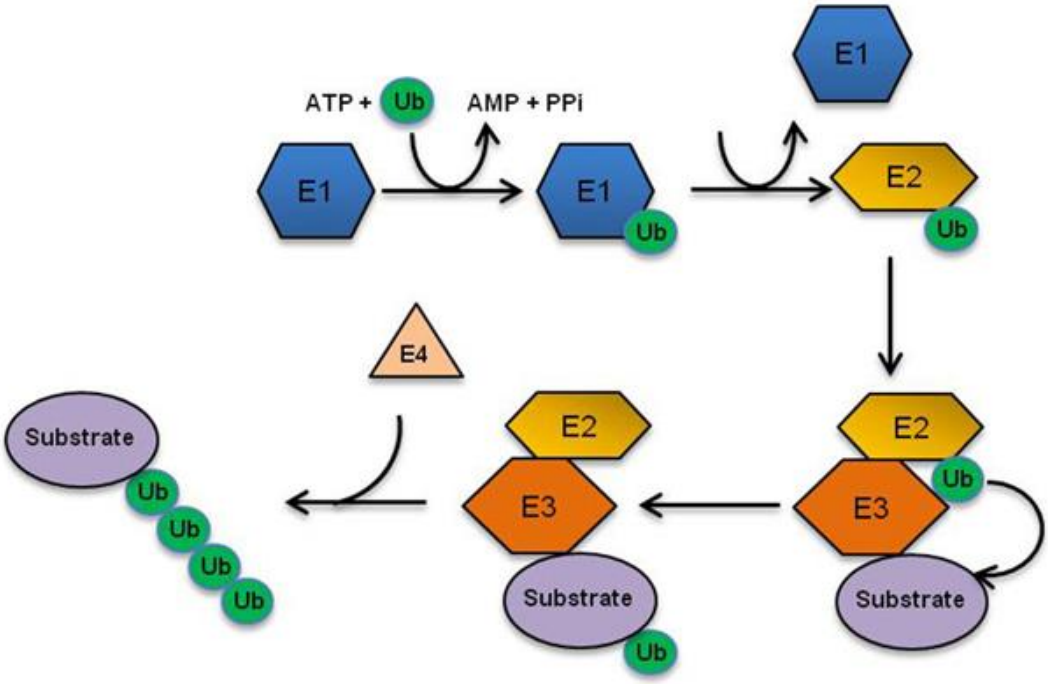

Figure 11. Mechanism of ubiquitination.
The ubiquitination process involves a three-enzyme cascade. The E1 enzyme first activates the carboxy terminus of the ubiquitin molecule, using the energy from converting an ATP molecule to AMP and pyrophosphate (PPi). The activated ubiquitin is attached to the sulfur of the E1 active-site cysteine residue. Ubiquitin is then transferred from E1 to E2, and E3 facilitates the transfer of ubiquitin from E2 to the substrate protein. In some cases, the extension of short ubiquitin chains requires additional elongation factors, termed E4 enzymes. (Modified from (Brinkmann, Schell et al. 2015)).

There are approximately 600 ubiquitin E3 ligases identified, with variable specificities to individual protein-substrates (Komander 2009). The specificity and type of ubiquitination is generated from substrate recognition by the E3 and the formation of different E2–E3 complex combinations that mediate ubiquitination (Weissman 2001). Ub itself contains seven lysine residues (Lys6, Lys11, Lys27, Lys29, Lys33, Lys48 and Lys63) that can be targeted in recurrent rounds of this cascade, giving rise to differently linked and branched Ub chains (polyUb). In this way, a complex Ub code can be generated. In fact, one ubiquitin C-terminus can be covalently linked to a second ubiquitin via one of the latter's seven Lys ε-amino groups or N-terminal amino group, forming ubiquitin chains. Thus, in addition to a single ubiquitin modification (monoubiquitination) or modification by one ubiquitin at multiple sites of the same substrate (multi-monoubiquitination or poly-monoubiquitination), substrates can be modified by ubiquitin chains (polyubiquitination)

(Callis 2014). Ubiquitination plays additional roles depending on the chain configuration and linkage (Komander 2009). There is increasing evidence for the formation of more complex topologies with mixed linkages, so-called atypical chain types, with unknown functions (Li and Ye 2008). In fact, the Ub polymers can also contain several linkage types in mixed ubiquitin chains, or one ubiquitin can be modified on multiple sites to form branched ubiquitin chains (heterotypic chains), generating a huge number of possible chain topologies (Nakasone, Livnat-Levanon et al. 2013). These types of Ub chains provide new functionalities in cells and constitute seemingly independent signals in degradation and signaling (Michel, Elliott et al. 2015). Thus, different ubiquitin-ubiquitin linkages form distinct conformations and consequently regulate different cellular processes (Haglund and Dikic 2005). Monoubiquitination may facilitate protein recognition, complex formation, or allosteric regulation, while most substrates require poly-ubiquitination to be delivered to the proteasome. Usually, the attachment of a Lys 48-linked polyUb chain to a protein is required for an efficient degradation, whereas the Lys 63-linked polyUb chain is mainly involved in non-proteolytic processes such as transcription, intracellular protein trafficking, autophagy, DNA-damage response, cellular signaling, and others (Komander and Rape 2012, Swatek and Komander 2016, Yau and Rape 2016). However, recent studies have added another level of complexity to this general process by demonstrating also the involvement of polyUb chains linked through Lys6, Lys11, Lys27, Lys29, Lys33 or Lys63 in targeting proteins to the proteasome for degradation (Saeki, Kudo et al. 2009).

3.1.1 Structure and function of the 26S proteasome

The degradation of the vast majority of intracellular mammalian proteins is performed mainly by the proteasome, also called **26S proteasome** in eukaryotes. The 26S proteasome is a cylinder-shaped multicatalytic ATP-dependent protease complex present in all eukaryotic cells. It consists of two subcomplexes: a central **20S core particle** (**CP**, about

700 kDa), capped with one or two **19S regulatory particles** (**RP** the most abundant form in mammals is called PA700, about 900 kDa) on one or both ends of the CP (Budenholzer, Cheng et al. 2017) (Figure 12).

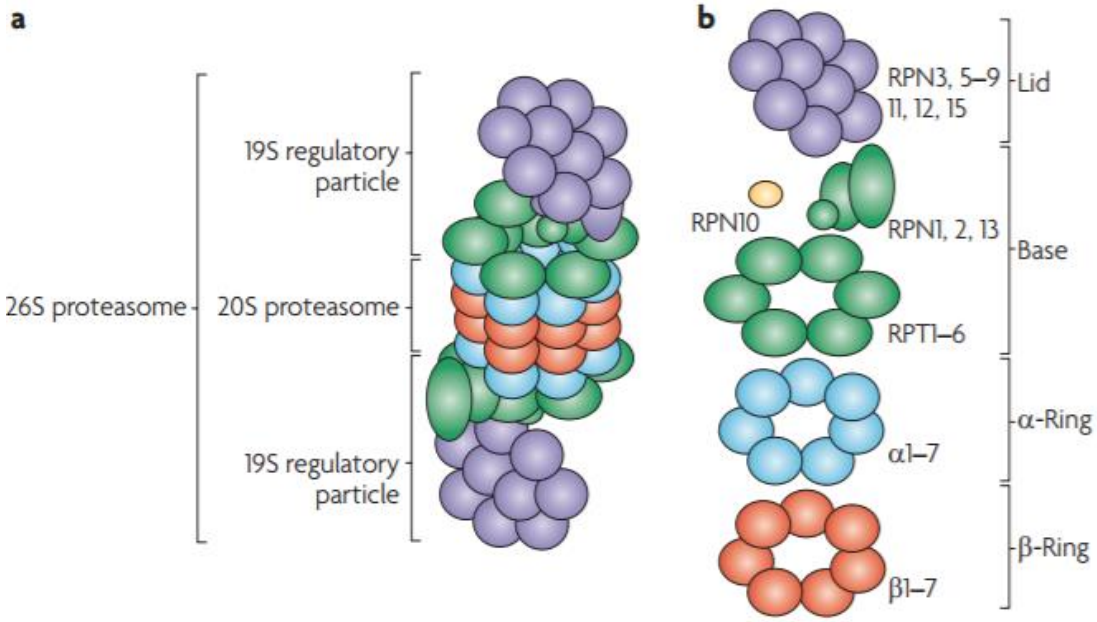

Figure 12. Scheme of 26S proteasome.
a | The 26S proteasome consists of the catalytic 20S proteasome (a barrel of four stacked rings: two outer alpha-rings and two inner beta-rings) and the 19S regulatory particle (RP, also known as PA700). b | Subunit composition of the 26S proteasome. The regulatory particle is further divided into the base and the lid subcomplexes, which are composed of regulatory particle triple-A (RPT) and regulatory particle non-ATPase (RPN) subunits. RPN10 is colored in yellow since it is thought to be located at the base–lid interface (modified from (Murata, Yashiroda et al. 2009)).

The **20S core particle** is responsible for the degradation of proteins into short peptides. It is composed of four stacked rings, two outer α-rings and two inner β-rings, forming a central cavity of 2-nm diameter. The two outer rings consist of seven different α subunits (α1- α7) that cap the two inner rings formed by seven different β subunits (β1-β7) (Budenholzer, Cheng et al. 2017). Only three β subunits (β1, β2 and β5) contain catalytically active sites, with threonine residues at their N-termini, that face the interior space of the 20S CP, while the other β-subunits, (β3, β4, β6 and β7) are catalytically inactive. The β catalytic subunits are associated with caspase-like, trypsin-like, and chymotrypsin-like activities, respectively, which confer the ability to cleave peptide bonds at the C-terminal side of acidic, basic, and hydrophobic aminoacid residues, respectively

(Budenholzer, Cheng et al. 2017). Different proteasome inhibitors have been developed that target these activities (Groll and Huber 2003). While β rings possess proteolytically active sites, the outer α rings forms a narrow channel (~ 13Å in diameter), mainly composed of α2, α3, and α4 subunits, which controls the access of substrates to the catalytic chamber and provides attachment sites for the 19S RP. In order to be degraded into peptides of 2–24 amino acids, substrate proteins must first be unfolded and then translocated into the proteolytic chamber via the narrow gate to access the active sites of catalytic enzymes at the center of the α-ring (Budenholzer, Cheng et al. 2017). Thus, UPS provides an essential source for aminoacids, and if the proteasome activity is inhibited, increased cell lethality due to severe storage of aminoacids occurs (Suraweera, Munch et al. 2012).

The **19S regulatory particle** is the key regulatory component of the 26S proteasome. It is responsible for recognition of ubiquitinated substrate followed by the removal of the ubiquitin chain via deubiquitinating enzymes, substrate unfolding, and translocation into the 20S catalytic chamber for degradation (Bar-Nun and Glickman 2012). The 19S RP is composed of at least 19 subunits that can be divided into two sub-complexes: the base and the lid (Lander, Estrin et al. 2012). The central part of the RP base consists of six AAA ATPases (Rpt1–Rpt6), Rpt1/S7, Rpt2/S4, Rpt3/S6, Rpt4/S10b, Rpt5/S6 and Rpt6/S8, which form an hesameric ring (Tomko, Funakoshi et al. 2010). The base also includes four non-ATPase subunits: Rpn1/S2, Rpn2/S1, Rpn10/S5a, and Rpn13/hRpn13 (Elsasser, Gali et al. 2002, Tomko, Funakoshi et al. 2010, Rosenzweig, Bronner et al. 2012). The hydrolysis of ATP provides the energy to unfold the substrates and translocate them into the 20S CP catalytic chamber (Smith, Chang et al. 2007). Significantly, the functions of the six ATPases are not redundant; in fact, they have to work together and coordinately. The non-ATPase proteins of the RP base, Rpn13, and Rpn10 possess ubiquitin-binding domains, and function as receptors for ubiquitinated substrates (Finley 2009). In addition, shuttling factors (Rad23, Dsk2, and Ddi1), members of the UBL/UBA protein family,

deliver ubiquitinated proteins to the proteasome for degradation. These proteins contain an ubiquitin-like (UBL) domain for binding to proteasome and one or more ubiquitin associated (UBA) domains for binding to poly-ubiquitinated chains (Wilkinson, Seeger et al. 2001, Elsasser, Gali et al. 2002). The lid complex includes also 9 non-ATPase subunits, Rpn3, Rpn5–Rpn9, Rpn11, Rpn12, and Sem1 (Lander, Estrin et al. 2012). It is connected to the base complex by interactions between Rpn12 and Rpn2, Rpn11 and Rpn1, and Rpn10 might be involved in stabilizing these interactions (Boehringer, Riedinger et al. 2012). One of the main functions of lid and base is proposed to be the removal of ubiquitin signals (a process called deubiquitination), carried out by specific enzymes, the deubiquitinases or deubiquitinating enzymes (DUBs) (Reyes-Turcu, Ventii et al. 2009).

3.1.2 Deubiquitinating enzymes

DUBs are a class of the human family of proteases that catalyse the removal of ubiquitin from target proteins and are also involved in ubiquitin maturation, recycling, and editing (Reyes-Turcu, Ventii et al. 2009, Clague, Barsukov et al. 2013). In particular, they produce free ubiquitin by releasing single molecules of Ub from the multiple fused ubiquitin moieties transcribed by ribosomes during the generation of *de novo* Ub. Another way to maintain the pool of free Ub is recycling ubiquitin from ubiquitin-protein conjugates. This process is vital for keeping sufficient levels of free ubiquitin that can be used for ubiquitin chain assembly. Deubiquitinating enzymes also cleave polyubiquitinated chains in specific locations inducing differential effects on the fate of the ubiquitinated proteins (Reyes-Turcu, Ventii et al. 2009). Moreover, DUBs can completely remove ubiquitin chains from ubiquitinated proteins and consequently stabilize proteins by preventing their degradation (Komander, Clague et al. 2009, Farshi, Deshmukh et al. 2015). Most DUBs regulate only a limited number of proteins and pathways, indicating that they operate with a limited number of specific target substrates (Hu, Li et al. 2005). In fact deubiquitinases exhibit

strong substrates specificity by using their ubiquitin-binding domain (UBD) (Nijman, Luna-Vargas et al. 2005, Komander, Clague et al. 2009). The number of known deubiquitinases is growing and varies depending on different organisms; for example, ~20 DUBs exist in *Saccharomyces cerevisiae*, while in humans there are ~100 enzymes (Clague, Barsukov et al. 2013) which are divided into six classes: ubiquitin-specific proteases (USPs, the largest family in human: about 60 members), ubiquitin carboxy-terminal hydrolases (UCHs), ovarian-tumour proteases (OTUs), Machado–Joseph disease protein domain proteases (MJD), JAMM/MPN domain-associated metallopeptidases (JAMMs) and monocyte chemotactic protein-induced protein (MCPIP) (Fraile, Quesada et al. 2012). Among the DUBs, three are associated with proteasome in humans to rescue ubiquitin chains before the degradation of the substrate protein: Rpn11/POH1 (Verma, Aravind et al. 2002), Ubp6/USP14 (Borodovsky, Kessler et al. 2001, Leggett, Hanna et al. 2002), and Uch37/UCHL5 (Lam, Xu et al. 1997) (yeast/human nomenclature) (Figure 13). Rpn11 is a metalloprotease, precisely a Zn2+-dependent DUB, which belongs to the JAMM domain family and is an integral part of the lid complex in 19S RP (Ambroggio, Rees et al. 2004), while Uch37 and Usp14 are cysteine proteases and members of the UCHs and USPs families, respectively. Both Usp14 and Uch37 are proteases reversibly associated to the base complex of the 19S RP: they release the ubiquitin chain from the substrate of proteasome and disassemble it. For an efficient proteolysis, the substrate has to be deubiquitinated. The covalently linked poly-ubiquitin chains of substrates sterically prevent the access to the opened channel into the 20S CP, thus the cleavage and removal of the ubiquitin chain is required for substrate translocation and degradation.

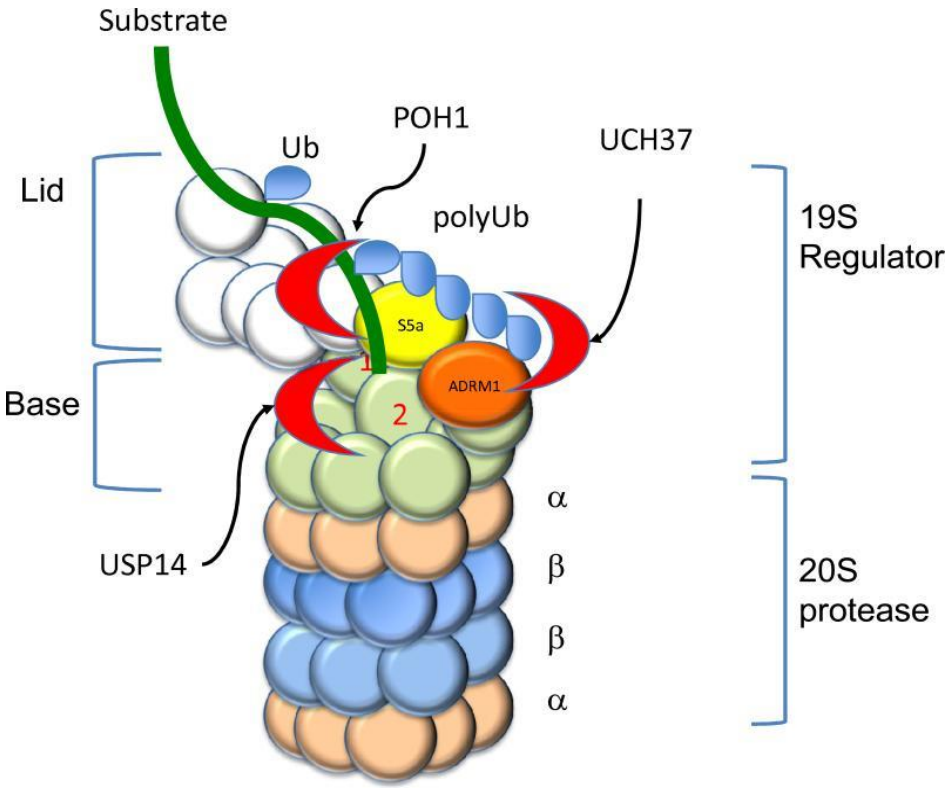

Figure 13. Proteasome bound deubiquitinating enzymes.
Deubiquitinating enzymes are indicated by red crescents, the substrate as a green line, and ubiquitin as blue ovals. POH1 catalyzes the release of a polyubiquitin chain "en bloc" as the substrate is engaged and translocated through the gated pore of the 20S protease. RPN10 (yellow) binds the polyubiquitin chain and the distal end of the chain can be removed by the action of UCH37 bound to ADRM1 (orange). USP14 is bound to the proteasome via interactions with RPN1 (purple) and probably removes mono ubiquitin attached to the substrate (modified from (Reyes-Turcu, Ventii et al. 2009)).

Rpn11 is the essential DUB for this aim: as a matter of fact, while Rpn11 promotes substrate degradation by removing the ubiquitin moiety as *en bloc* from the base of the chain, Uch37 and Usp14 are believed to antagonize substrate degradation. Both Usp14 and Uch37 trim the polyubiquitin chain to regulate the time of interaction between substrate and proteasome and the resulting rate of degradation (Leggett, Hanna et al. 2002, Stone, Hartmann-Petersen et al. 2004, Lee, Lee et al. 2011). Thus, the discrimination between these three DUBs resides in their proteolysis promoting activity.

3.1.3 Ubiquitin-Specific Protease14 (USP14)

USP14, the mammalian homolog of yeast Ubp6, is a cysteine protease that belongs to the ubiquitin specific proteases (USP) family. It is encoded by the *USP14* gene, located on chromosome 18p11.32, which is highly expressed in several mammalian tissues.

Alternative pre-RNA splicing results in two isoforms of USP14 but only one of them gives rise to a fully operative enzyme (Crimmins, Jin et al. 2006).

3.1.3.1. Structure and functions of USP14

USP14 encodes a protein that consists of 494 amino acids (about 60 kDa), composed of a 9 kDa N-terminal UBL domain (Wyndham, Baker et al. 1999), conserved between many eukaryotic species, and followed by a 45 kDa catalytic domain (Hu, Li et al. 2005). The UBL domain has a folding pattern similar to that observed in ubiquitin (Wyndham, Baker et al. 1999). It was first identified in USP14, but now it is known to be present in several members of the USP family (Komander, Clague et al. 2009). The UBL domain of Usp14 is critical for its reversible association with the Rpn1 subunit of the base in the 19S regulatory particle (Hu, Li et al. 2005). This association with the proteasome increases USP14 catalytic activity several hundredfold. In fact, USP14 is activated upon binding to the proteasome and catalyzes the cleavage of ubiquitin subunits from substrates before degradation by the proteasome (Borodovsky, Kessler et al. 2001, Hu, Li et al. 2005, Hanna, Hathaway et al. 2006), but it is also likely that free USP14 could have other proteasomal independent functions (Jung, Kim et al. 2013). The favourite substrates for USP14 are Lys48-linked polyUb chains which are cleaved from their distal end or within the chain (Hu, Li et al. 2005, Hanna, Hathaway et al. 2006), but recently, it has also been demonstrated an involvement of Usp14 in the regulation of the autophagy pathway by negatively controlling K63 ubiquitination of Beclin1, an important player of autophagy (Xu, Shan et al. 2016). Therefore, regulation of Usp14 activity provides a mechanism to control both proteasomal and autophagic degradation. Inhibition of Usp14 has been proposed as a strategy to promote both UPS and ALP for developing novel therapeutic approaches to use in neurodegenerative disease. The activity of Usp14 in deubiquitinating K63 Ub linkage is likely of physiological relevance given that inhibition of Usp14 *in vivo*

leads to enhanced K63-linked Ub conjugates in both spinal cord and neurons (Vaden, Bhattacharyya et al. 2015). However, the mechanism by which Usp14 regulates K63 ubiquitination in controlling cellular processes and its functional significance is not well characterized.

Beyond its function in controlling protein degradation, Usp14 has a critical role in ubiquitin recycling. Loss of ubiquitin pools severely impairs the ability of the proteasome to degrade unwanted proteins, being dependent on ubiquitin for tagging, thus resulting in protein accumulation. Depletion of free ubiquitin upregulates proteasome bound Usp14, while loss of Usp14 results in increased degradation of ubiquitin and decreased levels of monomeric ubiquitin (Hanna, Leggett et al. 2003, Hanna, Hathaway et al. 2006, Hanna, Meides et al. 2007). This specific role of Usp14 in stabilizing cellular ubiquitin levels was demonstrated in *Usp14* deficient mice with spontaneous ataxia mutation (axJ) which display decreased ubiquitin levels in all tissues with the most evident depletion observed at synaptic terminals (Wilson, Bhattacharyya et al. 2002, Anderson, Crimmins et al. 2005). The axJ mutation reduces dramatically the levels of Usp14 in both neuronal and non-neuronal tissues, resulting in severe tremors at 2–3 weeks of age followed by paralysis of hindlimbs and finally death in 2–3 months. This mutation consists in the insertion of an intracisternal A-particle (IAP), into intron 5 of the *Usp14* gene (Wilson, Bhattacharyya et al. 2002). axJ mice are characterized by defects in synaptic transmission in both the central and peripheral nervous systems rather than the ubiquitin-positive protein aggregates or neuronal cell loss observed in other neurodegenerative diseases. (Wilson, Bhattacharyya et al. 2002). Therefore, Usp14 regulates synaptic activity and neuronal development, and its massive reduction causes ataxia, but the neuronal specific expression of Usp14 can restore viability and motor system function. The ubiquitin monomer levels are also restored by Usp14 expression indicating that proteasome dysfunction could contribute to the neurological dysfunction in axJ mice (Crimmins, Jin et al. 2006, Chen, Bhattacharyya et al. 2011). Afterwards, Usp14 has been found to be essential for synaptic development and

function at neuromuscular junctions. In contrast to reduced levels of Usp14 in axJ mice, loss of *Usp14* causes developmental defects at motor neuron endplates which correlate with observed ubiquitin loss (Chen, Qin et al. 2009). Moreover, a study with a novel induced mutation (nmf375) in *Usp14*, indicates that Usp14 is also needed in adulthood. This mutation causes aberrant Usp14 mRNA splicing with a dramatic reduction of Usp14 amount, causing ubiquitin depletion and adult-onset motor endplate disease without reduced ubiquitin levels and neuromuscular junction abnormalities during the first 4-6 weeks of life, and early postnatal lethality characteristic of axJ mutation (Marshall, Watson et al. 2013). Overall, different genetic backgrounds have a great impact on the ubiquitin expression and influence the phenotypes caused by Usp14 deficiency.

Interestingly, recent studies suggest that a number of DUBs plays a prominent role in cancer development and progression (D'Arcy, Wang et al. 2015). Also, USP14 is thought to be involved in different cancers including, but not limited to, ovarian and colorectal cancer (Farshi, Deshmukh et al. 2015). High expression of USP14 has been found in several hematopoietic and solid tumor cell lines (for example: leukemic, colon cancer, and multiple myeloma cells) (Ishiwata, Katayama et al. 2001, Ishiwata, Ozawa et al. 2004, Tian, D'Arcy et al. 2014). Another engaging discovery is the identification of Usp14 among the candidate primary cilia proteins identified by proteomic analysis of mammalian primary cilia (Ishikawa, Thompson et al. 2012). Usp14 has never been implicated in cilia biology until now and this new evidence suggests a possible functional role of Usp14 in regulating ciliogenesis and maintenance of primary cilia, and a possible involvement of cilia in deubiquitination process.

3.1.3.2. IU1: a specific inhibitor of Usp14 deubiquitinating activity

Proteasome inhibitors are becoming attractive therapeutic agents. Researchers now propose that targeting specific aspects of the ubiquitin–proteasome pathway upstream of the 20S

proteasome (e.g. DUBs) might be advantageous with regards to efficacy as well as adverse effects. The main aspect that makes DUBs an attractive therapeutic target for diseases is the ability to modulate protein fate in a specific or selective manner (Farshi, Deshmukh et al. 2015). Therefore, targeting DUBs can modulate the status of the cell by modifying specific key aspects of pathological pathways to selectively direct the cell towards death or recovering from the pathological state. The importance of DUBs for proteasomal degradation has enhanced the interest in development of selective and specific DUBs inhibitors (Farshi, Deshmukh et al. 2015). Several inhibitors of pan-DUB that target both proteasomal and non-proteasomal DUBs have been described and the Usp14 inhibitor belongs to these. Thousands of compounds have been screened and 1-[1-(4-fluorophenyl)-2,5-dimethylpyrrol-3-yl]-2-pyrrolidin-1-ylethanone (IU1) represents the first small molecule we know that selectively, specifically and reversibly binds the proteasomal-associated form of USP14, thus inhibiting its deubiquitinase activity. The structure of IU1 is an active-site-directed thiol protease inhibitor which binds only the active form of Usp14 (Figure 14).

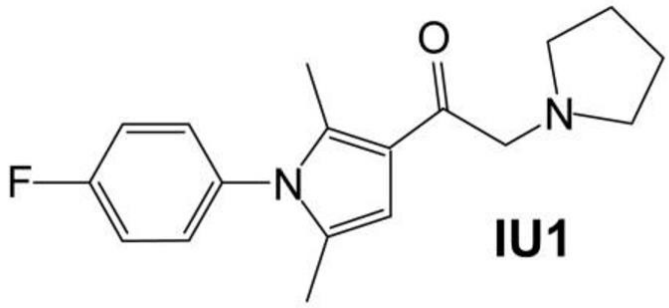

Figure 14. Chemical structures of IU1.
IU1 structure is an active-site-directed thiol protease inhibitor

IU1 increases proteasomal substrates degradation by enhancing proteasome activity and produces sharp reduction in the chain-trimming rate on ubiquitin chains of proteins associated with proteasomes through Usp14. Thus, inhibition of Usp14 has been proposed as a therapeutic strategy to accelerate proteasomal function in neurodegenerative diseases that are associated with the accumulation of misfolded and aggregated proteins such as tau

in Alzheimer's Disease and TDP-43 in Amyotropic lateral sclerosis (Lee, Lee et al. 2010).

3.2 Crosstalk between protein degradation and cilia

In recent years, the interest in understanding the correlation between primary cilia and degradative pathways has been exponentially growing, also because it has been found an intriguing crosstalk between ciliary growth and proteasome/autophagy activity. Changes in length and formation of cilia have been directly related to changes in functioning of degradative mechanisms. However, the regulatory role of degradation processes for the control of primary cilia is much more complex than it would appear, and for this reason there have been several conflicting reports. Indeed, blockage of autophagic or proteasomal pathways can either increase or decrease ciliary length. Part of these opposite effects are due to the fact that autophagy and proteasome can degrade proteins that contribute to ciliary growth (e.g. IFT20 essential for ciliogenesis) as well as regulatory proteins that inhibit ciliogenesis (e.g. Ofd1 associated to centriolar satellites) (Pampliega and Cuervo 2016, Shearer and Saunders 2016). The additional fascinating demonstrations that ciliopathy proteins can regulate signaling cascades by modulating proteolytic degradation (Liu, Tsai et al. 2014), together with the finding of proteasomal and autophagic components in proximity or into the primary cilia (Dikic 2017), have emphasized the interest for the relationship between ciliary proteins and degradation pathways.

3.2.1 Proteasome and cilia

The presence of functional proteins in appropriate quantities, maintained through balanced protein synthesis and degradation pathways, is necessary for viability of the cell. There are now various evidences that the primary cilium has a role in regulating protein homeostasis by influencing the ubiquitin-proteasome system (Malicki and Johnson 2017).

In the last years, interactions of different ciliary proteins with proteasomal components

were identified indicating a possible link between cilia and the proteasome. In line with this observation, we also demonstrated that cilioproteins play a crucial role in the regulation of paracrine signal transduction interacting directly with different proteasomal components and coordinating proteolytic degradation of signaling mediators (Liu, Tsai et al. 2014). Indeed, Ofd1 controls the composition of the proteasome components and its loss leads to a reduced proteasomal activity affecting the stability of proteins involved in Hh signaling (Liu, Tsai et al. 2014). The absence of other cilioproteins, such as Bbs4 and Bbs7, implicated in two forms of Bardet-Bield syndrome, is also associated with a decreased activity of the proteasome that leads to dysregulation of different cilia-related signaling pathways (Gerdes, Liu et al. 2007, Gascue, Tan et al. 2012, Liu, Tsai et al. 2014). The effect of these ciliary proteins has been referred to the proteasome localized at the centrosome, but only recently it has been demonstrated the real existence of a cilia-regulated proteasome. Three components of the 19S proteasomal subunit (Psmd2, Psmd3, and Psmd4, respectively) have been detected at the basal body of MEF cilia, and one component of the 20S proteasomal subunit (Psma5) along the entire cilium, thus supporting the likelihood of a ciliary involvement in proteasome assembly and/or function (Gerhardt, Lier et al. 2015). Moreover, the transition zone protein Rpgrip1l binds the ciliary regulatory proteasomal subunit Psmd2, and its depletion results in reduced proteasomal activity, specifically and exclusively at the ciliary base (Gerhardt, Lier et al. 2015), confirming the existence of a ciliary localization for the proteasome. In summary, some ciliary genes, whose mutations give rise to very severe ciliopathies, encode ciliary proteins that regulate proteasomal activity. Considering that the proteasome is involved in the formation, maintenance and function of several organs and structures of the human body, it is possible that proteasome dysfunction contributes to the manifestation of ciliopathies, and potentially, its decreased activity may influence the severity of the phenotypes observed in ciliopathies. Overall, all these discoveries suggest that the enhancement of proteasomal function might benefit ciliopathy patients. Additionally, using

a system biology approach, we also found that proteasomal components represent the largest community of "cilia/centrosome complex interactome (CCCI)" (Amato, Morleo et al. 2014), supporting that the close association of UPS with primary cilia may be functionally relevant.

Interestingly, protein degradation via UPS is also essential for regulating ciliogenesis, cilia disassembly and maintenance of cilia length during cell cycle. As said before, the primary cilium protrudes directly from the distal end of the mother centriole. In this context, UPS regulates the amount and availability of players involved in cilia formation localized to centrioles or close to these organelles. For examples, ciliogenesis is inhibited by Aurora A (AurA), a protein belonging to a repressor complex of cilia formation, which is bound and activated by the keratin-binding protein trichoplein at the centriole, preventing axoneme extension. The ubiquitin-proteasome system results indispensable to initiate ciliogenesis by removing trichoplein from the mother centrioles, thus causing inactivation of centriolar AurA, which promotes ciliogenesis. Therefore, degradation of polyubiquitinated trichoplein results in disassembly of the repressor complex, critical for the initiation of axoneme extension (Kasahara, Kawakami et al. 2014). Moreover, the E3 ubiquitin ligase Mindbomb 1 (MIB1), a new component of centriolar satellites, ubiquitinates Cep131 (also known as AZI1) and PCM1, and suppresses primary cilium formation (Villumsen, Danielsen et al. 2013). The E3 Ub ligase von Hippel-Lindau tumor suppressor (VHL) localizes to primary cilia and directly ubiquitinates Hypoxia-Inducible Factor-1α (HIF-1α), a transcriptional regulator of AurA, thus playing an indirect role in regulating ciliogenesis (Patil, Pabla et al. 2013). The activity of E3 ubiquitin ligase Anaphase-promoting complex (APC) controls the proper length of preformed cilia as well as the timely resorption of the cilium after serum induction. It also ubiquitinases Nek1, a ciliary kinase, and stimulate its proteolysis for regulating the stability of axonemal microtubules (Wang, Wu et al. 2014). Additionally, NDE1, a suppressor of the later stages of cilium formation, is also ubiquitinated and degraded through the UPS increasing ciliary length (Kim, Zaghloul et al.

2011, Maskey, Marlin et al. 2015). Altogether these results indicate that ubiquitination occurs during both the initiation and elongation stages of ciliogenesis, and it is important for controlling of cilia length.

Apart from the evident role of ubiquitination in the maintenance of centriolar satellites and cilium assembly, protein deubiquitination is also involved in ciliogenesis, correctly regulating protein levels. For example, cylindromatosis tumor suppressor gene (*CYLD*) encodes a deubiquitinating enzyme, and its mutation results in defects of cilium formation (Eguether, Ermolaeva et al. 2014). Ubiquitin-specific protease 8 (USP8) functions as a deubiquitinase of HIF1α by counteracting the VHL-mediated ubiquitination, and maintains basal expression levels of HIF1α, critical for ciliogenesis mediated by endosome trafficking (Eguether, Ermolaeva et al. 2014). Another study shows that Ubiquitin specific peptidase 21 (USP21) localizes strongly to the centrosome and microtubules, and its depletion greatly reduces cilia formation in human Retinal pigment epithelial (RPE) cells (Urbe, Liu et al. 2012). In summary, UPS results necessary to maintain the right balance of proteins involved in controlling primary cilia formation, length and function, by regulating both ubiquitination and deubiquitination mechanisms.

Based on these results, we can assume that ubiquitination, deubiquitination, and proteasomal degradation of key regulators of ciliogenesis represent mechanisms for controlling cilia formation, maintenance and length, and consequently all the sensory function played from primary cilia. To date the biological significance of the changes in cilia length during cellular processes it is not completely clear, but it is possible that primary cilia modify their sensing ability when they change their length, and, by doing so, subsequently sensitize and adapt cells to different metabolic, pathologic or physiologic necessities.

In conclusion, all these studies demonstrate that cilia and degradative pathways reciprocally affect each other. It seems that UPS is activated or inhibited to control primary cilia length both positively and negatively depending on the context. This highlights the

need for a fine-tune regulation of this processes to assure rapid adaptation of ciliary length to the cellular requirements. On the basis of the existing interplay across ubiquitin mediated degradation pathways, primary cilia, and ciliopathies, both academic laboratories and pharmaceutical companies are developing compounds that target specific components of this degradative system. Useful drugs have been already developed for clinical applications, but further studies on the crosstalk between cilia and proteasomal pathway are required thus continuing the production of conventional inhibitors or activators of specific enzymes, as well as supplying drugs able to direct the ubiquitin system to target, destroy, and thereby downregulate any specific protein. The result from these studies will lead to a better understanding of the pathophysiological implications derived from the perturbation of this interplay, and may lead to the identification of modulators capable to influence ciliary signaling pathways in order to improve the phenotype observed in ciliopathies.

MATERIALS AND METHODS

1. Cell culture

Usp14$^{+/+}$ and *Usp14*$^{-/-}$ MEFs (Mouse Embryonic Fibroblasts) were a gift provided by Dr. Scott Wilson and were previously described (Wilson, Bhattacharyya et al. 2002). MEFs were cultured in Dulbecco's Modified Eagle Medium (Gibco) containing 10% fetal bovine serum (FBS), 1% l-glutamine (Gibco), 1% sodium pyruvate (Gibco), and 1% antibiotics (penicillin/streptomycin) (Gibco) at 37^{o}C and 5% CO_2. HEK-293 or HEK- 293-FT cells and human dermal fibroblasts were grown in DMEM (Invitrogen) containing 10% FBS (Invitrogen) and 2 mM L-glutamine (Invitrogen). All cells were splitted upon reaching of confluence, by rinsing the monolayer twice with sterile filtered Phosphate-Buffered Saline (PBS, Gibco) and exposing cells to 0.25% Trypsin-EDTA for 2-3 minutes. Detached cells were centrifuged to eliminate Trypsin from the media and then plated at a density of 10^4 cells/cm2. To induce ciliogenesis, confluent MEFs were serum starved with medium containing 0.5% FBS for ≥30h.

2. Cell treatments

Shh, SAG, IU1 and MG132 treatments in MEFs cells were performed in DMEM Glucose Free (Gibco) supplemented with 0,5% FBS (Life Technologies). Hh signaling activation was performed by treatment with either Shh-N recombinant protein at a final concentration of 100ng/ml (R & D Systems (464-SH)) or SAG 200nM (Millipore) for 24h. IU1 (Cayman Chemical) was dissolved in DMSO at final concentration of 100mM and stored at -20°C. IU1 treatment was carried out at a final concentration of 40 μM for 6 or 24h. MG132 (Calbiochem) was dissolved in DMSO at a concentration of 10 mM and stored at -20°C. MG132. Drug treatment with MG132 was carried out at a final concentration of 30 μM for 6h, while SFN (Sigma-Aldrich) was used at a final concentration of 10 μM for 6h.

3. *In vitro* differentiation of ES cell–derived neurons

The Ofd1-deficient E14Tg2A.4 KOES line was obtained from BayGenomics. Both WT and Ofd1 KOESs were maintained in an undifferentiated state by culture on a monolayer of mitomycin C–inactivated fibroblasts in the presence of leukemia-inhibiting factor (LIF). To induce neural differentiation, we followed previously described protocols (Fico, Manganelli et al. 2008). Briefly, 48h after ES cells were seeded on gelatin-coated plates, they were dissociated and plated on gelatin-coated plates at 1,000 cells/cm^2 on day 0 (T0). The culture medium for neuronal differentiation (serum-free KnockOut Serum Replacement–supplemented medium; Invitrogen) contained knockout DMEM supplemented with 15% KSR (Invitrogen), 2 mM L-glutamine, 100 U/ml penicillin-streptomycin, and 0.1 mM β-mercaptoethanol and was replaced daily during the differentiation process.

4. Constructs and Transfections

Full-length murine Usp14 were tagged at the C terminus with a 3xFLAG tag by cloning it into the 3xFLAG-pCMV vector. The generated plasmid was verified by sequencing. pEGFP-N3-Kif7 construct was a gift from Kathrin Anderson's lab. pCDNA-HA-Ubiquitin construct was a gift provided by Di Marcotullio's lab.

The same number of MEFs were transfected in suspension with TransIT®-LT1 Transfection Reagent (Mirus) with a 3:1 ratio of TransIT-LT1 Reagent to DNA and following manufacture's instruction. Cells were starved for 30h, treated with Shh/SAG for 24h and collected 48h after transfection in two samples for RNA extraction and Western Blot analysis, respectively.

FuGene6 Transfection Reagent (Roche) was used for transfection of expression constructs, shRNA-expressing plasmids, in HEK293 cells. Then cells were cultured for 72h.

5. RNAi

To silence *Usp14,* MEF cells were transfected using siRNAs ON-TARGET plus smart pool against the murine *Usp14* and ON-TARGET Non-Targeting (Darmachon) as control to a final concentration of 100 nM. The transfection reagent was INTERFERIN (409–10, Polyplus). Equal numbers of MEFs transfected with siRNAs against murine *Usp14* and Non-Targeting RNA were plated. After 48h cells reached the confluence and were incubated in medium containing 0.5% FBS to induce ciliogenesis. 24h before harvesting, MEFs were treated with Shh-N or SAG to induce Hedgehog pathway activation. Silenced cells were used for RNA extraction, Western Blot and IF analyses 96h after transfections.

6. RT-PCR and qReal-Time PCR

Total RNA extracted from MEF cells, was isolated by using RNeasy Mini Kit (Qiagen) according to the manufacturer's instructions. During the extraction protocol, RNAs were digested with DNaseI (Qiagen) to remove DNA contaminating. Total RNA was then reverse-transcribed into cDNA by QuantiTect Reverse Transcription Kit (Qiagen) with random hexamers oligo. For quantitative real time PCR analysis (qRT-PCR), cDNAs were analysed with Roche Light Cycler 480 system using a LigthCycler 480 SYBR Green I Master (Roche). The final concentration of primers was of 0.8 μM. The ΔCT method was used for statistical analysis to determine gene expression levels. All experiments contained three technical replicates and were performed at least three times. The *Hprt* transcript was used as endogenous reference. The results are shown as means ± SEM of three independent biological replicates.

7. Western blot (WB) analysis

MEFs were lysed in RIPA buffer (Tris-HCl 50mM, pH 8, NaCl 150 mM, EDTA 1mM, NP-40 1%, SDS 0,1%, $C_{24}H_{39}NaO_4$ 0,5%) containing protease inhibitors (Sigma-Aldrich), phosphatase inhibitors (PhosSTOP, Roche) and proteasome inhibitor (Calbiochem), and

sonicated at appropriate intervals, followed by centrifugation at 4°C for 15 minutes. Protein concentrations in all lysates were measured using Pierce™ BCA Protein Assay Kit (Thermo Fisher) and a spectrophotometer reader (Biorad) at a wavelength of 595 nm. Protein samples were separated by 5% SDS-PAGE or 4-15% Precast Protein gel (Bio-Rad), and transferred to ImmunoBlot Polyvinylidene difluoride (PVDF) membranes (Millipore, US, Immobilon-P). Membranes were blocked in TBS containing 5% Non-Fat Dry Milk (Cell Signaling) and incubated with the following commercial primary antibodies:

Ab	**Company**	**Catalog number**	**Dilution**
anti-β-tubulin	Sigma	T 4026	1:5000
anti-GAPDH	Santa Cruz Biotechnology Inc.	sc-32233	1:10000
anti- HSP90	Cell Signaling	4874S	1:1000
anti-GLI2	R&D Systems	AF3635	1:200
anti-GLI3	R&D Systems	AF3690	1:400
anti- Flag	Sigma-Aldrich	F3165	1:1000
anti- Sp1	Santa Cruz Biotechnology Inc.	sc-14027	1:500
anti-Kif7	Abcam	ab95884	1:1000
anti- Usp14	Bethyl Laboratories	A300-920A	1:3000
anti-Ubiquitin	Santa Cruz Biotechnology Inc	Sc-8017	1:500
anti-Ubiquitin-Lys48-Specific	Merck Millipore	05-1307	1:3000
anti-GFP	Abcam	ab290	1:1000
anti-SUFU	Santa Cruz Biotechnology Inc	sc-10934	1:500
anti- mmOFD1	Antisera against a portion of murine OFD1 NM_177429 aa 461-884		1:200
anti- hsOFD1	antisera against human full-length OFD1 NM_003611		1:1000
anti-RPN10	Santa Cruz Biotechnology Inc	sc-10934	1:500
anti-20S	Novus	NB600-1016	1:400
anti-PA28γ	Novus	NBP1-54587	1:400

anti-RPT2	Boston Biochem	AP-107	1:1000
anti-RPT6	Enzo Life Sciences	BML-PW9265	1:400
anti-PA28γ	Novus	NBP1-54587	1:500

Proteins of interest were detected with horseradish peroxidase-conjugated goat anti-mouse or anti-rabbit IgG antibody (1:3000, GE Healthcare) and rabbit anti-goat IgG antibody (1:3000, Calbiochem), visualized with the Luminata Crescendo substrate (Millipore) or the Super Signal West Femto substrate (Thermo Scientific), according to the manufacturer's protocol. WB images were acquired using the Chemidoc-lt imaging system (UVP) and densitometric analysis was performed with ImageJ software. WB studies were performed at least in triplicate and representative images are shown.

8. Nuclear-Cytoplasmic Extraction

Nuclear-Cytoplasmic extractions were performed on ice with freshly harvested cells. Nuclear and Cytoplasmic fractions from MEF cells were isolated using NE-PER Nuclear and Cytoplasmic Extraction Kit (Thermo Scientific) according to the manufacturer's instructions. Each fraction for all samples was quantified before taking samples for gel electrophoresis to ensure that equal amounts of each fraction were loaded on the gel.

9. Affinity purification of proteasome complex

The 26S proteasome complex was purified following a previously described protocol (Wang, Chen et al. 2007) with modifications. Briefly, HEK-293-FT cells expressing stable HTBH-tagged hRPN11 (a gift from Lan Huang, University of California, Irvine, California, USA) were transfected with either pSuper control plasmid or pSuperOFD1 to knock down OFD1 expression. Seventy-two hours after transfection, cells were lysed in buffer A (100 mM NaCl, 50 mM Tris-HCl [pH 7.5], 10% glycerol, 2 mM ATP, 1 mM DTT, and 5 mM MgCl2) with 1× proteasome inhibitor (Roche). Lysates were centrifuged at 4°C for 15

minutes to remove cell debris. To purify proteasomes, an aliquot of the supernatant was incubated with streptavidin beads at 4°C overnight to precipitate HTBH-RPN11. The beads were then washed with buffer A three times, followed by one washing with TEB buffer (50 mM Tris-HCl, pH 7.5 and 10% glycerol). Finally, the beads were incubated in TEB buffer containing 1% TEV protease at 30°C for 1h, before SDS-PAGE and immunoblotting with anti-RPN11 (ab20239; Abcam).

10. Sucrose gradient sedimentation

HEK-293-FT cells were transfected and treated with nocodazole (10 μg/ml) and cytochalasin B (5 μg/ml) for 1h after 72h of transfection. To collect cytoplasmic lysates, cells were harvested in lysis buffer (1 mM HEPES [pH 7.3], 0.5% NP-40, 0.5 mM MgCl2, 0.1% β-ME, and 1× protease inhibitor), followed by centrifugation at 2,500 g for 10 minutes. After 10 mM HEPES and 5 U/ml DNase treatment for 30 minutes on ice, 1 ml of cytoplasmic lysates was layered on a discontinued sucrose gradient (70%, 50%, and 40% sucrose in the buffer containing 10 mM PIPES [pH 7.2], 0.1% NP-40, and 0.1% β-ME) and centrifuged for 1h at 195,000 g; 2% of lysates were kept before ultracentrifugation and served as an input. After ultracentrifugation, 13 fractions were collected and analysed by immunoblotting.

11. Generation of Ofd1$^{fl/y}$ CAG-Cre-ERTM mice by tamoxifen injections

Ofd1$^{fl/+}$ females were crossed with CAG-Cre-ERTM mice, a general deletor Cre line in which Cre-ER is ubiquitously expressed after tamoxifen injection. We treated pregnant mothers with a single intraperitoneal injection of 100 μg tamoxifen/g of weight at E18.5. Tamoxifen (Sigma-Aldrich) was diluted in 10% ethanol and 90% sesame oil at a final concentration of 10 mg/ml.

12. Primary cilia biogenesis assay

Equal numbers of MEFs transfected with siRNAs against murine *Usp14* and Non-Targeting RNA were seeded into 6-well dishes containing slides. When cells were attached on the slides, they were incubated in fresh complete medium. 96h after transfection slides were transferred into 24-well dishes and cells were fixed for immunofluorescence staining. The remaining cells from 6 wells were used for western blot analysis to evaluate silencing efficiency. Cells were seeded at different confluency to ensure that the cells reached the same confluence 96h after transfection. The same analysis was performed for MEFs after treatment with DMSO or IU1.

13. Immunofluorescence and image acquisition

MEFs were plated to be confluent after 24h and treated according to protocols described above with or without serum starvation or drug treatments. Cells were fixed with PFA 4% for 10 minutes at room temperature. Cells were then washed three times with PBS and then blocked with blocking buffer (2.5% BSA + 0.2% Triton X-100 in PBS) at room temperature for 45 minutes. Cells were incubated with primary antibodies either at 4°C overnight or at room temperature for 2h, washed three times with PBS and then incubated with the appropriate secondary antibodies conjugated to Alexa Fluor 488 or Alexa Fluor 568 (Invitrogen) for 1h at room temperature. DNA was stained with Hoechst. After three washings with PBS, slides were mounted on coverslips with Mowiol.

Images were acquired using LSM700 or LSM800 High-resolution confocal microscopes (Zeiss) and examined and processed using ZEN (Zeiss), ImageJ and Photoshop (Adobe) software. To quantify cilia length and localization of proteins to the cilia, images were taken as Z-stacks and rendered as maximum intensity projections. Fluorescence intensity at cilia was quantified by the ImageJ software and by measuring the sum of intensities in compressed z stacks images. The average intensities along the axoneme were measured and plotted against cilia length.

IF experiments were performed at least three times and representative images were shown. For analysis of IF data more than 100 cells were counted for each experiment. The significance of the results was calculated by Student's t-test and reported as p-value.

HEK-293 cells cultured on coverslips were fixed in methanol, blocked in normal goat serum (1:10 in PBS containing 5% BSA), and then probed with anti-RPN10 and anti–γ-tubulin, followed by secondary antibodies Alexa Fluor 488 IgG and Alexa Fluor 568 IgG. Finally, nuclei were visualized with Hoechst 33258 (Sigma-Aldrich). Images were captured with a Zeiss LSM 710 confocal microscope and analyzed with ImageJ software.

14. Ubiquitination experiments and IP

For Ubiquitination experiments, MEFs transfected with both the pEGF-Kif7 and HA-Ubiquitin plasmids were starved for 30h, treated with MG132 and DMSO or IU1 for 6h and collected 48h after transfection for IP experiments. For IP, approximately 1 mg of whole-cell was incubated with anti-OFD1, anti-Flag, or anti-GFP at 4°C overnight, followed by incubation with protein G–coupled agarose beads (Santa Cruz Biotechnology Inc.) at 4°C for 1 hour, or directly with anti-Flag M2 beads (A2220 Sigma-Aldrich). The beads were collected and washed with IP buffer (10% glycerol, 50 mM Tris-HCl [pH 7.5], 2.5 mM MgCl2, 1% NP40, and 200 mM NaCl). Proteins conjugated with the beads were then denatured and separated from the beads by boiling at 95°C to 100°C for 5 minutes before processing for immunoblotting. Proteins were resolved by SDS-PAGE, transferred onto PVDF membrane, and probed with the indicated antibodies.

15. Statistical analysis

In ciliary counts experiments the likelihood ratio test for Negative Binomial generalized linear models was applied. In all the remaining experiments, the statistical significance between two groups was evaluated by Student's t-test, $p<0.05$ was considered significant. Quantitative data are presented as the mean ± SEM (Standard Error of the Mean).

Results

1. Loss of *Ofd1* causes accumulation of Hh signaling mediators

In vertebrates, the cilium and the basal body are key components of signal transduction, and different phenotypes of ciliopathy patients have been attributed to defective paracrine signaling (Hildebrandt, Benzing et al. 2011), including polydactyly and neural tube defects due to defective Hh signaling (Eggenschwiler and Anderson 2007).

The increasing association of ciliary and basal body proteins with proteasomal functions; the involvement of proteasomal degradation in Hh signaling cascades; and the presence of proteasomal components to the primary cilium, led us to ask whether the ubiquitin-proteasome system could be a mechanism that contributes to the Hh signaling defects seen in OFD1 syndrome. We thus considered the possibility that loss of the basal body protein Ofd1 leads to changes in the stability of signaling mediators.

We examined the Hedgehog signaling, an established cilium-dependent signaling pathway (Eggenschwiler and Anderson 2007) which plays a critical role in determining proper embryonic patterning and cell fate determination in the CNS. We developed an *in vitro* neural differentiation model, in which embryonic wild type murine stem cells (WT ESs) and *Ofd1*-knockout murine embryonic stem cells (KO ESs) were cultured to generate neural progenitors (Figure 15). This model recapitulates the multi-step process of neural development in embryos (Fico, Manganelli et al. 2008). We used this method to differentiate ES cells in neurons and glial cells for studying the impact of *Ofd1* inhibition in proteasomal degradation of Hh signaling components.

ES cells were maintained in an undifferentiated state by culturing them in the presence of leukemia-inhibiting factor (LIF). To induce neural differentiation the culture medium for neuronal differentiation was daily replaced during the whole process. From day 8 (T8) to day12 (T12) of differentiation it is possible to observe the emergence of a rosette

conformation typical of neuronal precursors and, as time goes by, the presence of cells with neuronal morphology.

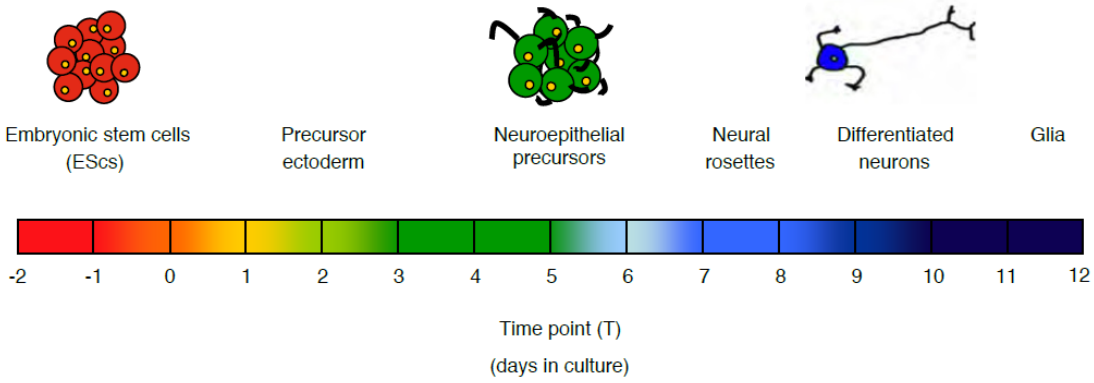

Figure 15. A model that recapitulates the multi-step process of neural development in embryos

KO ESs are male murine cells containing a gene trap mutation in *Ofd1*. As *Ofd1* is located on the X chromosome, *Ofd1* KO ESs are hemizygous for *Ofd1* and do not produce the protein (Singla and Reiter 2006).

To establish if the stability of Hh signaling mediators is altered upon depletion of *Ofd1*, we performed WB analysis and compared the total protein lysates obtained from *Ofd1* WT neurons differentiated from WT ESs to the total protein lysates obtained from *Ofd1* KO differentiated neurons derived from KO ESs. We found a significant increase in protein levels of Gli2FL and Sufu at the T8 time point in *Ofd1*-depleted neurons (Figure 16A). We also analyzed total lysates from *Ofd1*$^{\Delta 4–5/y}$ hemizygous male mouse embryos and WT littermates and we observed increased levels of Gli2FL and Sufu in *Ofd1*$^{\Delta 4–5/y}$ embryos compared to WT embryos (Figure 16B). In addition, also Gli3FL increased both in *Ofd1* KO neurons (Figure 16A) and in *Ofd1*$^{\Delta 4–5/y}$ mutant embryos (Figure 16B), with a concomitant decrease in Gli3R levels (Figure 16A and B), suggesting an involvement of Ofd1 in the regulation of the Hh pathway.

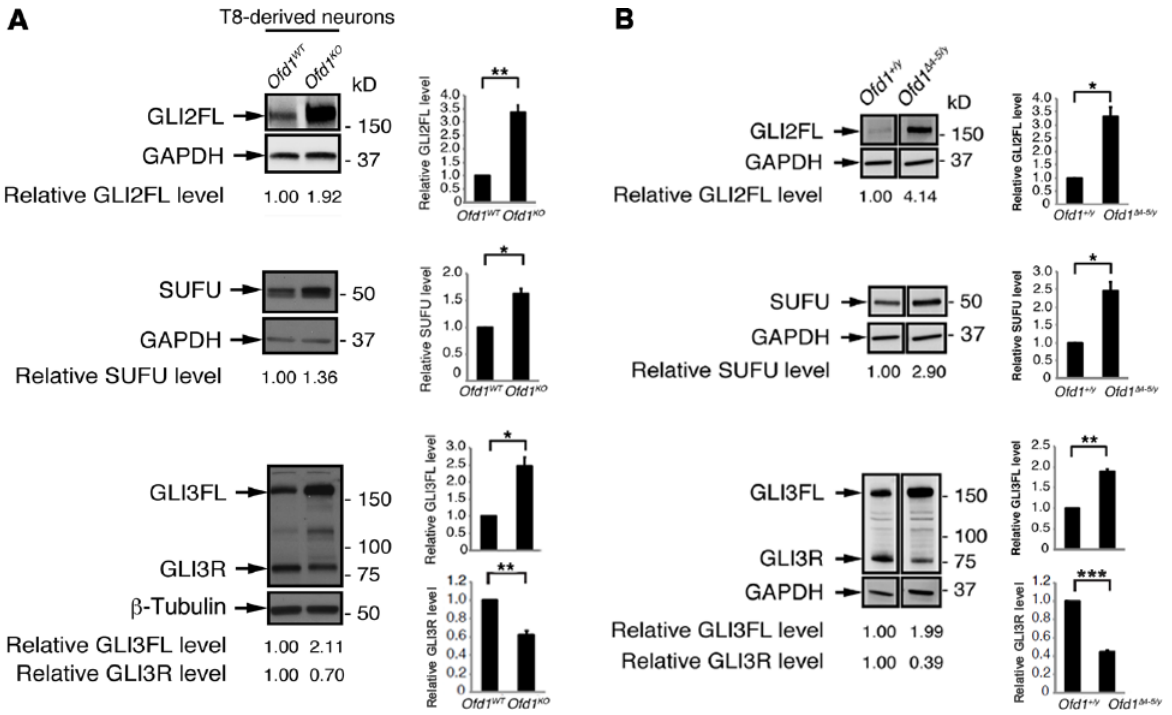

Figure 16. Accumulation of Shh signaling mediators upon *Ofd1* depletion
(A) Immunoblots show accumulation of Gli2FL, Gli3FL, and Sufu as well as reduction of Gli3R in T8-derived Ofd1^{KO} neurons. (B) At E10.5, accumulation of Gli2FL, Gli3FL, and Sufu as well as reduction of Gli3R were detected in protein lysates from *Ofd1*$^{\Delta 4-5/y}$ mice. *Ofd1*$^{+/y}$ mice are used as controls. Samples in each panel in B were run on the same gel but were noncontiguous. Bar graphs showing the SEM are plotted adjacent to each blot. *P < 0.05; **P < 0.01

Therefore, the perturbation of the Ofd1 ciliopathy protein alters the stability of Hh signaling mediators, such as Gli2, Gli3 and Sufu, demonstrating a role for Ofd1 in regulating proteasome-mediated degradation.

2. Loss of *Ofd1* selectively disrupts the UPS

Given our data on Hh mediators and the fact that the processing of components from this pathway is known to be mediated by the proteasome (Haycraft, Banizs et al. 2005), we asked whether proteasomal agonists could ameliorate the phenotypes observed in *Ofd1* depleted cells. The expression levels of three catalytic subunits of the proteasome, namely, proteasome subunit β types 5, 6, and 7 (PSMB5, PSMB6, and PSMB7, respectively), as well as the corresponding peptidase activities, increase upon treatment with sulforaphane (Kwak, Cho et al. 2007) [SFN; 1-isothiocyanato-4(R)-methylsulfinylbutane], an isothiocyanate extracted from cruciferous vegetables, rendering this compound an

attractive substrate for our studies. To address our hypothesis, we thus treated WT and T8 derived-*Ofd1* KO neurons with this drug and performed WB analysis to evaluate the amounts of Hh mediator proteins. We found that treatment with SFN reduced the protein levels of Gli2FL, Gli3FL, and Sufu when *Ofd1* is lost, in comparison with the untreated *Ofd1* KO counterpart (Figure 17A), thus rescuing the previously observed accumulation of these mediators in the absence of *Ofd1*. Consistent with the participation of the proteasome in both processing and degradation of Gli2/3, treatment with SFN also reduced Gli3R protein levels (Figure 17A).

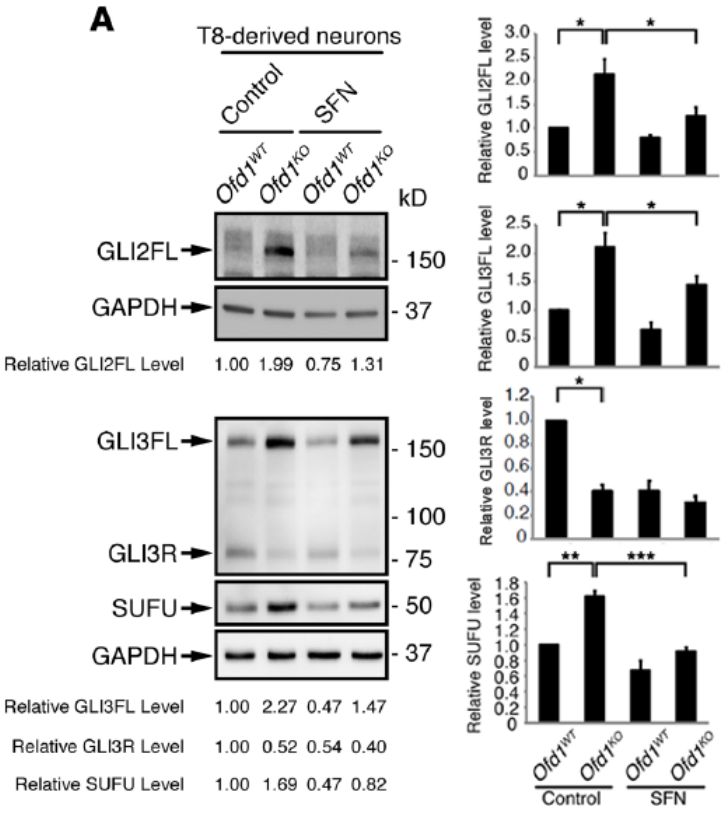

Figure 17. Disruption of proteasomal degradation caused by loss of Ofd1
(A) Treatment of proteasomal agonist SFN ameliorated the accumulation of Gli3FL, Gli2FL, and Sufu in T8-derived *Ofd1*^{KO} neurons. Bar graphs showing the SEM are plotted adjacent to each blot. *P < 0.05; **P < 0.01; ***P<0.001

Therefore, defects in proteasome-dependent processing and degradation of Gli2/3, and Sufu in *Ofd1* depleted neurons can be ameliorated by increasing the expression of the corresponding proteasomal subunits through SFN treatment as this treatment improves the ability of the cell to eliminate proteins targeted for degradation.

3. Ofd1 regulates the proteasome complex

Our observations in differentiated neurons suggested that Ofd1 is responsible for regulating proteasomal degradation of Hh mediators but the mechanism is still unclear. We therefore explored the possibility of a direct biochemical relationship between OFD1 and the proteasome.

First, an unbiased mass spectrometry screen was conducted to identify putative OFD1-interacting proteins. This experiment uncovered a spectrum of different UPS components including the regulatory proteasome ATPase subunit 6 (RPT6). To confirm this putative interaction, we performed a semiendogenous coimmunoprecipitation. We transfected 3xFlag-RPT6 expressing vector or 3xFlag empty vector in WT cells. RPT6 or OFD1 were immunoprecipitated with Flag antibody, or OFD1 antibody that recognized the endogenous protein, respectively, and the immunoblot confirmed the interaction between OFD1 and the Flag-tagged RPT6 (Figure 18A).

To probe the relevance of these interactions, we asked whether loss of *OFD1* alters the composition of the proteasome respect to its subunits and the association of deubiquitinase enzymes to the proteasome. Using a stable HEK-293 cell line expressing tagged regulatory proteasome non-ATPase subunit 11 (RPN11) (Lee, Lee et al. 2010), we suppressed *OFD1* by transfection with short hairpin RNA (shRNA)-expressing plasmids, purified 26S proteasome complexes, and analyzed the binding of some proteasomal subunits and deubiquitinases. We observed a robust reduction (60% ± 8%) of 26S-bound regulatory proteasome ATPase subunit 2 (RPT2) in *OFD1*-depleted cells compared to controls, while total RPT2 protein abundance was not affected by *OFD1* depletion (Figure 18B). We also found increased levels of USP14 deubiquitinase bound to proteasome in *OFD1* depleted cells, while the binding of the other proteasomal DUB, UCH37, did not change (Figure 18B). Therefore, the depletion of *OFD1* alters the association of some UPS components to

the proteasomal complex, such as RPT2 and USP14, demonstrating a role for OFD1 in regulating proteasome composition.

Given that the centrosome was identified as a site for concentration of the proteasome and associated regulatory proteins, we also tested the localization of some regulatory subunits. We analyzed the regulatory proteasome non-ATPase subunit 10 (RPN10) around the centrosome in *OFD1* HEK-293 depleted cells by quantifying the RPN10 signal that localized around centrosomal γ-tubulin. We performed immunofluorescence (IF) analysis and observed a 43% ± 2% reduction of pericentriolar RPN10 levels (normalized to cytoplasmic RPN10 levels) in *OFD1*-depleted cells (Figure 18C), suggesting that OFD1 is necessary for the proper localization of the centrosomal proteasome.

On the basis of these data, we also tested whether loss of *OFD1* altered the composition of RPN10, RPT2, and other proteasomal components by sucrose gradient sedimentation. Based on the commercial availability of reliable antibodies against proteasomal subunits, we found that RPN10, RPN13, RPT2, and RPT6 were enriched in γ-tubulin–enriched fractions in cells transfected with pSuper control plasmid. Depletion of *OFD1* by transfecting pSuperOFD1 plasmid to knock down OFD1 expression, resulted in a shift in the peak expression of the proteasomal subunits with a decrease in the overlap between γ-tubulin–enriched fractions and 19S subunit–enriched fractions (Figure 18D), indicating an involvement of the basal body OFD1 protein in the regulation of proteasome composition at the centrosome.

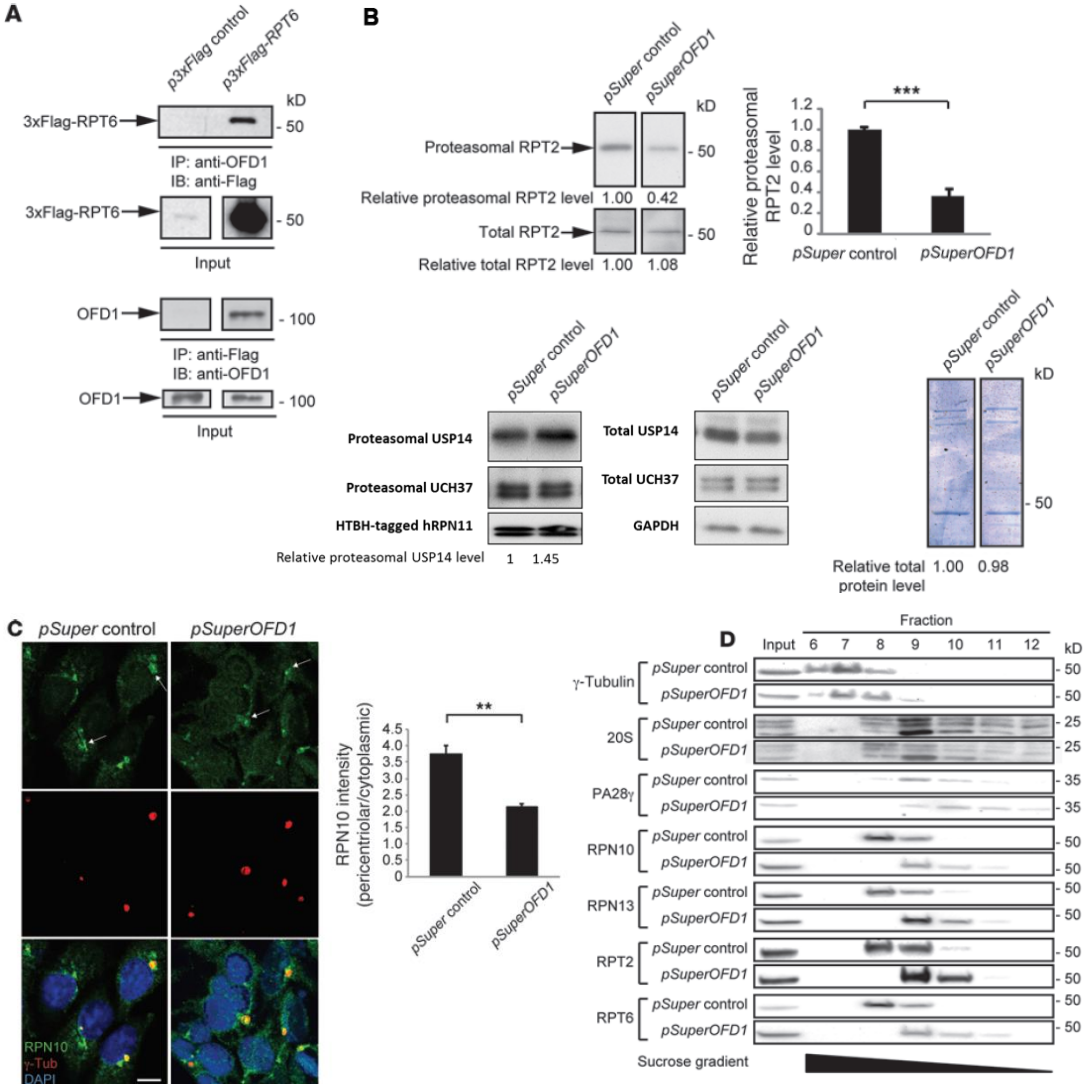

Figure 18. OFD1 interacts with proteasomal components and regulates proteasome composition
(A) Immunoblots of immunoprecipitation analysis show interaction between endogenous OFD1 and Flag-tagged RPT6. (B) Immunoblots show that suppression of *OFD1* in HEK-293 cells reduced RPT2 and increased USP14 protein levels in purified 26S proteasome. Densitometry measurements of proteasomal RPT2 (n = 3) and USP14 protein levels were plotted (n = 2), and no significant difference in total RPT2 and Usp14 abundance was detected. Coomassie blue staining were carried out as a loading control to measure the efficiency of the 26S proteasomal purification process. (C) Suppression of *OFD1* in HEK-293 cells result in the reduction of pericentriolar RPN10 levels (normalized to cytoplasmic RPN10 levels). RPN10 in green, γ-Tubulin marks centrosome (red) and DAPI for nuclei (blue). Scale bar: 10 μm. (D) HEK-293 cells transfected with pSuper control and pSuperOFD1 were subjected to sucrose gradient centrifugation. Fractions (fractions 6–12 of 13 fractions) were then analyzed by immunoblotting with antibodies against γ-tubulin and proteasomal subunits.
**P < 0.01; ***P < 0.001.

Taken together, these data suggest that OFD1 regulates the composition of the centrosomal proteasome, likely through direct biochemical interactions with specific regulatory subunits and that its depletion perturbs the cilia-associated Hedgehog signaling pathway due to impaired proteasome-mediated degradation of signaling mediators.

Our observations led us to conclude that the relationship between ciliary proteins and the proteasome is of relevant functional importance. In support of this idea, the two main proteomic studies on mammalian primary cilia, performed by different approaches (Ishikawa, Thompson et al. 2012, Mick, Rodrigues et al. 2015), show common UPS components, and in particular, one of them is Usp14, suggesting a relationship between primary cilia functions and deubiquitination process. Furthermore, given the importance of protein degradation mediated by the ubiquitin-proteasome system on cilia formation, cilia elongation and ciliary signal transduction we decided to investigate the involvement of Usp14 in cilia biology.

4. Usp14 controls ciliogenesis and cilia length

First, we hypothesized that inhibition of *Usp14* may have an effect on ciliogenesis *in vitro*. To test this hypothesis *Usp14* was silenced in cycling mouse embryonic fibroblasts (MEFs) in complete medium. The transfection efficiency of small interfering RNA targeting *Usp14* (*Usp14* siRNA) was confirmed by WB analysis of Usp14 protein levels. We observed about 80% reduction of relative Usp14 levels in *Usp14*-depleted cells respect to cells transfected with non-targeting control siRNAs (control) (Figure 19A), thus ensuring an efficient decrease of Usp14 expression.

The effects of *Usp14* silencing on ciliogenesis were determined by IF analysis 96h after siRNAs transfection. Surprisingly, despite the cells being cultured in 10% FBS medium, knockdown of *Usp14* had a strong effect on cilium formation. About 14% of silenced cells had visible cilia, labeled with an antibody that recognizes Arl13b, a protein specifically localized at primary cilia; while the cycling serum-stimulated control MEFs remained mostly unciliated, as expected for not quiescent cells, with about 4% of ciliated cells (Figure 19B). Our results indicate that the Usp14 depletion induces formation of primary cilia, demonstrating a role for Usp14 in regulating ciliogenesis.

To provide evidence that Usp14 inhibition promotes cilia formation through its deubiquitinase activity we treated WT MEFs with IU1, an inhibitor of the catalytic activity of Usp14 that reduces the trimming of ubiquitin chains and enhances the proteasome degradation activity of specific targets (Lee, Lee et al. 2010). Cells were scored for the presence of cilia under serum stimulus, at 6h and 24h of IU1 treatment: the number of ciliated cells increased over time (~15% at 6h and 20% at 24h), while DMSO treated controls remained unciliated (~5-7% at 0, 6 and 24h) (Figure 19C). Then, to verify the suppression of ubiquitin removal by IU1 we performed WB analysis which showed increased ubiquitination levels of total protein lysates after 6h of treatment, which was even more evident after 24h (Figure 19D).

Proteasomal activity seems to impact different stages of ciliogenesis, allowing for proper cilia biogenesis and elongation (Kim, Zaghloul et al. 2011, Kasahara, Kawakami et al. 2014, Maskey, Marlin et al. 2015), we thus next examined whether depletion of *Usp14* may influence axoneme elongation. *Usp14* siRNA-treated MEFs were analyzed by IF analysis 48h after serum starvation and displayed increased ciliary length compared to controls (Figure 20A). Using Arl13b as a cilia marker, we found that the length of cilia from control MEFs was ~2.8μm, whereas the length of mutant cilia was ~3.6μm in *Usp14* depleted MEFs. Thus, Usp14 mutant cilia were ~30% longer, on average, and more variable in length, compared to controls.

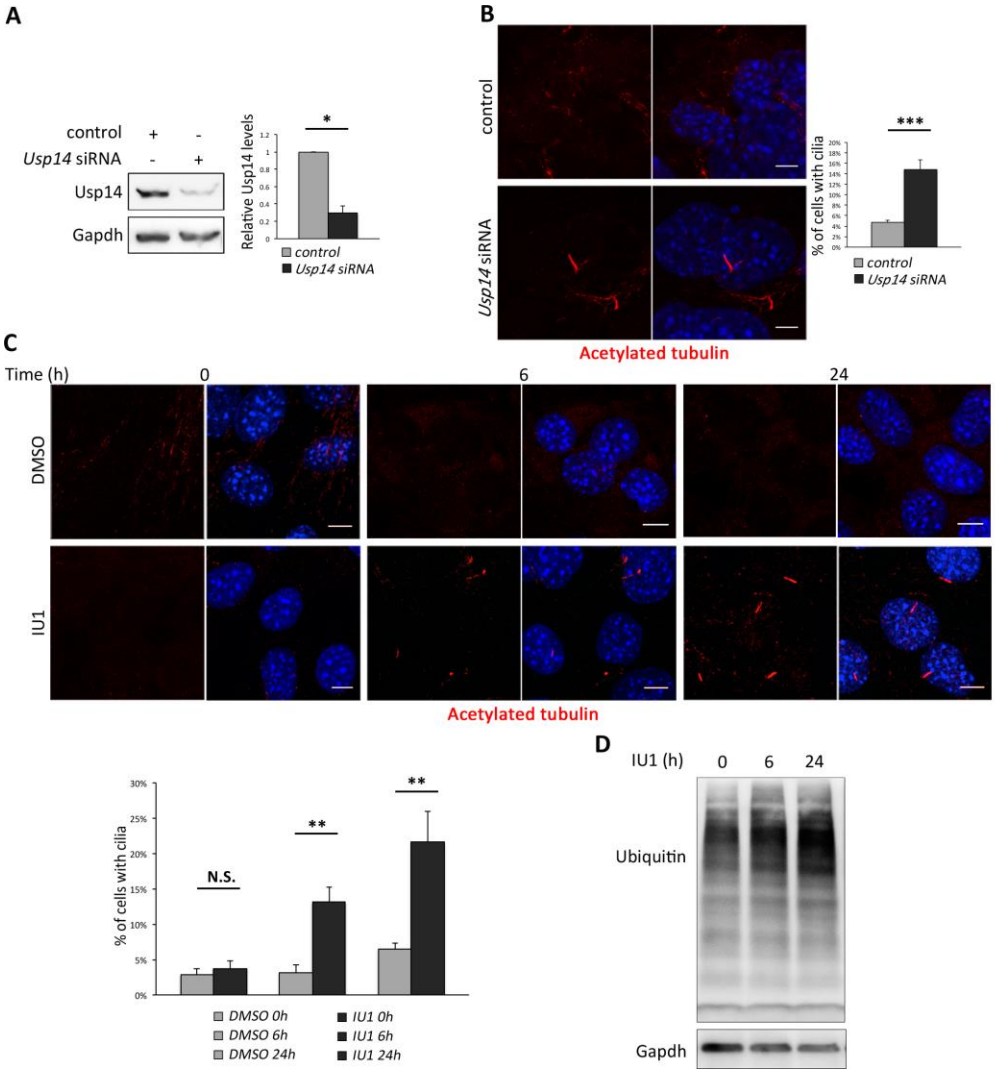

Figure 19. Usp14 controls ciliogenesis

(A) WB analysis of *Usp14*-depleted MEFs that were transfected with Usp14 specific or control siRNAs. (B) Representative confocal images of cycling MEFs in complete medium (with FBS), transfected with siRNA targeting Usp14 (*Usp14* siRNA) and non-targeting negative control siRNA (control) for 96-hours. Acetylated-α-tubulin (red) marks cilia. Hoechst (blue) labels nuclei. (C) Representative confocal images of primary cilia in cycling MEFs in complete medium (with FBS), treated with IU1 or DMSO for 0, 6 and 24h. Acetylated-α-tubulin (red) marks cilia. Hoechst (blue) labels nuclei. (D) WB analysis of the suppression of ubiquitin chain trimming by IU1 was verified at 6 and 24h.

Bar graphs showing the SEM are plotted adjacent to each panel. *P < 0.05; **P < 0.01; ***P<0.001. Scale bar = 5μm. More than 100 cells were analyzed per sample.

To supply an independent evidence, *Usp14* WT and knockout MEFs (*Usp14*$^{+/+}$ and U*sp14*$^{-/-}$, respectively) were plated in complete medium and serum-starved (0,5% FBS) for 48h to induce cilia formation. Cilia of *Usp14*$^{-/-}$ MEFs showed morphological defects similar to those observed in Usp14 silenced cells, with an average length remarkably increased compared to WT MEFs (Figure 20B). An increased ciliary length was also observed in WT MEFs that were plated in complete medium, serum-starved for 48h and treated with IU1

for 24h, suggesting that the Usp14 catalytic proteasome inhibitor activity acts also on cilia elongation (Figure 20C). Consistent with these observations, transfection of *Usp14*$^{-/-}$ MEFs with the 3xFLAG-Usp14 construct rescued the cilia length (Figure 20D), confirming that Usp14 acts as inhibitor of cilia elongation.

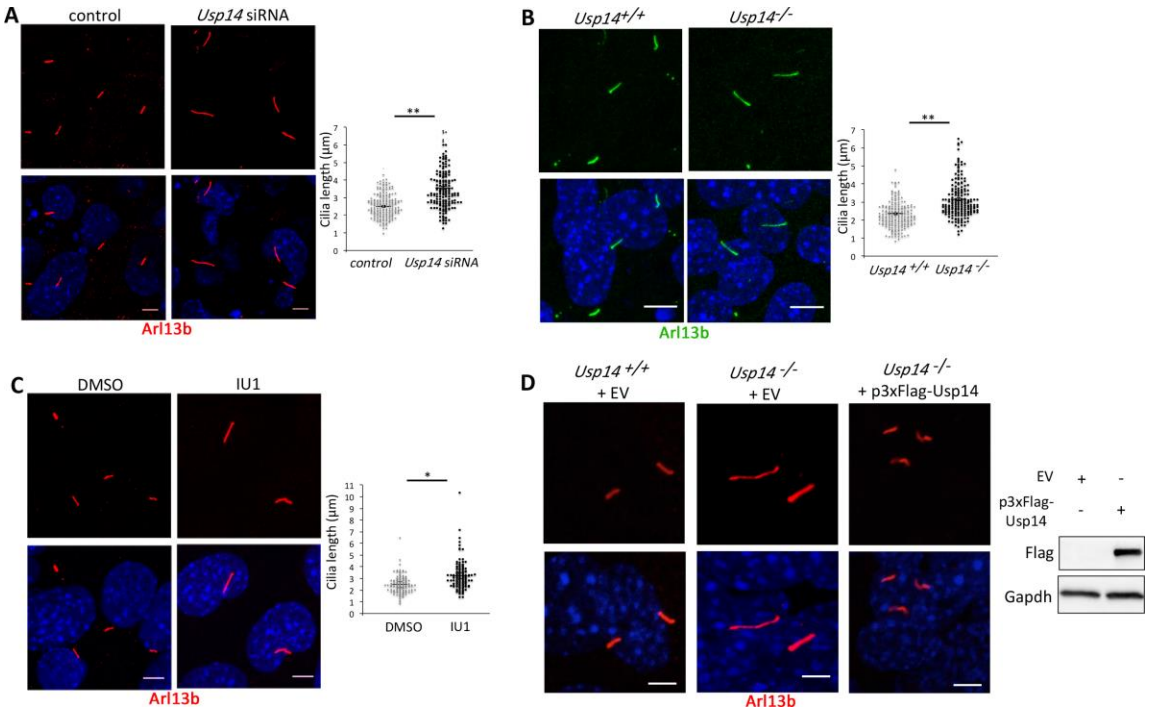

Figure 20. Usp14 controls cilia length

(A) Representative confocal images of primary cilia in Usp14-siRNA depleted and control MEFs, after 48h of serum starvation. Arl13b marks primary cilia (red) and Hoechst labels nuclei (blue). (B) Primary cilia stained with Arl13b (green) and Hoechst in blue, in 48h FBS starved WT *Usp14*$^{+/+}$ and knockout *Usp14*$^{-/-}$ MEFs. (C) Primary cilia stained with Arl13b (red) and Hoechst in blue, in 48h starved WT MEFs treated with IU1 and DMSO for 24h. (D) Primary cilia stained with Arl13b (red) and Hoechst in blue, in 48h starved WT and *Usp14*$^{-/-}$ MEFs transfected with the empty vector (EV) and *Usp14*$^{-/-}$ expressing 3xFlag-Usp145 vector (left). WB analysis of Usp14 expression in *Usp14*$^{-/-}$ MEFs transfected with either the empty vector (EV) or the 3xFlag-Usp14 construct (right).

The histograms on the right of each panel show the quantification of primary cilia length. Scale bar = 5µm. More than 100 cells analyzed per sample. Data are expressed as mean +/- SEM (n=3); *P < 0.05; **P < 0.01.

Taken together, our results reveal a role for Usp14 in the control of ciliogenesis *in vitro* and indicate that pharmacological induction of proteasomal activity positively affects cilia formation and elongation.

5. Usp14 is required for the proper localization of Hh components to primary cilia

In order to evaluate the functionality of abnormally long primary cilia observed when Usp14 is inhibited, we decided to analyze the signaling cascade of the Hh pathway which needs cilia to properly transduce its signals and activate the transcription of target genes in order to exert its physiological functions (Nozawa, Lin et al. 2013). A major event associated with active Hh signaling is the increased levels of pathway mediators along the primary cilium under Hh stimulus. In basal conditions, Gli proteins are present in low amounts at the ciliary tip where enriched after Hh signaling activation. We thus determined whether the levels/localization of Hh signaling components were affected in longer cilia of *Usp14*$^{-/-}$ embryonic fibroblasts. We assayed the ciliary localization of Gli2 and Gli3 by fluorescence staining with endogenous antibodies, whereas anti Arl13b/Acetylated tubulin antibodies were used for labeling of primary cilia. We then bordered the perimeter of each cilium and measured fluorescence intensity to quantify the total ciliary amounts of Gli2 and Gli3 in unstimulated conditions or after 24h of stimulation either with the Smoothened agonist (SAG) or the ligand Sonic Hedgehog (Shh) recombinant protein.

We rarely observed Gli2 staining in the tips of WT cilia in unstimulated conditions (NT), while the staining significantly enriched upon induction either with SAG or Shh in *Usp14*$^{-/-}$ cilia. Gli2 also shifted localization, and many *Usp14* mutant cells showed multiple sites of concentrated Gli2 under the tip and throughout the axoneme, compared to WT MEFs (Figure 21A). Moreover, the analysis of Gli3 ciliary localization revealed a pattern similar to that observed for Gli2. The fluorescence intensity of Gli3 was significantly stronger along *Usp14*$^{-/-}$ cilia compared to WT cells under Hh pathway activation (Figure 21B), suggesting that Usp14 is essential for controlling the proper localization of Gli proteins at the primary cilia. To provide independent evidence and support these findings, *Usp14* was silenced using specific siRNA directed against Usp14 in WT MEFs and the cells were stimulated with SAG for 24h. Immunofluorescence experiments showed that also the

transient silencing of *Usp14* had a strong effect on Gli2 ciliary localization compared to controls, as demonstrated by quantification of ciliary fluorescent intensity (Figure 21C). We then asked whether Usp14 inhibition promotes recruitment of Hh signaling effectors to cilia through its catalytic activity. WT MEFs were plated in complete medium, serum-starved for 48h and treated with IU1 inhibitor for 24h. Confocal analysis revealed increased ciliary fluorescence intensity for Gli2, confirming that the catalytic proteasome inhibitor activity of Usp14 acts also on the ciliary localization of Hh signaling components (Figure 21D).

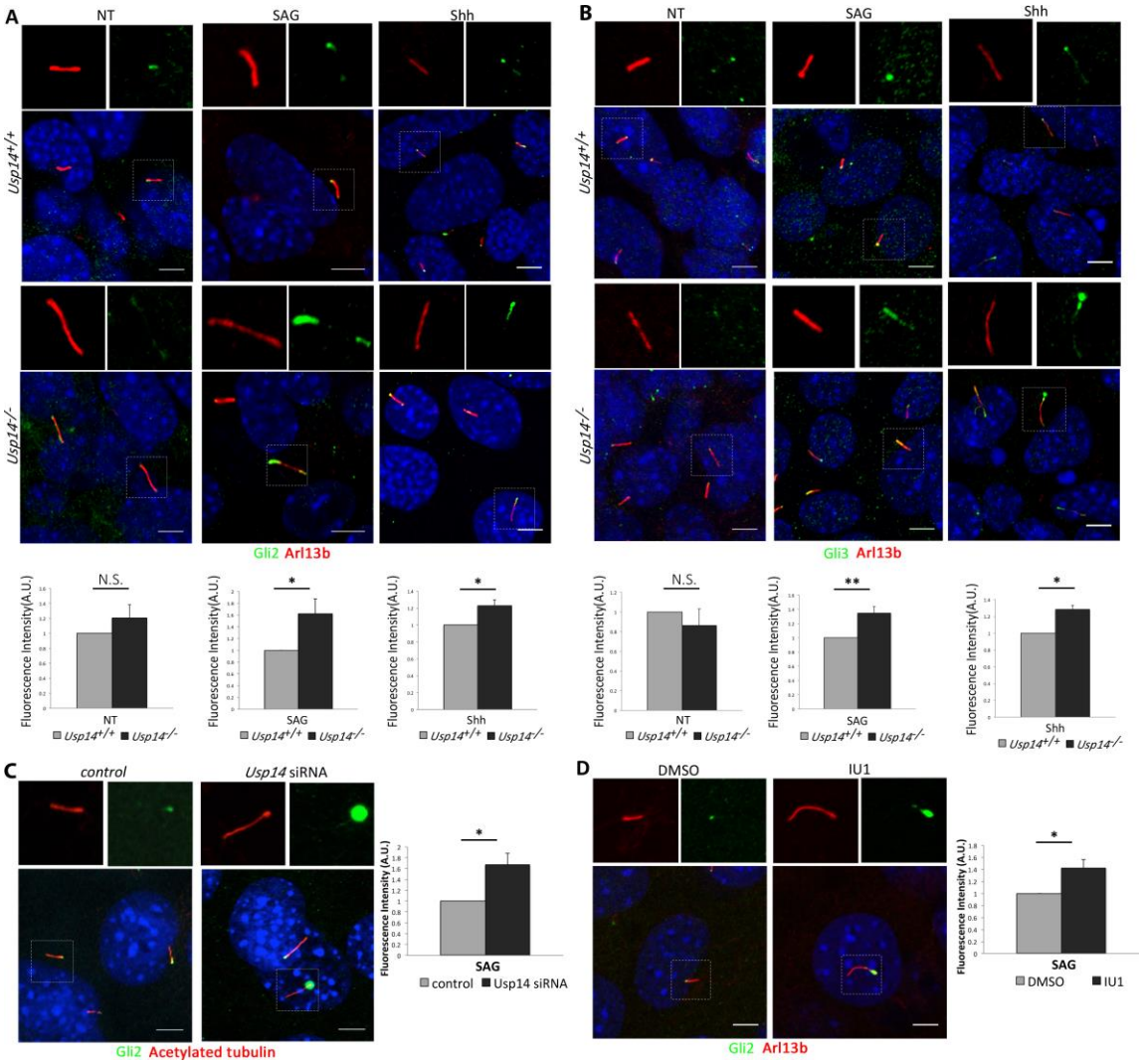

Figure 21. Usp14 controls localization of Hh mediators at cilia

(A) Representative confocal images of endogenous Gli2 (green) and (B) Gli3 (green) localization at cilia in *Usp14*$^{+/+}$ and *Usp14*$^{-/-}$ starved MEFs in basal condition (NT) and under SAG/Shh stimuli. Arl13b marks primary cilia (red) and Hoechst in blue. Gli2 and Gli3 staining were rarely observed in WT cilia in unstimulated conditions while they were significantly enriched in cilia in *Usp14*$^{-/-}$ MEFs upon induction both with SAG or Shh compared to *Usp14*$^{+/+}$ cells. The histograms show the quantification of the fluorescence intensity of ciliary Gli2 (A) and Gli3 (B), respectively, for NT, SAG and Shh stimulated MEFs. (C) IF

staining of the endogenous Gli2 (green) on *Usp14* siRNA depleted MEFs and control under SAG stimulus for 24h. Acetylated tubulin marks primary cilia (red). The histogram shows the quantification of Gli2 fluorescence intensity on cilia which increased in Usp14 depleted cells compared to controls. (D) IF staining of the endogenous Gli2 (green) on WT MEFs treated with IU1 inhibitor and DMSO for 24h, under SAG stimulus for 24h. Acetylated tubulin marks primary cilia (red). The histogram shows the quantification of Gli2 fluorescence intensity on cilia which increased in IU1 treated cells compared to controls.
Data are expressed as mean+- SEM (n=3); *P < 0.05; **P < 0.01; ***P < 0.001. Scale bar = 5μm. More than 100 cells analyzed per sample. SAG= Smoothened agonist, Shh=recombinant N-Shh

Consistent with these observations, transfection of *Usp14*$^{-/-}$ MEFs with the 3xFLAG-Usp14 construct rescued the Gli2 ciliary localization compared to cells transfected with the empty vector (Figure 22A), thus proving the specificity of action of Usp14.

On the basis of these observations, we treated *Usp14*$^{-/-}$ MEFs with MG132, a proteasome inhibitor, to establish if the observed ciliary phenotypes can be modulated by regulating proteasomal activity. We found that the MG132 treatment was able to rescue the ciliary fluorescence intensity of Gli2 and Gli3 in *Usp14*$^{-/-}$ MEFs, compared to DMSO treated cells (Figure 22B), confirming an involvement of the proteasomal activity in modulating the localization of Gli proteins at the primary cilia.

In order to demonstrate that the enhanced recruitment of Gli2/3 to cilia, consequent to inhibition of Usp14, does not depend on increased levels of total Gli proteins, we performed WB analysis and compared the total protein lysates obtained from WT and *Usp14*$^{-/-}$ MEFs. We didn't find a significant increase in protein levels of Gli2 and Gli3 in *Usp14*-/- cells, as well as in *Usp14* silenced and IU1 treated cells (Figure 22C), confirming that the enhanced ciliary localization of Hh mediators is not due to increased protein levels. Therefore, our observations suggest that the efficiency of the ciliary recruitment and transport of Hh regulatory proteins, and perhaps other cargos, is controlled by Usp14, putting forward the possibility of an 'ubiquitin-dependent' regulation.

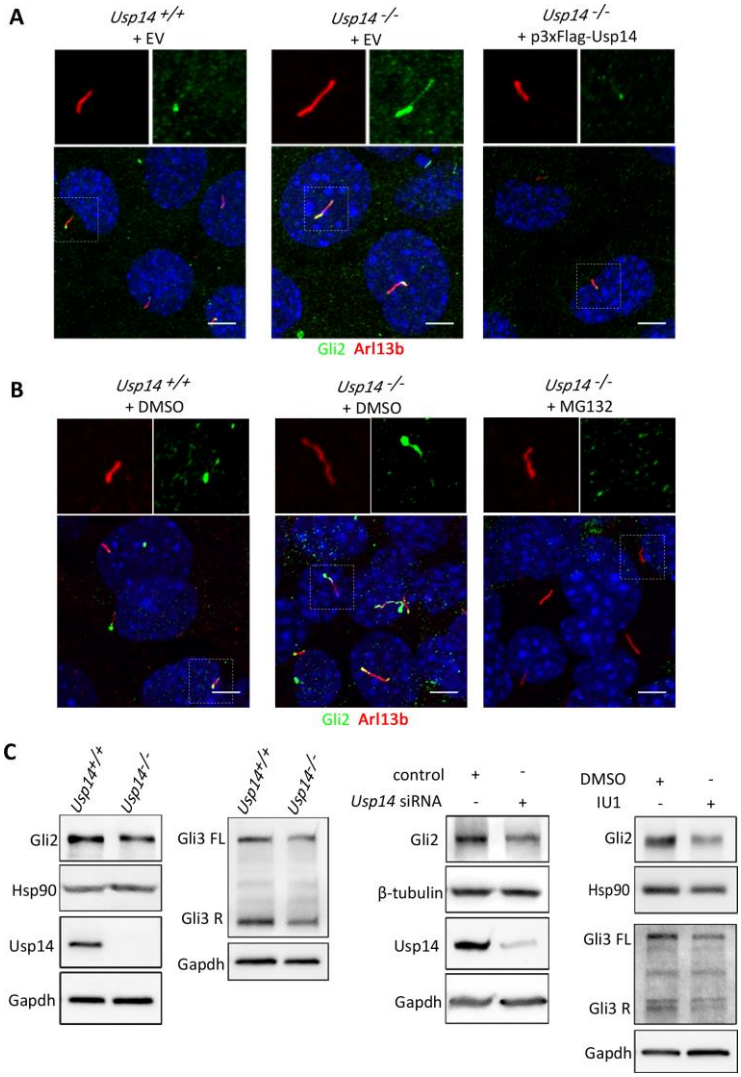

Figure 22. Proteasomal activity regulates localization of Hh mediators at cilia
(A) IF in 48h starved WT and *Usp14*$^{-/-}$ MEFs transfected with the empty vector (EV) and *Usp14*$^{-/-}$ cells transfected with the 3xFlag-Usp14 construct. Primary cilia stained with Arl13b (red), endogenous Gli2 in green and Hoechst in blue. Scale bar=5µm. (B) Representative confocal images of endogenous Gli2 (green in upper panel) and Gli3 (green in lower panel) localization at cilia in WT and Usp14$^{-/-}$ MEFs treated with DMSO or MG132 under SAG stimulus. Arl13b marks primary cilia (red) and Hoechst in blue. (C) WB analysis of Gli2 and Gli3 protein levels in *Usp14*$^{-/-}$ MEFs, *Usp14* siRNA depleted MEFs and IU1 treated cells, compared to their controls.

6. Loss of *Usp14* enhances migration of Gli2 to the nucleus

The Hh phenotype observed in *Usp14* depleted models could also be associated to defective retrograde transport. We thus evaluated whether Gli proteins normally translocated to the nucleus to activate transcription of target genes.

To analyze the nuclear migration of Gli2 we decided to employ a subcellular fractionation analysis. We plated WT MEFs at confluency. The cells then underwent serum starvation for 48h and the Hh pathway was activated by SAG treatment. Finally, the cells were

treated with IU1 in order to inhibit the catalytic activity of Usp14. At this point we separated the nuclear fractions from the cytoplasmic fractions and measured the amounts of Gli2 protein in DMSO or IU1 treated samples. IU1 treatment of SAG stimulated WT MEFs revealed an increased nuclear amount of Gli2, the main Hh transcriptional activator, compared to the amount detected in untreated cells. On the contrary, IU1 treated cells displayed lower amount of cytoplasmic Gli2 protein compared to untreated MEFs (Figure 23A, left panels). Nuclear and cytoplasmic fractions obtained were not cross-contaminated, as indicated by the absence of Gapdh and Sp1, used as controls, in nuclear and cytoplasmic extracts, respectively. The same findings were observed for SAG stimulated *Usp14* siRNA-treated and *Usp14*$^{-/-}$ MEF cells (Figure 23A, central and right panels, respectively). Conversely, transfection of 3xFLAG-Usp14 in *Usp14*$^{-/-}$ SAG stimulated MEFs resulted in increased cytoplasmic levels and reduced nuclear amounts of Gli2 compared to cells transfected with the empty vector, as the protein is retained in the cytoplasm (Figure 23B).

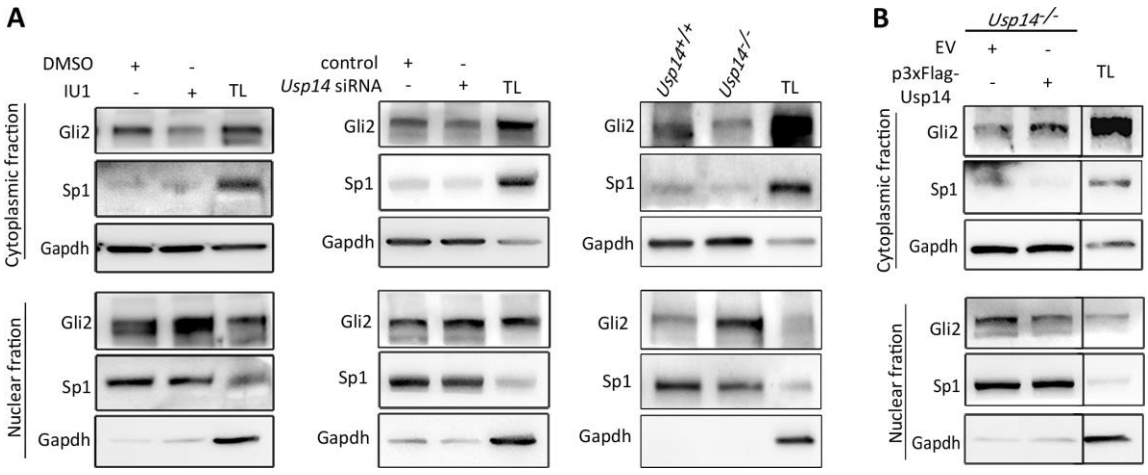

Figure 23. Usp14 controls migration of Gli2 to the nucleus
(A) WB analysis of Gli2 protein levels in cytoplasmic and nuclear fractions from IU1 or DMSO treated MEFs (left), *Usp14* siRNA depleted MEFs and control (center), and *Usp14*$^{+/+}$ and *Usp14*$^{-/-}$ MEFs lysates (right). In all conditions, nuclear amounts of Gli2 are increased, and cytoplasmic amounts of Gli2 are decreased in Usp14 depleted cells compared to the respective control. (B) WB analysis of Gli2 protein levels in cytoplasmic and nuclear fractions from *Usp14*$^{-/-}$ cells transiently transfected with the EV or p3xFlag-Usp14 for 48h. In Usp14-/- cells transfected with the p3xFlag-Usp14 construct, the Gli2 cytoplasmic levels resulted increased, while the nuclear amounts of Gli2 resulted decreased compared to cells transfected with the EV. For all experiments MEFs were stimulated with SAG for 24h. Gapdh and Sp1 were used as control for the quality of cytoplasmic and nuclear fractions. TL=total lysate.

To evaluate the functionality of the increased nuclear amounts of Gli2 observed in the absence of *Usp14*, we analyzed the expression levels of *Gli1*, the main downstream direct target gene, used as readout of the Hh pathway activation. For this purpose, we exposed starved MEF cells to both SAG and Shh stimulus for 24h and then monitored the *Gli1* transcriptional levels by quantitative Real-Time PCR (qPCR). We found that the mRNA levels of *Gli1* were significantly higher in IU1 treated cells (Figure 24A, top left panel), as well as in *Usp14*$^{-/-}$ MEFs and *Usp14* siRNA depleted cells (Figure 24A, right and bottom left panels, respectively), demonstrating that genetic or pharmacological inhibition of Usp14 resulted in enhanced activation of the Hh signaling pathway. Consistent with these observations, to demonstrate the specificity of action of Usp14, we transfected 3xFLAG-Usp14 in *Usp14*$^{-/-}$ MEFs and rescued *Gli1* mRNA expression levels compared to cells transfected with the empty vector (Figure 24B), confirming an inhibitory role of Usp14 in Hh signal transduction pathway.

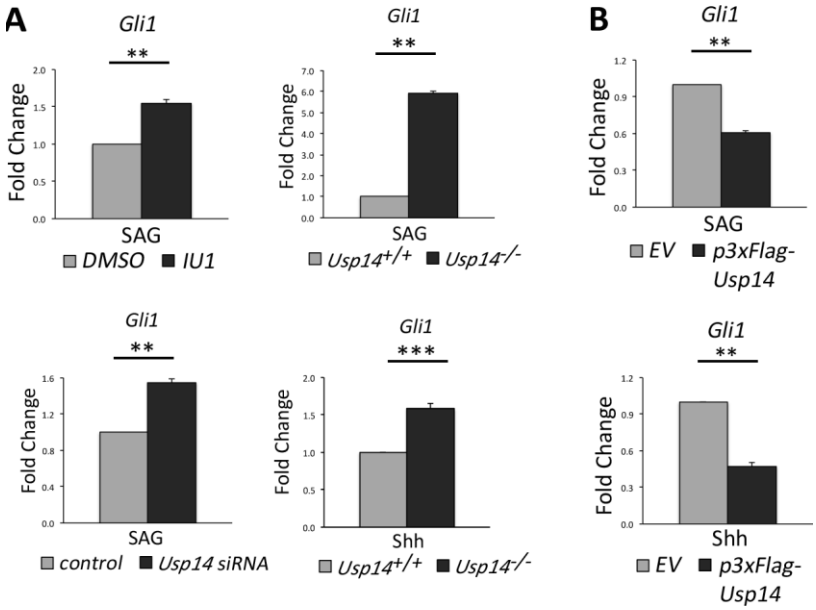

Figure 24. Usp14 controls activation of Hedgehog signaling
(A) qRT-PCR analysis. The transcriptional levels of *Gli1* are increased in IU1, *Usp14*$^{-/-}$ or *Usp14* siRNA depleted MEFs under SAG treatment compared to the corresponding control. The levels of Gli1 are also increased in *Usp14*$^{-/-}$ cells under Shh treatment (bottom right). (B) Conversely, *Gli1* transcriptional levels are decreased in *Usp14*$^{-/-}$ cells transiently transfected for 48h with the p3xFlag-Usp14 construct under SAG and Shh treatment. Data are expressed as mean+- SEM (n=3); *P < 0.05; **P < 0.01; ***P < 0.001

The above-described results reveal a critical role for Usp14 and proteasomal activity not only in the control of ciliogenesis and cilia elongation, but also in Hedgehog signaling.

On the basis of these data, at this point, we also wondered whether the suppression of Usp14's deubiquitinase activity altered the stability of specific regulator of cilia maintenance and functionality.

7. Usp14 inhibition promotes Kif7 degradation

We reasoned that Kif7, a kinesin-4 family protein, could be an interesting putative target of Usp14, since Kif7 has been shown to inhibit Hh signaling, to control localization of Hh mediators and axonemal length. In particular, depletion of *Kif7* causes a relatively mild activation of Hh signaling, induces elongation and instability of cilia, and ectopic puncta of Hh signaling components along *Kif7* mutant cilia (Ingham and McMahon 2009, He, Subramanian et al. 2014). We thus hypothesized that Usp14 may act on cilia and Hh signaling through the Kif7 protein.

In order to evaluate whether Kif7 is target of the proteasome, we treated WT MEFs with the proteasome inhibitor MG132, and analyzed whole-cell lysates by WB analysis. We observed a time dependent accumulation of Kif7 protein levels after MG132 treatment, indicating a degradation of Kif7 mediated by UPS (Figure 25A). Then we evaluated the effect of genetic and pharmacological inhibition of Usp14 on Kif7 stability. We first treated WT MEFs at different time points with IU1 and we quantified the protein amounts of Kif7 after 24h of MG132 treatment by WB analysis. In addition, we also analyzed lysates from *Usp14* silenced and KO cells. We found that protein amounts of endogenous Kif7 were dramatically decreased in IU1 treated WT cells (Figure 25B), *Usp14* siRNA-treated MEFs (Figure 25C), and *Usp14*$^{-/-}$ MEFs (Figure 25D) compared to the respective controls. Conversely, 3xFLAG-Usp14 overexpression increased Kif7 protein levels in WT MEFs compared to cells transfected with the empty vector (Figure 25E).

Given that Usp14 is a deubiquitinating enzyme we further investigated whether Usp14 may regulate the ubiquitination status of Kif7. WT MEFs were transfected with a GFP-Kif7 construct and treated either with IU1 or DMSO. The exogenous tagged Kif7 was immunoprecipitated using the GFP antibody. Then, samples from Usp14-inhibited or -not inhibited MEFs were immunoblotted with an antibody specifically recognizing the K48 ubiquitin chains that mediate the degradation of proteins by the UPS. In order to detect specifically the ubiquitination on Kif7 and not on non-covalently interacting proteins, we used a stringent condition for cell lysis, immunoprecipitation and washing (see methods). Our results indicated that inhibition of the catalytic activity of Usp14 increased the levels of ubiquitination of Kif7 as demonstrated by the stronger smear of high molecular weight observed in IU1 treated cells compared to DMSO treated controls (Figure 25F). Taken together these findings strongly suggest that Kif7 is a target of Usp14.

Furthermore, we asked whether Kif7 instability could be connected to the cellular phenotypes observed in *Usp14* depleted cells. *Usp14*$^{-/-}$ MEFs were transfected with the empty vector alone or the GFP-Kif7 plasmid for 48h, followed by nuclear and cytoplasmic fractionation to study Gli2 migration into the nucleus. Immunoblotting showed that Kif7 overexpression rescued the Gli2 nuclear accumulation observed in *Usp14* depleted conditions (Figure 25G), suggesting that Usp14 has a role in regulating Gli2 nuclear translocation trough Kif7. In addition, we also evaluated activation of the Hh pathway. We thus performed qPCR on extracts of *Usp14*$^{-/-}$ cells transfected either with pGFP-Kif7 or EV. We found a downregulation of *Gli1* expression levels in Usp14 mutated cells overexpressing tagged Kif7 (Figure 25H), confirming an action of Kif7 downstream of Usp14 and demonstrating the ability of Kif7 overexpression to rescue the iper-activation of the Hh signaling pathway caused by Usp14 inhibition.

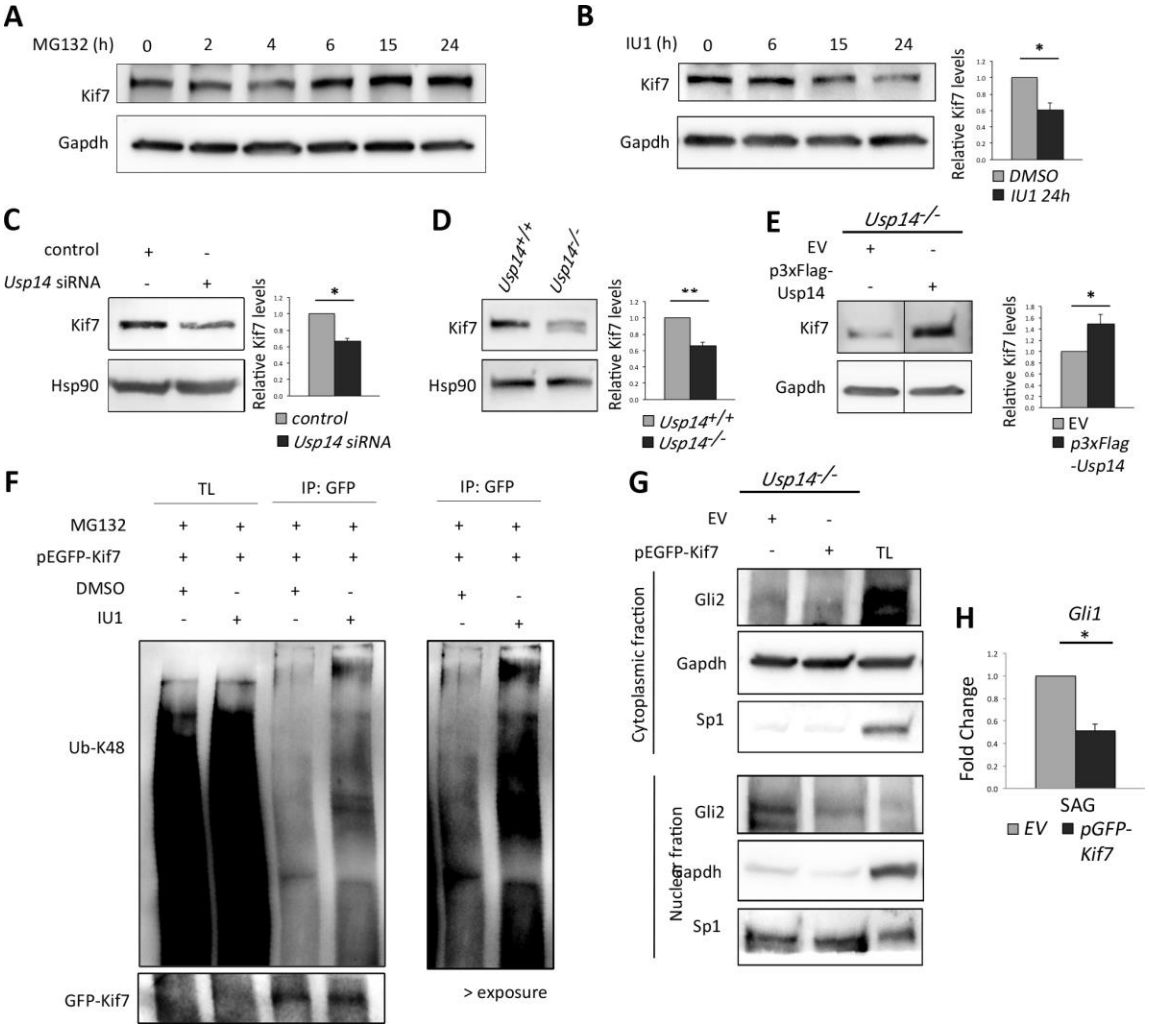

Figure 25. Usp14 inhibition promotes Kif7 degradation

(A) WB analysis of Kif7 protein levels from WT MEFs cells treated with MG132 at different time points. (B) WB analysis of Kif7 protein levels from WT MEFs cells treated with IU1 at different time points. The histogram shows quantification of band intensities for relative Kif7 levels after 24h of treatment. (C-E) WB analysis of Kif7 protein levels from *Usp14* siRNA depleted MEFs and control (C), *Usp14*$^{+/+}$ and *Usp14*$^{-/-}$ MEFs lysates (D) and *Usp14*$^{-/-}$ MEFs transiently transfected with the EV or the p3xFlag-Usp14 construct for 48h (E). For all three conditions, MEFs are stimulated by SAG for 24h. Histograms show quantification of band intensities for relative Kif7 levels (C-E). (F) MEFs were transfected with the pEGFP-Kif7 construct and treated with IU1 or DMSO for 6h in the presence of MG132. Protein extracts were immunoprecipitated in denaturing conditions using an antibody against GFP, and Ubiquitin-K48 and GFP-Kif7 were analyzed by WB. (G) WB analysis on Gli2 protein levels in cytoplasmic and nuclear fractions from *Usp14*$^{-/-}$ cells transiently transfected with EV or pGFP-Kif7 for 48h, under SAG stimulus. Gapdh and Sp1 were used as controls for the quality of cytoplasmic and nuclear fractions. TL=total lysate. (H) qPCR analysis on mRNA expression levels of *Gli1* under SAG treatment in *Usp14*$^{-/-}$ cells transiently transfected for 48h with the EV vector or the pGFP-Kif7 construct.

These findings suggest a new mechanism by which cilia maintenance and the Hh pathway are regulated by Usp14, a major inhibitor of proteasome degradation, via modulation of the stability of the ciliopathy protein Kif7.

8. Inhibition of Usp14 rescues Hh related phenotypes in *Pkd1*$^{-/-}$ MEFs

The Hh signaling pathway is essential for embryonic development in vertebrates. Consequently, impaired Hh signaling results in severe human diseases, and is responsible for some of the clinical signs observed in ciliopathies (Wong and Reiter 2008). We thus tested if Usp14 may play a role in Hh-related phenotypes observed in ciliopathies cellular models. We analyzed Usp14 and Kif7 protein amounts in *in vitro* models (MEFs) depleted for the *Intraflagellar transport 20* (*Ift20*$^{-/-}$), *Ofd1* (*Ofd1*$^{-/-}$), and *Pkd1* (*Pkd1*$^{-/-}$) transcripts. WB analysis showed increased protein levels of Usp14 and Kif7 in all the three ciliopathy models analyzed (Figure 26A), suggesting an involvement of Usp14 and Kif7 in the manifestations of the Hh phenotypes observed in ciliopathies.

Mutations in *Ift20* and *Ofd1* disrupt assembly of cilia and result in Hh signaling impairment (Clement, Kristensen et al. 2009, Liu, Tsai et al. 2014), while *Pkd1* mutations are not associated to defects in cilia formation (Lee and Somlo 2014). Polycystin-1 and -2 localize at the primary cilium of diverse cell types, but vertebrates lacking functional polycystins do not have structurally abnormal cilia, suggesting that polycystins, may modulate sensory functions of cilia, rather than proper cilia formation (Gascue, Katsanis et al. 2011, Lee and Somlo 2014). We thus decided to perform IF analysis in order to evaluate Gli2 ciliary localization in *Pkd1*$^{-/-}$ cells. Our results showed a proper localization of endogenous Gli2 to cilia in WT and *Pkd1*$^{-/-}$ MEFs, although the Gli2 fluorescence intensity resulted fainter on the ciliary tips of *Pkd1* mutant MEFs compared to WT (Figure 26B). We then wondered whether inhibition of Usp14 could promote recruitment of Gli2 to cilia in *Pkd1*$^{-/-}$ MEFs, and could improve the Gli proteins translocation defects observed in *Pkd1*$^{-/-}$ cells. IF experiment showed rescued amount of Gli2 protein on ciliary tips of *Pkd1*$^{-/-}$ MEFs transfected with siRNA against *Usp14* (Figure 26C), confirming the role of Usp14 in regulating the ciliary localization of Gli2 also in the *Pkd1* cellular model. We then exposed WT and *Pkd1*$^{-/-}$ MEFs to SAG treatment and evaluated Hh signaling activation by Real Time PCR. Our results indicated that *Gli1* transcriptional levels, as

already shown in other ciliopathies models (Clement, Kristensen et al. 2009, Liu, Tsai et al. 2014), were downregulated in *Pkd1*$^{-/-}$ cells compared to WT, in basal condition and after Hh pathway activation (Figure 26D). We thus hypothesized that by inhibiting the activity of Usp14 we could also modulate the activation of the Hh signaling. Consistent with these idea, silencing of *Usp14* in *Pkd1*$^{-/-}$ MEFs enhanced *Gli1* mRNA expression levels compared to cells transfected with the empty vector (Figure 26E), demonstrating the role of Usp14 on the proper activation of the Hh signal transduction pathway. We also enhanced the ciliary amount of Gli2 and the mRNA expression levels of *Gli1* in *Pkd1*$^{-/-}$ MEFs after treatment with IU1, confirming the role of Us14deubiquitinase activity in Hh signaling pathway (Figure 26F-G).

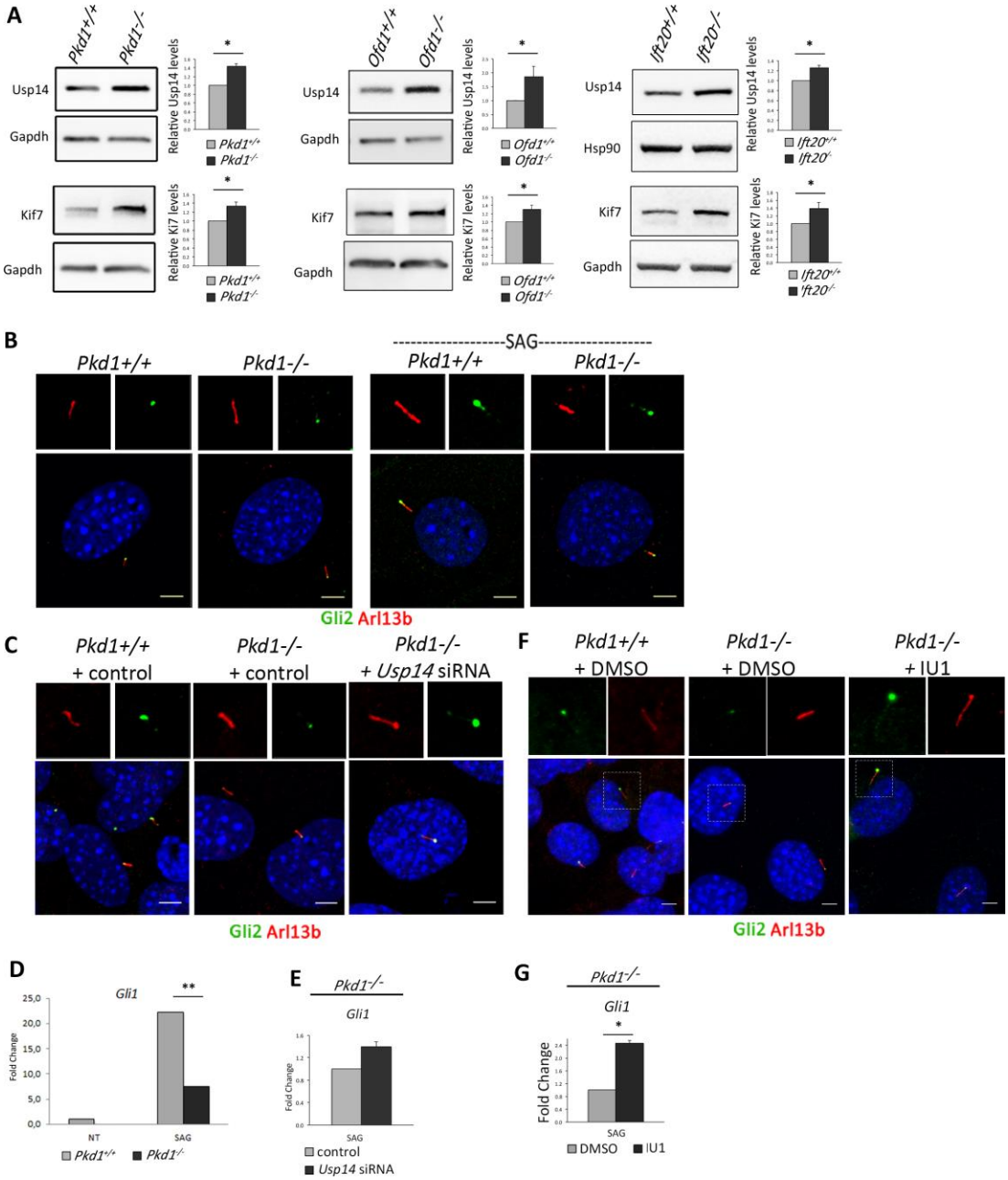

Figure 26. Usp14 inhibition rescues Hh related phenotypes of *Pkd1*$^{-/-}$ MEFs

(A) WB blot analysis of *Ift20*$^{-/-}$, *Pkd1*$^{-/-}$ and *Ofd1*$^{-/-}$ MEFs show increased protein levels of Usp14 and Kif7 in all models analyzed. (B) Representative confocal images of endogenous Gli2 (green) localization to cilia in *Pkd1*$^{+/+}$ and *Pkd1*$^{-/-}$ starved MEFs in basal condition (NT) and under SAG stimulus. Arl13b marks primary cilia (red) and Hoechst labels nuclei (blue). Scale bar=5µm. (C) IF experiments in 48h starved WT and *Pkd1*$^{-/-}$ MEFs transfected with non-targeting siRNA (control) and *Pkd1*$^{-/-}$ cells transfected with siRNA directed against *Usp14*. Primary cilia are stained with Arl13b (red), endogenous Gli2 is in green and Hoechst in blue. Scale bar=5µm. (D) qPCR analysis on mRNA expression levels of *Gli1* in basal condition and under SAG treatment in *Pkd1*$^{+/+}$ and *Pkd1*$^{-/-}$ starved MEFs, (E) and in *Pkd1*$^{-/-}$ cells transfected with Usp14 siRNA under SAG stimulus. (F) IF experiments in 48h starved WT and *Pkd1*$^{-/-}$ MEFs treated with DMSO and *Pkd1*$^{-/-}$ cells treated with IU1. Primary cilia are stained with Arl13b (red), endogenous Gli2 is in green and Hoechst in blue. Scale bar=5µm. (G) qPCR analysis on mRNA expression levels of *Gli1* under SAG stimulus in *Pkd1*$^{-/-}$ cells treated with DMSO or IU1.

Discussion

In recent years primary cilia have become the focus of intensive studies for their importance in development, inherited human disease and cancer (Brown and Witman 2014). Since most mammalian cells have cilia, loss of primary cilia or defects in ciliary functions affect different organ systems, and are associated with severe developmental diseases, collectively called ciliopathies (Hildebrandt, Benzing et al. 2011). It is well established that primary cilia act as the cell's antenna and play important roles in the correct transmission of several signal transduction pathways. One of the most convincing and solid experimental evidence in cilia biology is that vertebrate cells require intact and functioning primary cilia to respond to Hh family ligands (Lee, Zhao et al. 2016). Moreover, many important aspects of the phenotypes observed in ciliopathies, such as neural tube defects, polydactyly skeletal defects and craniofacial malformations, which include also the classical clinical features of OFD type 1 syndrome (Toprak, Uzum et al. 2006, Macca and Franco 2009), can be explained by misregulation of the Hh signaling (Toprak, Uzum et al. 2006, Macca and Franco 2009). Mutations in ciliary genes result in either loss or increase of Hh signaling. This is particularly evident in craniofacial structures, where cilia impairment can lead to both narrowing of the head with incomplete separation of the forebrain hemispheres (holoprosencephaly, associated with loss of Hh signaling) and widening of the mid-face (associated with gain of Hh signaling) (Cordero, Marcucio et al. 2004, Brugmann, Allen et al. 2010).

The study of the connections between cilia and developmental signaling has begun to clarify the basis of human diseases associated with ciliary dysfunction. The proper course of several cilia-associated signaling pathways is also mediated by ubiquitin-dependent proteolysis. In particular, besides the ubiquitin-dependent protein degradation, the proteasome is able to proteolytically process proteins. A well-designed processing event is the transformation of full-length activating Gli proteins into their shorter repressor forms

(Gerhardt, Leu et al. 2016), highlighting the possibility of regulating the Hh pathway activity through UPS modulation. Despite significant advances in identifying ciliopathy genes, the causative mechanisms at the base of ciliopathies are still poorly understood. To better understand the processes of Hh signal transduction related to the cilium, we directed our study towards the analysis of the relationship between ciliary function and the ubiquitin proteasome pathway. Our hypothesis is grounded on the previously cited observations and on the presence of several regulatory subunits of the proteasome in the available ciliary proteome databases (Ishikawa, Thompson et al. 2012, Goel, Murthy et al. 2013). In addition, the proteasome is known to alter its composition under certain conditions, such as cellular stress (Schmidt and Finley 2014). Conversely, it has been shown that in response to cellular stress primary cilia length and ciliogenesis are affected (Keeling, Tsiokas et al. 2016). Therefore, we wondered whether loss of the OFD1 ciliopathy protein affects proteasome composition, and performed functional evaluation of appropriate degradation/processing of Hh mediators; and we also asked whether the modulation of UPS components or proteasomal activity could ameliorate ciliary dysfunctions. Our data suggest a simple model, in which the Ofd1 centrosomal/basal body protein plays a role in Hh signal transduction regulation through a direct interaction with regulatory subunits of the proteasome, and by controlling the context-dependent proteolytic degradation. We tested the robustness of this model by demonstrating that cells ablated for Ofd1 show defects in proteasomal clearance of specific Hh signaling components including Gli2, Gli3, and Sufu. An altered composition of multiple subunits in the proteasome occurs during cellular stress (Hanna, Meides et al. 2007), and it is plausible that alteration of ciliary signaling can have a similar effect. Thus, we evaluated whether the ablation of the centrosomal OFD1 protein, which causes impairment of Hh signaling, can affect the proteasomal composition. The centrosome is a site of action for the UPS (Vora and Phillips 2016), and in the absence of OFD1, the centrosomal proteasome is mislocalized and changes its composition, as demonstrated by the reduction of RPT2

regulatory subunit and increased levels of USP14 deubiquitinase, which is a major inhibitor of proteasomal activity. Furthermore, we demonstrated that enhancement of the proteasomal activity, by SFN treatment, has an ameliorative effect by improving the Hh signaling defects through the chemical upregulation of proteasomal components. Notably, we observed sucrose fraction sedimentation changes in multiple proteasomal subunits in the absence of OFD1, suggesting that ciliopathy phenotypes are unlikely to be driven by specific defects in only one subunit, consistent with the observation that mice haploinsufficient for the subunit Rpn10 are phenotypically normal, at least by looking at the gross pathology, while homozygous $Rpn10^{-/-}$ mutants are embryonic lethal (Hamazaki, Sasaki et al. 2007). Ciliopathy proteins also play a central role in the regulation of the actin cytoskeleton and in the control of cilia length (Hernandez-Hernandez, Pravincumar et al. 2013, Keeling, Tsiokas et al. 2016). Defects in ciliary length are in fact associated with ciliopathies. It is intriguing to note that several renal cystic diseases have been associated with long cilia. Kidney tubules and cultured renal tubular cells from Bbs4-null mice displayed elongated cilia with an intact microtubular structure following prolonged culture (Mokrzan, Lewis et al. 2007), and Juvenile cystic kidneys (jck) mice (carrying a mutation in Nek8) also displayed long cilia (Smith, Bukanov et al. 2006, Sohara, Luo et al. 2008). Kidney tissues from a fetus affected with mutations in MKS3 displayed longer cilia compared to the control tissue, as measured by alpha-acetylated tubulin staining (Tammachote, Hommerding et al. 2009). Cells depleted for three genes responsible for three different forms of Joubert syndrome (JBTS): KIF7 (JBTS12) (He, Subramanian et al. 2014), KIAA0556 (JBTS26) (Sanders, de Vrieze et al. 2015) and TMEM67 (JBTS6) also have abnormally long cilia (Stayner, Poole et al. 2017).

Research on the UPS has demonstrated that proteins involved in ubiquitin-dependent signaling and proteolysis are important for a variety of cellular functions (Dikic 2017, Varshavsky 2017). Indeed, it has recently been suggested that the ubiquitin proteasomal system is one of the core mechanisms in regulating the formation and maintenance of

primary cilia (Malicki and Johnson 2017). Moreover, results from functional genomics and proteomics screen indicate that many UPS components may play a role in ciliogenesis. Although a large body of evidence indicated the potential importance of UPS in the dynamic profile of cilia, the role of the proteasome complex in ciliogenesis has been poorly studied and needs to be fully understood. Here, we report that a specific DUB, Usp14, reveals a novel signaling mechanism in both ciliogenesis and the control of the Hh pathway. We provide evidence that both genetic and pharmacological inhibition of Usp14 promotes ciliogenesis and cilia length elongation. Since the control of primary cilia length is an important and dynamic process, intimately related to ciliary signaling (Goetz and Anderson 2010), it is clear that alterations of cilia morphology and/or length can have dramatic functional implications. In order to evaluate the functionality of the abnormally long observed cilia, we studied the Hedgehog pathway, as its signal transduction is closely related to cilia integrity and is mediated by Gli proteins translocation to the cilia tip (Robbins, Fei et al. 2012). Strikingly, here we report that both genetic and pharmacological modulation using a drug that activate proteasome by Usp14 inhibition not only influenced ciliogenesis but also promoted translocation of Gli proteins to the cilia, into the nucleus and activation of the Hh pathway.

Recent studies of ciliary regulators and components have uncovered multiple mechanisms that control the movement of Hh players and the activation of the pathway (Goetz, Ocbina et al. 2009). IFT is integral for Hh transduction by trafficking signaling components within cilia: loss of most IFT complex B proteins, which mediate anterograde IFT, causes the absence of cilia and the inability to transduce Hh signals (Huangfu, Liu et al. 2003, Huangfu and Anderson 2005). In contrast, loss of IFT complex A proteins, Thm1 and Ift122, which largely mediate retrograde IFT, sequesters proteins in bulb-like structures at the distal tip of shortened cilia and causes inappropriate activation of the Hh pathway (Tran, Haycraft et al. 2008, Qin, Lin et al. 2011). Unlike most complex B proteins, Ift25 and Ift27 are not essential for ciliogenesis but form a subcomplex which is critical for ciliary import

of Gli2. As a result, loss of Ift25 or Ift27 does not alter cilia structure but disrupts activation of the Hh pathway (Keady, Samtani et al. 2012, Eguether, San Agustin et al. 2014, Liew, Ye et al. 2014). More recently, the phospholipid content of the ciliary membrane has also been shown to be a critical regulator of the pathway. INPP5E encodes for a phophoinositide phosphatase that creates a distinct phosphoinositide distribution in the ciliary membrane. Mutations in INPP5E cause Joubert syndrome, a well-known ciliopathy (Jacoby, Cox et al. 2009), and increase ciliary localization of Hh negative modulators, resulting in inactivation of the pathway. Furthermore, the transport of proteins in the ciliary axoneme is also driven by microtubule-dependent motors, the kinesins (Kif proteins). A null mutation in Kif3a has also been shown to disrupt Hh signaling (Goetz, Ocbina et al. 2009), while pathogenic mutations of KIF7, show not only upregulation of direct targets of Hh signaling but also elongation of primary cilia (Putoux, Thomas et al. 2011). KIF7 is the only evolutionarily conserved component of the core Hh signal transduction pathway that controls the axoneme length and the ciliary localization of Hh signaling molecules (He, Subramanian et al. 2014). Mutations in human KIF7 have been reported in several classes of severe ciliopathies associated with perinatal lethality, including fetal hydrolethalus, acrocallosal syndrome, and Joubert syndrome (Dafinger, Liebau et al. 2011, Putoux, Thomas et al. 2011, Ali, Silhavy et al. 2012, Barakeh, Faqeih et al. 2015:Walsh, 2013 #76, Ibisler, Hehr et al. 2015, Karaer, Yuksel et al. 2015, Tunovic, Baranano et al. 2015). Affected individuals show a spectrum of developmental defects including brain abnormalities, skeletal malformations, and craniofacial dysmorphisms, consistent with a role for KIF7 in the mammalian Hh pathway. Based on these observations, we propose a model where Usp14-mediated degradation of Kif7 regulates both ciliogenesis and Hh signaling. Consistent with our model, the levels of both Usp14 and Kif7 were increased in three different types of ciliopathies, confirming that Usp14 is intimately related to cilia biology. The mechanistic cause of this elevation has not yet been determined, and it is necessary to understand whether the increased Usp14 levels influence

or simply accompany the progression of the ciliopathies cellular phenotype. Moreover, we evaluated the effects of Usp14 inhibition on Hh signaling in $Pkd1^{-/-}$ MEFs, that do not display altered cilia formation. At the molecular level, one of the evident differences between proteins codified by genes responsible for ADPKD and proteins codified by transcripts mutated in other forms of inherited polycystic kidney disease is that while most cilioproteins responsible for renal cystic diseases have a fundamental role in ciliogenesis, polycystins (involved in ADPKD) do not seem to be essential for cilia formation and both Pkd1 and Pkd2, when inactivated, are not associated to cilia impairment (Gascue, Katsanis et al. 2011, Lee and Somlo 2014). Surprisingly, we showed that loss of *Pkd1* is associated to a dramatic decrease of Hh signaling and to impaired Gli2 ciliary localization following Hh activation, which was rescued by IU1 treatment even in the presence of apparently normal cilia (as in the case of the $Pkd1^{-/-}$ model) suggesting that Hh signaling may be involved in renal cytogenesis independently from the normal length of cilia. Additional experiments in the different available ADPKD *in vitro* and *in vivo* models accompanied by ultrastructural analysis of cilia will help in clarifying this hypothesis. Evidence that Hh signaling is involved in renal cystogenesis in animal models not due to mutations in the ADPKD loci are recently emerging (Attanasio, Uhlenhaut et al. 2007, Tran, Haycraft et al. 2008, Jonassen, SanAgustin et al. 2012, Tran, Talbott et al. 2014). On the basis of these considerations one of the challenges in understanding the molecular mechanisms of ADPKD is to discover the specific ciliary signaling process/es regulated by polycystins. In this regard, the mammalian Hh pathway may be a good starting point. As mentioned above, to the best of my knowledge a detailed analysis of the Hh signaling in PKD mouse models *in vivo* has not been reported yet and it will be needed to determine a possible functional role for Hh signaling in the renal cystic disease observed in ADPKD.

Therefore, our findings not only support the previously reported suggestion of an involvement of the UPS in cilia signaling and biogenesis but also contribute to the understanding of the role of the catalytic activation of proteasomal degradation in linking

ciliogenesis and Hh signaling transduction. To the best of our knowledge, this is the first example in which activation of proteasomal degradation has been shown to lead to an elongation of cilia, and to Hh signaling activation. Our results linking ciliopathy proteins, proteasomal function, cilia maintenance and Hh signaling represent a significant advance in the understanding of this organelle and indicate new potential therapeutic applications. In contrast to proteasome inhibitors, small molecules that can activate or enhance proteasome activity are rare and not well studied. Intriguingly, Lee et al. demonstrated that IU1, the selective small-molecule inhibitor of Usp14, accelerates proteasomal degradation of specific targets (Lee, Lee et al. 2010). Since we demonstrated that IU1 promotes ciliogenesis and Hh signaling, the activation of the proteasome could become a useful therapeutic strategy in ciliopathies. Our findings may therefore provide interesting new insights to better understand the spectrum of actions of proteasome activating compounds and may warrant further investigation into application of some of these compounds in treatment. Therefore, although the proteasomal dysfunction is just one of the contributor to the pathology of ciliopathies, our results can help in the design of future UPS-related therapies aimed at improving Hh-mediated phenotypes.

Conclusions

In conclusion, we demonstrated, both *in vitro* and *in vivo*, that loss of Ofd1 causes accumulation of Hh signaling mediators that is rescued by enhancing proteasomal activity. We also demonstrated that OFD1, as well as other cilioproteins, regulates the proteasomal composition at the centrosome through a direct interaction with specific regulatory proteasomal subunits. This part of the thesis was published in 2014 (Liu, Tsai et al. 2014), and is reported in the appendix.

Our observation led us to further investigate USP14, a proteasomal deubiquitinase identified in mammalian primary cilia through proteomic approaches that was found more bound to the proteasome in *Ofd1*-depleted models. Indeed, our results indicate that USP14 controls ciliogenesis and cilia length and has also a role in Hh signaling. Indeed Usp14 inactivation, depletion or inhibition by using a specific small molecule, modulate localization of Hh signaling components to primary cilia and activation of the pathway. Our results were also tested and validated in other ciliopathy models.

In summary, our studies support the involvement of the Ubiquitin Proteasome System in cilia signaling and biogenesis and contribute information to the emerging data linking proteasomal degradation, ciliogenesis and Hh signal transduction. Our findings may also provide insights for the potential therapeutic use of UPS-related therapies aimed at improving Hh-mediated ciliopathy phenotypes.

Collaboration and definition of the work performed by the applicant

The experimental work presented in this thesis was performed in collaboration with research groups located in the United States and in particular with Prof. Nicholas Katsanis at the Center for Human Disease Modeling, Duke University, Durham and with the research group of Prof Daniel Finley at the Department of Cell Biology, Harward Medical School, Boston. The experiments in Figures 18A, 18B, 18D were conducted by the external collaborators, all other experiments were carried out by the candidate.

References

Adams, M., U. M. Smith, C. V. Logan and C. A. Johnson (2008). "Recent advances in the molecular pathology, cell biology and genetics of ciliopathies." J Med Genet **45**(5): 257-267.

Ali, B. R., J. L. Silhavy, N. A. Akawi, J. G. Gleeson and L. Al-Gazali (2012). "A mutation in KIF7 is responsible for the autosomal recessive syndrome of macrocephaly, multiple epiphyseal dysplasia and distinctive facial appearance." Orphanet J Rare Dis **7**: 27.

Alman, B. A. (2015). "The role of hedgehog signalling in skeletal health and disease." Nat Rev Rheumatol **11**(9): 552-560.

Amato, R., M. Morleo, L. Giaquinto, D. di Bernardo and B. Franco (2014). "A network-based approach to dissect the cilia/centrosome complex interactome." BMC Genomics **15**: 658.

Ambroggio, X. I., D. C. Rees and R. J. Deshaies (2004). "JAMM: a metalloprotease-like zinc site in the proteasome and signalosome." PLoS Biol **2**(1): E2.

Anderson, C., S. Crimmins, J. A. Wilson, G. A. Korbel, H. L. Ploegh and S. M. Wilson (2005). "Loss of Usp14 results in reduced levels of ubiquitin in ataxia mice." J Neurochem **95**(3): 724-731.

Angers, S. and R. T. Moon (2009). "Proximal events in Wnt signal transduction." Nat Rev Mol Cell Biol **10**(7): 468-477.

Attanasio, M., N. H. Uhlenhaut, V. H. Sousa, J. F. O'Toole, E. Otto, K. Anlag, C. Klugmann, A. C. Treier, J. Helou, J. A. Sayer, D. Seelow, G. Nurnberg, C. Becker, A. E. Chudley, P. Nurnberg, F. Hildebrandt and M. Treier (2007). "Loss of GLIS2 causes nephronophthisis in humans and mice by increased apoptosis and fibrosis." Nat Genet **39**(8): 1018-1024.

Badano, J. L., N. Mitsuma, P. L. Beales and N. Katsanis (2006). "The ciliopathies: an emerging class of human genetic disorders." Annu Rev Genomics Hum Genet **7**: 125-148.

Bai, C. B. and A. L. Joyner (2001). "Gli1 can rescue the in vivo function of Gli2." Development **128**(24): 5161-5172.

Bar-Nun, S. and M. H. Glickman (2012). "Proteasomal AAA-ATPases: structure and function." Biochim Biophys Acta **1823**(1): 67-82.

Barakeh, D., E. Faqeih, S. Anazi, S. A.-D. M, A. Softah, F. Albadr, H. Hassan, A. M. Alazami and F. S. Alkuraya (2015). "The many faces of KIF7." Hum Genome Var **2**: 15006.

Beachy, P. A., S. S. Karhadkar and D. M. Berman (2004). "Tissue repair and stem cell renewal in carcinogenesis." Nature **432**(7015): 324-331.

Benmerah, A. (2013). The ciliary pocket. Curr Opin Cell Biol. **25:** 78-84.

Bernabe-Rubio, M. and M. A. Alonso (2017). "Routes and machinery of primary cilium biogenesis." Cell Mol Life Sci.

Bianchi, M., E. Giacomini, R. Crinelli, L. Radici, E. Carloni and M. Magnani (2015). "Dynamic transcription of ubiquitin genes under basal and stressful conditions and new insights into the multiple UBC transcript variants." Gene **573**(1): 100-109.

Bimonte, S., A. De Angelis, L. Quagliata, F. Giusti, R. Tammaro, R. Dallai, M. G. Ascenzi, G. Diez-Roux and B. Franco (2011). "Ofd1 is required in limb bud patterning and endochondral bone development." Dev Biol **349**(2): 179-191.

Bisschoff, I. J., C. Zeschnigk, D. Horn, B. Wellek, A. Riess, M. Wessels, P. Willems, P. Jensen, A. Busche, J. Bekkebraten, M. Chopra, H. D. Hove, C. Evers, K. Heimdal, A. S. Kaiser, E. Kunstmann, K. L. Robinson, M. Linne, P. Martin, J. McGrath, W. Pradel, K. E. Prescott, B. Roesler, G. Rudolf, U. Siebers-Renelt, N. Tyshchenko, D. Wieczorek, G. Wolff, W. B. Dobyns and D. J. Morris-Rosendahl (2013). "Novel mutations including deletions of the entire OFD1 gene in 30 families with type 1 orofaciodigital syndrome: a study of the extensive clinical variability." Hum Mutat **34**(1): 237-247.

Boehringer, J., C. Riedinger, K. Paraskevopoulos, E. O. Johnson, E. D. Lowe, C. Khoudian, D. Smith, M. E. Noble, C. Gordon and J. A. Endicott (2012). "Structural and functional characterization of Rpn12 identifies residues required for Rpn10 proteasome incorporation." Biochem J **448**(1): 55-65.

Borodovsky, A., B. M. Kessler, R. Casagrande, H. S. Overkleeft, K. D. Wilkinson and H. L. Ploegh (2001). "A novel active site-directed probe specific for deubiquitylating enzymes reveals proteasome association of USP14." EMBO J **20**(18): 5187-5196.

Bowers, M., L. Eng, Z. Lao, R. K. Turnbull, X. Bao, E. Riedel, S. Mackem and A. L. Joyner (2012). "Limb anterior-posterior polarity integrates activator and repressor functions of GLI2 as well as GLI3." Dev Biol **370**(1): 110-124.

Breslow, D. K., E. F. Koslover, F. Seydel, A. J. Spakowitz and M. V. Nachury (2013). "An in vitro assay for entry into cilia reveals unique properties of the soluble diffusion barrier." J Cell Biol **203**(1): 129-147.

Brinkmann, K., M. Schell, T. Hoppe and H. Kashkar (2015). "Regulation of the DNA damage response by ubiquitin conjugation." Front Genet **6**: 98.

Briscoe, J. and P. P. Therond (2013). "The mechanisms of Hedgehog signalling and its roles in development and disease." Nat Rev Mol Cell Biol **14**(7): 416-429.

Brown, J. M. and G. B. Witman (2014). "Cilia and Diseases." Bioscience **64**(12): 1126-1137.

Bruel, A. L., B. Franco, Y. Duffourd, J. Thevenon, L. Jego, E. Lopez, J. F. Deleuze, D. Doummar, R. H. Giles, C. A. Johnson, M. A. Huynen, V. Chevrier, L. Burglen, M. Morleo, I. Desguerres, G. Pierquin, B. Doray, B. Gilbert-Dussardier, B. Reversade, E. Steichen-Gersdorf, C. Baumann, I. Panigrahi, A. Fargeot-Espaliat, A. Dieux, A. David, A. Goldenberg, E. Bongers, D. Gaillard, J. Argente, B. Aral, N. Gigot, J. St-Onge, D. Birnbaum, S. R. Phadke, V. Cormier-Daire, T. Eguether, G. J. Pazour, V. Herranz-Perez, J. S. Goldstein, L. Pasquier, P. Loget, S. Saunier, A. Megarbane, O. Rosnet, M. R. Leroux, J. B. Wallingford, O. E. Blacque, M. V. Nachury, T. Attie-Bitach, J. B. Riviere, L. Faivre and C. Thauvin-Robinet (2017). "Fifteen years of research on oral-facial-digital syndromes: from 1 to 16 causal genes." J Med Genet **54**(6): 371-380.

Brugmann, S. A., N. C. Allen, A. W. James, Z. Mekonnen, E. Madan and J. A. Helms (2010). "A primary cilia-dependent etiology for midline facial disorders." Hum Mol Genet **19**(8): 1577-1592.

Budenholzer, L., C. L. Cheng, Y. Li and M. Hochstrasser (2017). "Proteasome Structure and Assembly." J Mol Biol.

Budny, B., W. Chen, H. Omran, M. Fliegauf, A. Tzschach, M. Wisniewska, L. R. Jensen, M. Raynaud, S. A. Shoichet, M. Badura, S. Lenzner, A. Latos-Bielenska and H. H. Ropers (2006). "A novel X-linked recessive mental retardation syndrome comprising macrocephaly and ciliary dysfunction is allelic to oral-facial-digital type I syndrome." Hum Genet **120**(2): 171-178.

Burglin, T. R. (2008). "The Hedgehog protein family." Genome Biol **9**(11): 241.

Callis, J. (2014). "The ubiquitination machinery of the ubiquitin system." Arabidopsis Book **12**: e0174.

Cardenas-Rodriguez, M. and J. L. Badano (2009). "Ciliary biology: understanding the cellular and genetic basis of human ciliopathies." Am J Med Genet C Semin Med Genet **151C**(4): 263-280.

Chen, M. H., C. W. Wilson, Y. J. Li, K. K. Law, C. S. Lu, R. Gacayan, X. Zhang, C. C. Hui and P. T. Chuang (2009). "Cilium-independent regulation of Gli protein function by Sufu in Hedgehog signaling is evolutionarily conserved." Genes Dev **23**(16): 1910-1928.

Chen, P. C., B. J. Bhattacharyya, J. Hanna, H. Minkel, J. A. Wilson, D. Finley, R. J. Miller and S. M. Wilson (2011). "Ubiquitin homeostasis is critical for synaptic development and function." J Neurosci **31**(48): 17505-17513.

Chen, P. C., L. N. Qin, X. M. Li, B. J. Walters, J. A. Wilson, L. Mei and S. M. Wilson (2009). "The proteasome-associated deubiquitinating enzyme Usp14 is essential for the maintenance of synaptic ubiquitin levels and the development of neuromuscular junctions." J Neurosci **29**(35): 10909-10919.

Cheung, H. O., X. Zhang, A. Ribeiro, R. Mo, S. Makino, V. Puviindran, K. K. Law, J. Briscoe and C. C. Hui (2009). "The kinesin protein Kif7 is a critical regulator of Gli transcription factors in mammalian hedgehog signaling." Sci Signal **2**(76): ra29.

Chiang, C., Y. Litingtung, E. Lee, K. E. Young, J. L. Corden, H. Westphal and P. A. Beachy (1996). "Cyclopia and defective axial patterning in mice lacking Sonic hedgehog gene function." Nature **383**(6599): 407-413.

Ciechanover, A., A. Orian and A. L. Schwartz (2000). "The ubiquitin-mediated proteolytic pathway: mode of action and clinical implications." J Cell Biochem Suppl **34**: 40-51.

Clague, M. J., I. Barsukov, J. M. Coulson, H. Liu, D. J. Rigden and S. Urbe (2013). "Deubiquitylases from genes to organism." Physiol Rev **93**(3): 1289-1315.

Clement, C. A., S. G. Kristensen, K. Mollgard, G. J. Pazour, B. K. Yoder, L. A. Larsen and S. T. Christensen (2009). "The primary cilium coordinates early cardiogenesis and hedgehog signaling in cardiomyocyte differentiation." J Cell Sci **122**(Pt 17): 3070-3082.

Clement, D. L., S. Mally, C. Stock, M. Lethan, P. Satir, A. Schwab, S. F. Pedersen and S. T. Christensen (2013). "PDGFRalpha signaling in the primary cilium regulates NHE1-

dependent fibroblast migration via coordinated differential activity of MEK1/2-ERK1/2-p90RSK and AKT signaling pathways." J Cell Sci **126**(Pt 4): 953-965.

Coene, K. L., R. Roepman, D. Doherty, B. Afroze, H. Y. Kroes, S. J. Letteboer, L. H. Ngu, B. Budny, E. van Wijk, N. T. Gorden, M. Azhimi, C. Thauvin-Robinet, J. A. Veltman, M. Boink, T. Kleefstra, F. P. Cremers, H. van Bokhoven and A. P. de Brouwer (2009). "OFD1 is mutated in X-linked Joubert syndrome and interacts with LCA5-encoded lebercilin." Am J Hum Genet **85**(4): 465-481.

Collins, G. A. and A. L. Goldberg (2017). "The Logic of the 26S Proteasome." Cell **169**(5): 792-806.

Corbit, K. C., P. Aanstad, V. Singla, A. R. Norman, D. Y. Stainier and J. F. Reiter (2005). "Vertebrate Smoothened functions at the primary cilium." Nature **437**(7061): 1018-1021.

Cordero, D., R. Marcucio, D. Hu, W. Gaffield, M. Tapadia and J. A. Helms (2004). "Temporal perturbations in sonic hedgehog signaling elicit the spectrum of holoprosencephaly phenotypes." J Clin Invest **114**(4): 485-494.

Crimmins, S., Y. Jin, C. Wheeler, A. K. Huffman, C. Chapman, L. E. Dobrunz, A. Levey, K. A. Roth, J. A. Wilson and S. M. Wilson (2006). "Transgenic rescue of ataxia mice with neuronal-specific expression of ubiquitin-specific protease 14." J Neurosci **26**(44): 11423-11431.

Czarnecki, P. G. and J. V. Shah (2012). "The ciliary transition zone: from morphology and molecules to medicine." Trends Cell Biol **22**(4): 201-210.

D'Angelo, A., A. De Angelis, B. Avallone, I. Piscopo, R. Tammaro, M. Studer and B. Franco (2012). "Ofd1 controls dorso-ventral patterning and axoneme elongation during embryonic brain development." PLoS One **7**(12): e52937.

D'Angelo, A. and B. Franco (2009). "The dynamic cilium in human diseases." Pathogenetics **2**(1): 3.

D'Arcy, P., X. Wang and S. Linder (2015). "Deubiquitinase inhibition as a cancer therapeutic strategy." Pharmacol Ther **147**: 32-54.

Dafinger, C., M. C. Liebau, S. M. Elsayed, Y. Hellenbroich, E. Boltshauser, G. C. Korenke, F. Fabretti, A. R. Janecke, I. Ebermann, G. Nurnberg, P. Nurnberg, H. Zentgraf, F. Koerber, K. Addicks, E. Elsobky, T. Benzing, B. Schermer and H. J. Bolz (2011). "Mutations in KIF7 link Joubert syndrome with Sonic Hedgehog signaling and microtubule dynamics." J Clin Invest **121**(7): 2662-2667.

Dai, P., H. Akimaru, Y. Tanaka, T. Maekawa, M. Nakafuku and S. Ishii (1999). "Sonic Hedgehog-induced activation of the Gli1 promoter is mediated by GLI3." J Biol Chem **274**(12): 8143-8152.

Davis, E. E. and N. Katsanis (2012). "The ciliopathies: a transitional model into systems biology of human genetic disease." Curr Opin Genet Dev **22**(3): 290-303.

de Conciliis, L., A. Marchitiello, M. C. Wapenaar, G. Borsani, S. Giglio, M. Mariani, G. G. Consalez, O. Zuffardi, B. Franco, A. Ballabio and S. Banfi (1998). "Characterization of Cxorf5 (71-7A), a novel human cDNA mapping to Xp22 and encoding a protein containing coiled-coil alpha-helical domains." Genomics **51**(2): 243-250.

Del Giudice, E., M. Macca, F. Imperati, A. D'Amico, P. Parent, L. Pasquier, V. Layet, S. Lyonnet, V. Stamboul-Darmency, C. Thauvin-Robinet, B. Franco and I. C. G. Oral-Facial-Digital Type (2014). "CNS involvement in OFD1 syndrome: a clinical, molecular, and neuroimaging study." Orphanet J Rare Dis **9**: 74.

Deltas, C. and G. Papagregoriou (2010). "Cystic diseases of the kidney: molecular biology and genetics." Arch Pathol Lab Med **134**(4): 569-582.

DeLuca, A. P., M. C. Weed, C. M. Haas, J. A. Halder and E. M. Stone (2015). "Apparent Usher Syndrome Caused by the Combination of BBS1-Associated Retinitis Pigmentosa and SLC26A4-Associated Deafness." JAMA Ophthalmol **133**(8): 967-968.

Di Marcotullio, L., E. Ferretti, E. De Smaele, I. Screpanti and A. Gulino (2006). "Suppressors of hedgehog signaling: Linking aberrant development of neural progenitors and tumorigenesis." Mol Neurobiol **34**(3): 193-204.

Di Marcotullio, L., E. Ferretti, A. Greco, E. De Smaele, I. Screpanti and A. Gulino (2007). "Multiple ubiquitin-dependent processing pathways regulate hedgehog/gli signaling: implications for cell development and tumorigenesis." Cell Cycle **6**(4): 390-393.

Dikic, I. (2017). "Proteasomal and Autophagic Degradation Systems." Annu Rev Biochem **86**: 193-224.

Dirksen, E. R. (1991). "Centriole and basal body formation during ciliogenesis revisited." Biol Cell **72**(1-2): 31-38.

Ebrahimi, A., L. Larijani, A. Moradi and M. R. Ebrahimi (2013). "Hedgehog signalling pathway: carcinogenesis and targeted therapy." Iran J Cancer Prev **6**(1): 36-43.

Eggenschwiler, J. T. and K. V. Anderson (2007). "Cilia and developmental signaling." Annu Rev Cell Dev Biol **23**: 345-373.

Eguether, T., M. A. Ermolaeva, Y. Zhao, M. C. Bonnet, A. Jain, M. Pasparakis, G. Courtois and A. M. Tassin (2014). "The deubiquitinating enzyme CYLD controls apical docking of basal bodies in ciliated epithelial cells." Nat Commun **5**: 4585.

Eguether, T., J. T. San Agustin, B. T. Keady, J. A. Jonassen, Y. Liang, R. Francis, K. Tobita, C. A. Johnson, Z. A. Abdelhamed, C. W. Lo and G. J. Pazour (2014). "IFT27 links the BBSome to IFT for maintenance of the ciliary signaling compartment." Dev Cell **31**(3): 279-290.

Elsasser, S., R. R. Gali, M. Schwickart, C. N. Larsen, D. S. Leggett, B. Muller, M. T. Feng, F. Tubing, G. A. Dittmar and D. Finley (2002). "Proteasome subunit Rpn1 binds ubiquitin-like protein domains." Nat Cell Biol **4**(9): 725-730.

Emes, R. D. and C. P. Ponting (2001). "A new sequence motif linking lissencephaly, Treacher Collins and oral-facial-digital type 1 syndromes, microtubule dynamics and cell migration." Hum Mol Genet **10**(24): 2813-2820.

Endoh-Yamagami, S., M. Evangelista, D. Wilson, X. Wen, J. W. Theunissen, K. Phamluong, M. Davis, S. J. Scales, M. J. Solloway, F. J. de Sauvage and A. S. Peterson (2009). "The mammalian Cos2 homolog Kif7 plays an essential role in modulating Hh signal transduction during development." Curr Biol **19**(15): 1320-1326.

Engel, B. D., W. B. Ludington and W. F. Marshall (2009). "Intraflagellar transport particle size scales inversely with flagellar length: revisiting the balance-point length control model." J Cell Biol **187**(1): 81-89.

Farshi, P., R. R. Deshmukh, J. O. Nwankwo, R. T. Arkwright, B. Cvek, J. Liu and Q. P. Dou (2015). "Deubiquitinases (DUBs) and DUB inhibitors: a patent review." Expert Opin Ther Pat **25**(10): 1191-1208.

Feather, S. A., P. J. Winyard, S. Dodd and A. S. Woolf (1997). "Oral-facial-digital syndrome type 1 is another dominant polycystic kidney disease: clinical, radiological and histopathological features of a new kindred." Nephrol Dial Transplant **12**(7): 1354-1361.

Feather, S. A., A. S. Woolf, D. Donnai, S. Malcolm and R. M. Winter (1997). "The oral-facial-digital syndrome type 1 (OFD1), a cause of polycystic kidney disease and associated malformations, maps to Xp22.2-Xp22.3." Hum Mol Genet **6**(7): 1163-1167.

Ferrante, M. I., A. Barra, J. P. Truong, S. Banfi, C. M. Disteche and B. Franco (2003). "Characterization of the OFD1/Ofd1 genes on the human and mouse sex chromosomes and exclusion of Ofd1 for the Xpl mouse mutant." Genomics **81**(6): 560-569.

Ferrante, M. I., G. Giorgio, S. A. Feather, A. Bulfone, V. Wright, M. Ghiani, A. Selicorni, L. Gammaro, F. Scolari, A. S. Woolf, O. Sylvie, L. Bernard, S. Malcolm, R. Winter, A. Ballabio and B. Franco (2001). "Identification of the gene for oral-facial-digital type I syndrome." Am J Hum Genet **68**(3): 569-576.

Ferrante, M. I., L. Romio, S. Castro, J. E. Collins, D. A. Goulding, D. L. Stemple, A. S. Woolf and S. W. Wilson (2009). "Convergent extension movements and ciliary function are mediated by ofd1, a zebrafish orthologue of the human oral-facial-digital type 1 syndrome gene." Hum Mol Genet **18**(2): 289-303.

Ferrante, M. I., A. Zullo, A. Barra, S. Bimonte, N. Messaddeq, M. Studer, P. Dolle and B. Franco (2006). "Oral-facial-digital type I protein is required for primary cilia formation and left-right axis specification." Nat Genet **38**(1): 112-117.

Fico, A., G. Manganelli, M. Simeone, S. Guido, G. Minchiotti and S. Filosa (2008). "High-throughput screening-compatible single-step protocol to differentiate embryonic stem cells in neurons." Stem Cells Dev **17**(3): 573-584.

Field, M., I. E. Scheffer, D. Gill, M. Wilson, L. Christie, M. Shaw, A. Gardner, G. Glubb, L. Hobson, M. Corbett, K. Friend, S. Willis-Owen and J. Gecz (2012). "Expanding the molecular basis and phenotypic spectrum of X-linked Joubert syndrome associated with OFD1 mutations." Eur J Hum Genet **20**(7): 806-809.

Finley, D. (2009). "Recognition and processing of ubiquitin-protein conjugates by the proteasome." Annu Rev Biochem **78**: 477-513.

Forsythe, E. and P. L. Beales (1993). Bardet-Biedl Syndrome. GeneReviews(R). R. A. Pagon, M. P. Adam, H. H. Ardinger et al. Seattle (WA).

Fraile, J. M., V. Quesada, D. Rodriguez, J. M. Freije and C. Lopez-Otin (2012). "Deubiquitinases in cancer: new functions and therapeutic options." Oncogene **31**(19): 2373-2388.

Franco, B. and C. Thauvin-Robinet (2016). "Update on oral-facial-digital syndromes (OFDS)." Cilia **5**: 12.

Gascue, C., N. Katsanis and J. L. Badano (2011). "Cystic diseases of the kidney: ciliary dysfunction and cystogenic mechanisms." Pediatr Nephrol **26**(8): 1181-1195.

Gascue, C., P. L. Tan, M. Cardenas-Rodriguez, G. Libisch, T. Fernandez-Calero, Y. P. Liu, S. Astrada, C. Robello, H. Naya, N. Katsanis and J. L. Badano (2012). "Direct role of Bardet-Biedl syndrome proteins in transcriptional regulation." J Cell Sci **125**(Pt 2): 362-375.

Gerdes, J. M., E. E. Davis and N. Katsanis (2009). "The vertebrate primary cilium in development, homeostasis, and disease." Cell **137**(1): 32-45.

Gerdes, J. M., Y. Liu, N. A. Zaghloul, C. C. Leitch, S. S. Lawson, M. Kato, P. A. Beachy, P. L. Beales, G. N. DeMartino, S. Fisher, J. L. Badano and N. Katsanis (2007). "Disruption of the basal body compromises proteasomal function and perturbs intracellular Wnt response." Nat Genet **39**(11): 1350-1360.

Gerhardt, C., T. Leu, J. M. Lier and U. Ruther (2016). "The cilia-regulated proteasome and its role in the development of ciliopathies and cancer." Cilia **5**: 14.

Gerhardt, C., J. M. Lier, S. Burmuhl, A. Struchtrup, K. Deutschmann, M. Vetter, T. Leu, S. Reeg, T. Grune and U. Ruther (2015). "The transition zone protein Rpgrip1l regulates proteasomal activity at the primary cilium." J Cell Biol **210**(1): 115-133.

Giorgio, G., M. Alfieri, C. Prattichizzo, A. Zullo, S. Cairo and B. Franco (2007). "Functional characterization of the OFD1 protein reveals a nuclear localization and physical interaction with subunits of a chromatin remodeling complex." Mol Biol Cell **18**(11): 4397-4404.

Gluenz, E., J. L. Hoog, A. E. Smith, H. R. Dawe, M. K. Shaw and K. Gull (2010). "Beyond 9+0: noncanonical axoneme structures characterize sensory cilia from protists to humans." FASEB J **24**(9): 3117-3121.

Goel, R., K. R. Murthy, S. M. Srikanth, S. M. Pinto, M. Bhattacharjee, D. S. Kelkar, A. K. Madugundu, G. Dey, S. S. Mohan, V. Krishna, T. K. Prasad, S. Chakravarti, H. C. Harsha and A. Pandey (2013). "Characterizing the normal proteome of human ciliary body." Clin Proteomics **10**(1): 9.

Goetz, S. C. and K. V. Anderson (2010). "The primary cilium: a signalling centre during vertebrate development." Nat Rev Genet **11**(5): 331-344.

Goetz, S. C., P. J. Ocbina and K. V. Anderson (2009). "The primary cilium as a Hedgehog signal transduction machine." Methods Cell Biol **94**: 199-222.

Groll, M. and R. Huber (2003). "Substrate access and processing by the 20S proteasome core particle." Int J Biochem Cell Biol **35**(5): 606-616.

Gundersen, G. G. and J. C. Bulinski (1986). "Distribution of tyrosinated and nontyrosinated alpha-tubulin during mitosis." J Cell Biol **102**(3): 1118-1126.

Haglund, K. and I. Dikic (2005). "Ubiquitylation and cell signaling." EMBO J **24**(19): 3353-3359.

Hamazaki, J., K. Sasaki, H. Kawahara, S. Hisanaga, K. Tanaka and S. Murata (2007). "Rpn10-mediated degradation of ubiquitinated proteins is essential for mouse development." Mol Cell Biol **27**(19): 6629-6638.

Hanna, J., N. A. Hathaway, Y. Tone, B. Crosas, S. Elsasser, D. S. Kirkpatrick, D. S. Leggett, S. P. Gygi, R. W. King and D. Finley (2006). "Deubiquitinating enzyme Ubp6 functions noncatalytically to delay proteasomal degradation." Cell **127**(1): 99-111.

Hanna, J., D. S. Leggett and D. Finley (2003). "Ubiquitin depletion as a key mediator of toxicity by translational inhibitors." Mol Cell Biol **23**(24): 9251-9261.

Hanna, J., A. Meides, D. P. Zhang and D. Finley (2007). "A ubiquitin stress response induces altered proteasome composition." Cell **129**(4): 747-759.

Harris, P. C. and V. E. Torres (1993). Polycystic Kidney Disease, Autosomal Dominant. GeneReviews(R). R. A. Pagon, M. P. Adam, H. H. Ardinger et al. Seattle (WA).

Haycraft, C. J., B. Banizs, Y. Aydin-Son, Q. Zhang, E. J. Michaud and B. K. Yoder (2005). "Gli2 and Gli3 localize to cilia and require the intraflagellar transport protein polaris for processing and function." PLoS Genet **1**(4): e53.

He, M., R. Subramanian, F. Bangs, T. Omelchenko, K. F. Liem, Jr., T. M. Kapoor and K. V. Anderson (2014). "The kinesin-4 protein Kif7 regulates mammalian Hedgehog signalling by organizing the cilium tip compartment." Nat Cell Biol **16**(7): 663-672.

Henkel, K. E., R. A. Pfeiffer and H. Stoss (1993). "[Meckel-Gruber syndrome]." Pathologe **14**(1): 32-35.

Hernandez-Hernandez, V., P. Pravincumar, A. Diaz-Font, H. May-Simera, D. Jenkins, M. Knight and P. L. Beales (2013). "Bardet-Biedl syndrome proteins control the cilia length through regulation of actin polymerization." Hum Mol Genet **22**(19): 3858-3868.

Hildebrandt, F., T. Benzing and N. Katsanis (2011). "Ciliopathies." N Engl J Med **364**(16): 1533-1543.

Horani, A., T. W. Ferkol, S. K. Dutcher and S. L. Brody (2016). "Genetics and biology of primary ciliary dyskinesia." Paediatr Respir Rev **18**: 18-24.

Hsia, E. Y., Y. Gui and X. Zheng (2015). "Regulation of Hedgehog signaling by ubiquitination." Front Biol (Beijing) **10**(3): 203-220.

Hu, C. K., M. Coughlin, C. M. Field and T. J. Mitchison (2011). "KIF4 regulates midzone length during cytokinesis." Curr Biol **21**(10): 815-824.

Hu, M., P. Li, L. Song, P. D. Jeffrey, T. A. Chenova, K. D. Wilkinson, R. E. Cohen and Y. Shi (2005). "Structure and mechanisms of the proteasome-associated deubiquitinating enzyme USP14." EMBO J **24**(21): 3747-3756.

Huangfu, D. and K. V. Anderson (2005). "Cilia and Hedgehog responsiveness in the mouse." Proc Natl Acad Sci U S A **102**(32): 11325-11330.

Huangfu, D., A. Liu, A. S. Rakeman, N. S. Murcia, L. Niswander and K. V. Anderson (2003). "Hedgehog signalling in the mouse requires intraflagellar transport proteins." Nature **426**(6962): 83-87.

Hui, C. C. and S. Angers (2011). "Gli proteins in development and disease." Annu Rev Cell Dev Biol **27**: 513-537.

Humke, E. W., K. V. Dorn, L. Milenkovic, M. P. Scott and R. Rohatgi (2010). "The output of Hedgehog signaling is controlled by the dynamic association between Suppressor of Fused and the Gli proteins." Genes Dev **24**(7): 670-682.

Ibisler, A., U. Hehr, A. Barth, M. Koch, J. T. Epplen and S. Hoffjan (2015). "Novel KIF7 Mutation in a Tunisian Boy with Acrocallosal Syndrome: Case Report and Review of the Literature." Mol Syndromol **6**(4): 173-180.

Ingham, P. W. and A. P. McMahon (2009). "Hedgehog signalling: Kif7 is not that fishy after all." Curr Biol **19**(17): R729-731.

Ingham, P. W., Y. Nakano and C. Seger (2011). "Mechanisms and functions of Hedgehog signalling across the metazoa." Nat Rev Genet **12**(6): 393-406.

Ishikawa, H., J. Thompson, J. R. Yates, 3rd and W. F. Marshall (2012). "Proteomic analysis of mammalian primary cilia." Curr Biol **22**(5): 414-419.

Ishiwata, S., J. Katayama, H. Shindo, Y. Ozawa, K. Itoh and M. Mizugaki (2001). "Increased expression of queuosine synthesizing enzyme, tRNA-guanine transglycosylase, and queuosine levels in tRNA of leukemic cells." J Biochem **129**(1): 13-17.

Ishiwata, S., Y. Ozawa, J. Katayama, S. Kaneko, H. Shindo, Y. Tomioka, T. Ishiwata, G. Asano, S. Ikegawa and M. Mizugaki (2004). "Elevated expression level of 60-kDa subunit of tRNA-guanine transglycosylase in colon cancer." Cancer Lett **212**(1): 113-119.

Jacoby, M., J. J. Cox, S. Gayral, D. J. Hampshire, M. Ayub, M. Blockmans, E. Pernot, M. V. Kisseleva, P. Compere, S. N. Schiffmann, F. Gergely, J. H. Riley, D. Perez-Morga, C. G. Woods and S. Schurmans (2009). "INPP5E mutations cause primary cilium signaling defects, ciliary instability and ciliopathies in human and mouse." Nat Genet **41**(9): 1027-1031.

Janke, C. and J. C. Bulinski (2011). "Post-translational regulation of the microtubule cytoskeleton: mechanisms and functions." Nat Rev Mol Cell Biol **12**(12): 773-786.

Janke, C. and M. Kneussel (2010). "Tubulin post-translational modifications: encoding functions on the neuronal microtubule cytoskeleton." Trends Neurosci **33**(8): 362-372.

Jessell, T. M. (2000). "Neuronal specification in the spinal cord: inductive signals and transcriptional codes." Nat Rev Genet **1**(1): 20-29.

Jia, J., A. Kolterud, H. Zeng, A. Hoover, S. Teglund, R. Toftgard and A. Liu (2009). "Suppressor of Fused inhibits mammalian Hedgehog signaling in the absence of cilia." Dev Biol **330**(2): 452-460.

Jiang, J. and C. C. Hui (2008). "Hedgehog signaling in development and cancer." Dev Cell **15**(6): 801-812.

Johnson, R. L., R. D. Riddle, E. Laufer and C. Tabin (1994). "Sonic hedgehog: a key mediator of anterior-posterior patterning of the limb and dorso-ventral patterning of axial embryonic structures." Biochem Soc Trans **22**(3): 569-574.

Jonassen, J. A., J. SanAgustin, S. P. Baker and G. J. Pazour (2012). "Disruption of IFT complex A causes cystic kidneys without mitotic spindle misorientation." J Am Soc Nephrol **23**(4): 641-651.

Jung, H., B. G. Kim, W. H. Han, J. H. Lee, J. Y. Cho, W. S. Park, M. M. Maurice, J. K. Han, M. J. Lee, D. Finley and E. H. Jho (2013). "Deubiquitination of Dishevelled by Usp14 is required for Wnt signaling." Oncogenesis **2**: e64.

Kaesler, S., B. Luscher and U. Ruther (2000). "Transcriptional activity of GLI1 is negatively regulated by protein kinase A." Biol Chem **381**(7): 545-551.

Karaer, K., Z. Yuksel, A. Ichkou, C. Calisir and T. Attie-Bitach (2015). "A novel KIF7 mutation in two affected siblings with acrocallosal syndrome." Clin Dysmorphol **24**(2): 61-64.

Kasahara, K., Y. Kawakami, T. Kiyono, S. Yonemura, Y. Kawamura, S. Era, F. Matsuzaki, N. Goshima and M. Inagaki (2014). "Ubiquitin-proteasome system controls ciliogenesis at the initial step of axoneme extension." Nat Commun **5**: 5081.

Ke, Z., I. Kondrichin, Z. Gong and V. Korzh (2008). "Combined activity of the two Gli2 genes of zebrafish play a major role in Hedgehog signaling during zebrafish neurodevelopment." Mol Cell Neurosci **37**(2): 388-401.

Keady, B. T., R. Samtani, K. Tobita, M. Tsuchya, J. T. San Agustin, J. A. Follit, J. A. Jonassen, R. Subramanian, C. W. Lo and G. J. Pazour (2012). "IFT25 links the signal-dependent movement of Hedgehog components to intraflagellar transport." Dev Cell **22**(5): 940-951.

Keeling, J., L. Tsiokas and D. Maskey (2016). "Cellular Mechanisms of Ciliary Length Control." Cells **5**(1).

Kent, D., E. W. Bush and J. E. Hooper (2006). "Roadkill attenuates Hedgehog responses through degradation of Cubitus interruptus." Development **133**(10): 2001-2010.

Kestler, H. A. and M. Kuhl (2008). "From individual Wnt pathways towards a Wnt signalling network." Philos Trans R Soc Lond B Biol Sci **363**(1495): 1333-1347.

Kim, J., M. Kato and P. A. Beachy (2009). "Gli2 trafficking links Hedgehog-dependent activation of Smoothened in the primary cilium to transcriptional activation in the nucleus." Proc Natl Acad Sci U S A **106**(51): 21666-21671.

Kim, S., N. A. Zaghloul, E. Bubenshchikova, E. C. Oh, S. Rankin, N. Katsanis, T. Obara and L. Tsiokas (2011). "Nde1-mediated inhibition of ciliogenesis affects cell cycle re-entry." Nat Cell Biol **13**(4): 351-360.

Kiprilov, E. N., A. Awan, R. Desprat, M. Velho, C. A. Clement, A. G. Byskov, C. Y. Andersen, P. Satir, E. E. Bouhassira, S. T. Christensen and R. E. Hirsch (2008). "Human embryonic stem cells in culture possess primary cilia with hedgehog signaling machinery." J Cell Biol **180**(5): 897-904.

Kisselev, A. F. and A. L. Goldberg (2001). "Proteasome inhibitors: from research tools to drug candidates." Chem Biol **8**(8): 739-758.

Kobayashi, T. and B. D. Dynlacht (2011). "Regulating the transition from centriole to basal body." J Cell Biol **193**(3): 435-444.

Kogerman, P., T. Grimm, L. Kogerman, D. Krause, A. B. Unden, B. Sandstedt, R. Toftgard and P. G. Zaphiropoulos (1999). "Mammalian suppressor-of-fused modulates nuclear-cytoplasmic shuttling of Gli-1." Nat Cell Biol **1**(5): 312-319.

Komander, D. (2009). "The emerging complexity of protein ubiquitination." Biochem Soc Trans **37**(Pt 5): 937-953.

Komander, D., M. J. Clague and S. Urbe (2009). "Breaking the chains: structure and function of the deubiquitinases." Nat Rev Mol Cell Biol **10**(8): 550-563.

Komander, D. and M. Rape (2012). "The ubiquitin code." Annu Rev Biochem **81**: 203-229.

Konno, A., M. Setou and K. Ikegami (2012). "Ciliary and flagellar structure and function--their regulations by posttranslational modifications of axonemal tubulin." Int Rev Cell Mol Biol **294**: 133-170.

Kozminski, K. G., K. A. Johnson, P. Forscher and J. L. Rosenbaum (1993). "A motility in the eukaryotic flagellum unrelated to flagellar beating." Proc Natl Acad Sci U S A **90**(12): 5519-5523.

Kwak, M. K., J. M. Cho, B. Huang, S. Shin and T. W. Kensler (2007). "Role of increased expression of the proteasome in the protective effects of sulforaphane against hydrogen peroxide-mediated cytotoxicity in murine neuroblastoma cells." Free Radic Biol Med **43**(5): 809-817.

Lam, Y. A., W. Xu, G. N. DeMartino and R. E. Cohen (1997). "Editing of ubiquitin conjugates by an isopeptidase in the 26S proteasome." Nature **385**(6618): 737-740.

Lander, G. C., E. Estrin, M. E. Matyskiela, C. Bashore, E. Nogales and A. Martin (2012). "Complete subunit architecture of the proteasome regulatory particle." Nature **482**(7384): 186-191.

Lecker, S. H., A. L. Goldberg and W. E. Mitch (2006). "Protein degradation by the ubiquitin-proteasome pathway in normal and disease states." J Am Soc Nephrol **17**(7): 1807-1819.

Lee, B. H., M. J. Lee, S. Park, D. C. Oh, S. Elsasser, P. C. Chen, C. Gartner, N. Dimova, J. Hanna, S. P. Gygi, S. M. Wilson, R. W. King and D. Finley (2010). "Enhancement of proteasome activity by a small-molecule inhibitor of USP14." Nature **467**(7312): 179-184.

Lee, J. E., J. L. Silhavy, M. S. Zaki, J. Schroth, S. L. Bielas, S. E. Marsh, J. Olvera, F. Brancati, M. Iannicelli, K. Ikegami, A. M. Schlossman, B. Merriman, T. Attie-Bitach, C. V. Logan, I. A. Glass, A. Cluckey, C. M. Louie, J. H. Lee, H. R. Raynes, I. Rapin, I. P. Castroviejo, M. Setou, C. Barbot, E. Boltshauser, S. F. Nelson, F. Hildebrandt, C. A. Johnson, D. A. Doherty, E. M. Valente and J. G. Gleeson (2012). "CEP41 is mutated in Joubert syndrome and is required for tubulin glutamylation at the cilium." Nat Genet **44**(2): 193-199.

Lee, M. J., B. H. Lee, J. Hanna, R. W. King and D. Finley (2011). "Trimming of ubiquitin chains by proteasome-associated deubiquitinating enzymes." Mol Cell Proteomics **10**(5): R110 003871.

Lee, R. T., Z. Zhao and P. W. Ingham (2016). "Hedgehog signalling." Development **143**(3): 367-372.

Lee, S. H. and S. Somlo (2014). "Cyst growth, polycystins, and primary cilia in autosomal dominant polycystic kidney disease." Kidney Res Clin Pract **33**(2): 73-78.

Leggett, D. S., J. Hanna, A. Borodovsky, B. Crosas, M. Schmidt, R. T. Baker, T. Walz, H. Ploegh and D. Finley (2002). "Multiple associated proteins regulate proteasome structure and function." Mol Cell **10**(3): 495-507.

Li, J., C. Wang, Y. Pan, Z. Bai and B. Wang (2011). "Increased proteolytic processing of full-length Gli2 transcription factor reduces the hedgehog pathway activity in vivo." Dev Dyn **240**(4): 766-774.

Li, W. and Y. Ye (2008). "Polyubiquitin chains: functions, structures, and mechanisms." Cell Mol Life Sci **65**(15): 2397-2406.

Liem, K. F., Jr., M. He, P. J. Ocbina and K. V. Anderson (2009). "Mouse Kif7/Costal2 is a cilia-associated protein that regulates Sonic hedgehog signaling." Proc Natl Acad Sci U S A **106**(32): 13377-13382.

Liew, G. M., F. Ye, A. R. Nager, J. P. Murphy, J. S. Lee, M. Aguiar, D. K. Breslow, S. P. Gygi and M. V. Nachury (2014). "The intraflagellar transport protein IFT27 promotes BBSome exit from cilia through the GTPase ARL6/BBS3." Dev Cell **31**(3): 265-278.

Lilienbaum, A. (2013). "Relationship between the proteasomal system and autophagy." Int J Biochem Mol Biol **4**(1): 1-26.

Liu, J., H. Zeng and A. Liu (2015). "The loss of Hh responsiveness by a non-ciliary Gli2 variant." Development **142**(9): 1651-1660.

Liu, Y. P., I. C. Tsai, M. Morleo, E. C. Oh, C. C. Leitch, F. Massa, B. H. Lee, D. S. Parker, D. Finley, N. A. Zaghloul, B. Franco and N. Katsanis (2014). "Ciliopathy proteins regulate paracrine signaling by modulating proteasomal degradation of mediators." J Clin Invest **124**(5): 2059-2070.

Lopes, C. A., S. L. Prosser, L. Romio, R. A. Hirst, C. O'Callaghan, A. S. Woolf and A. M. Fry (2011). "Centriolar satellites are assembly points for proteins implicated in human ciliopathies, including oral-facial-digital syndrome 1." J Cell Sci **124**(Pt 4): 600-612.

Lum, L. and P. A. Beachy (2004). "The Hedgehog response network: sensors, switches, and routers." Science **304**(5678): 1755-1759.

Macca, M. and B. Franco (2009). "The molecular basis of oral-facial-digital syndrome, type 1." Am J Med Genet C Semin Med Genet **151C**(4): 318-325.

Malicki, J. J. and C. A. Johnson (2017). "The Cilium: Cellular Antenna and Central Processing Unit." Trends Cell Biol **27**(2): 126-140.

Marshall, A. G., J. A. Watson, J. J. Hallengren, B. J. Walters, L. E. Dobrunz, L. Francillon, J. A. Wilson, S. E. Phillips and S. M. Wilson (2013). "Genetic background alters the severity and onset of neuromuscular disease caused by the loss of ubiquitin-specific protease 14 (usp14)." PLoS One **8**(12): e84042.

Marshall, W. F., H. Qin, M. Rodrigo Brenni and J. L. Rosenbaum (2005). "Flagellar length control system: testing a simple model based on intraflagellar transport and turnover." Mol Biol Cell **16**(1): 270-278.

Marshall, W. F. and J. L. Rosenbaum (2001). "Intraflagellar transport balances continuous turnover of outer doublet microtubules: implications for flagellar length control." J Cell Biol **155**(3): 405-414.

Maskey, D., M. C. Marlin, S. Kim, S. Kim, E. C. Ong, G. Li and L. Tsiokas (2015). "Cell cycle-dependent ubiquitylation and destruction of NDE1 by CDK5-FBW7 regulates ciliary length." EMBO J **34**(19): 2424-2440.

Maurya, A. K., J. Ben, Z. Zhao, R. T. Lee, W. Niah, A. S. Ng, A. Iyu, W. Yu, S. Elworthy, F. J. van Eeden and P. W. Ingham (2013). "Positive and negative regulation of Gli activity by Kif7 in the zebrafish embryo." PLoS Genet **9**(12): e1003955.

May-Simera, H. L. and M. W. Kelley (2012). "Cilia, Wnt signaling, and the cytoskeleton." Cilia **1**(1): 7.

McAnany, J. J., M. A. Genead, S. Walia, A. V. Drack, E. M. Stone, R. K. Koenekoop, E. I. Traboulsi, A. Smith, R. G. Weleber, S. G. Jacobson and G. A. Fishman (2013). "Visual acuity changes in patients with leber congenital amaurosis and mutations in CEP290." JAMA Ophthalmol **131**(2): 178-182.

Michel, M. A., P. R. Elliott, K. N. Swatek, M. Simicek, J. N. Pruneda, J. L. Wagstaff, S. M. Freund and D. Komander (2015). "Assembly and specific recognition of k29- and k33-linked polyubiquitin." Mol Cell **58**(1): 95-109.

Mick, D. U., R. B. Rodrigues, R. D. Leib, C. M. Adams, A. S. Chien, S. P. Gygi and M. V. Nachury (2015). "Proteomics of Primary Cilia by Proximity Labeling." Dev Cell **35**(4): 497-512.

Mitch, W. E. and A. L. Goldberg (1996). "Mechanisms of muscle wasting. The role of the ubiquitin-proteasome pathway." N Engl J Med **335**(25): 1897-1905.

Mokrzan, E. M., J. S. Lewis and K. Mykytyn (2007). "Differences in renal tubule primary cilia length in a mouse model of Bardet-Biedl syndrome." Nephron Exp Nephrol **106**(3): e88-96.

Morleo, M. and B. Franco (2008). "Dosage compensation of the mammalian X chromosome influences the phenotypic variability of X-linked dominant male-lethal disorders." J Med Genet **45**(7): 401-408.

Murata, S., H. Yashiroda and K. Tanaka (2009). "Molecular mechanisms of proteasome assembly." Nat Rev Mol Cell Biol **10**(2): 104-115.

Nakasone, M. A., N. Livnat-Levanon, M. H. Glickman, R. E. Cohen and D. Fushman (2013). "Mixed-linkage ubiquitin chains send mixed messages." Structure **21**(5): 727-740.

Nijman, S. M., M. P. Luna-Vargas, A. Velds, T. R. Brummelkamp, A. M. Dirac, T. K. Sixma and R. Bernards (2005). "A genomic and functional inventory of deubiquitinating enzymes." Cell **123**(5): 773-786.

Novarino, G., N. Akizu and J. G. Gleeson (2011). "Modeling human disease in humans: the ciliopathies." Cell **147**(1): 70-79.

Nozawa, Y. I., C. Lin and P. T. Chuang (2013). "Hedgehog signaling from the primary cilium to the nucleus: an emerging picture of ciliary localization, trafficking and transduction." Curr Opin Genet Dev **23**(4): 429-437.

Ou, C. Y., C. H. Wang, J. Jiang and C. T. Chien (2007). "Suppression of Hedgehog signaling by Cul3 ligases in proliferation control of retinal precursors." Dev Biol **308**(1): 106-119.

Paces-Fessy, M., D. Boucher, E. Petit, S. Paute-Briand and M. F. Blanchet-Tournier (2004). "The negative regulator of Gli, Suppressor of fused (Sufu), interacts with SAP18, Galectin3 and other nuclear proteins." Biochem J **378**(Pt 2): 353-362.

Pampliega, O. and A. M. Cuervo (2016). "Autophagy and primary cilia: dual interplay." Curr Opin Cell Biol **39**: 1-7.

Pan, Y., C. B. Bai, A. L. Joyner and B. Wang (2006). "Sonic hedgehog signaling regulates Gli2 transcriptional activity by suppressing its processing and degradation." Mol Cell Biol **26**(9): 3365-3377.

Parisi, M. and I. Glass (1993). Joubert Syndrome. GeneReviews(R). R. A. Pagon, M. P. Adam, H. H. Ardinger et al. Seattle (WA).

Patil, M., N. Pabla, S. Huang and Z. Dong (2013). "Nek1 phosphorylates Von Hippel-Lindau tumor suppressor to promote its proteasomal degradation and ciliary destabilization." Cell Cycle **12**(1): 166-171.

Pedersen, L. B. and A. Akhmanova (2014). "Kif7 keeps cilia tips in shape." Nat Cell Biol **16**(7): 623-625.

Pedersen, L. B. and J. L. Rosenbaum (2008). "Intraflagellar transport (IFT) role in ciliary assembly, resorption and signalling." Curr Top Dev Biol **85**: 23-61.

Petrova, R. and A. L. Joyner (2014). "Roles for Hedgehog signaling in adult organ homeostasis and repair." Development **141**(18): 3445-3457.

Piperno, G., M. LeDizet and X. J. Chang (1987). "Microtubules containing acetylated alpha-tubulin in mammalian cells in culture." J Cell Biol **104**(2): 289-302.

Prattichizzo, C., M. Macca, V. Novelli, G. Giorgio, A. Barra, B. Franco and I. C. G. Oral-Facial-Digital Type (2008). "Mutational spectrum of the oral-facial-digital type I syndrome: a study on a large collection of patients." Hum Mutat **29**(10): 1237-1246.

Putoux, A., S. Nampoothiri, N. Laurent, V. Cormier-Daire, P. L. Beales, A. Schinzel, D. Bartholdi, C. Alby, S. Thomas, N. Elkhartoufi, A. Ichkou, J. Litzler, A. Munnich, F. Encha-Razavi, R. Kannan, L. Faivre, N. Boddaert, A. Rauch, M. Vekemans and T. Attie-Bitach (2012). "Novel KIF7 mutations extend the phenotypic spectrum of acrocallosal syndrome." J Med Genet **49**(11): 713-720.

Putoux, A., S. Thomas, K. L. Coene, E. E. Davis, Y. Alanay, G. Ogur, E. Uz, D. Buzas, C. Gomes, S. Patrier, C. L. Bennett, N. Elkhartoufi, M. H. Frison, L. Rigonnot, N. Joye, S. Pruvost, G. E. Utine, K. Boduroglu, P. Nitschke, L. Fertitta, C. Thauvin-Robinet, A. Munnich, V. Cormier-Daire, R. Hennekam, E. Colin, N. A. Akarsu, C. Bole-Feysot, N. Cagnard, A. Schmitt, N. Goudin, S. Lyonnet, F. Encha-Razavi, J. P. Siffroi, M. Winey, N. Katsanis, M. Gonzales, M. Vekemans, P. L. Beales and T. Attie-Bitach (2011). "KIF7 mutations cause fetal hydrolethalus and acrocallosal syndromes." Nat Genet **43**(6): 601-606.

Qin, J., Y. Lin, R. X. Norman, H. W. Ko and J. T. Eggenschwiler (2011). "Intraflagellar transport protein 122 antagonizes Sonic Hedgehog signaling and controls ciliary localization of pathway components." Proc Natl Acad Sci U S A **108**(4): 1456-1461.

Quarmby, L. M. and J. D. Parker (2005). "Cilia and the cell cycle?" J Cell Biol **169**(5): 707-710.

Quinlan, R. J., J. L. Tobin and P. L. Beales (2008). "Modeling ciliopathies: Primary cilia in development and disease." Curr Top Dev Biol **84**: 249-310.

Reiter, J. F. and M. R. Leroux (2017). "Genes and molecular pathways underpinning ciliopathies." Nat Rev Mol Cell Biol.

Reyes-Turcu, F. E., K. H. Ventii and K. D. Wilkinson (2009). "Regulation and cellular roles of ubiquitin-specific deubiquitinating enzymes." Annu Rev Biochem **78**: 363-397.

Robbins, D. J., D. L. Fei and N. A. Riobo (2012). "The Hedgehog signal transduction network." Sci Signal **5**(246): re6.

Rohatgi, R., L. Milenkovic and M. P. Scott (2007). "Patched1 regulates hedgehog signaling at the primary cilium." Science **317**(5836): 372-376.

Rohatgi, R. and W. J. Snell (2010). "The ciliary membrane." Curr Opin Cell Biol **22**(4): 541-546.

Romio, L., A. M. Fry, P. J. Winyard, S. Malcolm, A. S. Woolf and S. A. Feather (2004). "OFD1 is a centrosomal/basal body protein expressed during mesenchymal-epithelial transition in human nephrogenesis." J Am Soc Nephrol **15**(10): 2556-2568.

Romio, L., V. Wright, K. Price, P. J. Winyard, D. Donnai, M. E. Porteous, B. Franco, G. Giorgio, S. Malcolm, A. S. Woolf and S. A. Feather (2003). "OFD1, the gene mutated in oral-facial-digital syndrome type 1, is expressed in the metanephros and in human embryonic renal mesenchymal cells." J Am Soc Nephrol **14**(3): 680-689.

Rosenzweig, R., V. Bronner, D. Zhang, D. Fushman and M. H. Glickman (2012). "Rpn1 and Rpn2 coordinate ubiquitin processing factors at proteasome." J Biol Chem **287**(18): 14659-14671.

Roy, S. (2009). "The motile cilium in development and disease: emerging new insights." Bioessays **31**(7): 694-699.

Ruiz i Altaba, A. (1997). "Catching a Gli-mpse of Hedgehog." Cell **90**(2): 193-196.

Ruiz i Altaba, A., C. Mas and B. Stecca (2007). "The Gli code: an information nexus regulating cell fate, stemness and cancer." Trends Cell Biol **17**(9): 438-447.

Ruiz i Altaba, A., V. Palma and N. Dahmane (2002). "Hedgehog-Gli signalling and the growth of the brain." Nat Rev Neurosci **3**(1): 24-33.

Saal, S., L. Faivre, B. Aral, N. Gigot, A. Toutain, L. Van Maldergem, A. Destree, I. Maystadt, J. P. Cosyns, P. S. Jouk, B. Loeys, D. Chauveau, E. Bieth, V. Layet, M. Mathieu, J. Lespinasse, A. Teebi, B. Franco, E. Gautier, C. Binquet, A. Masurel-Paulet, C. Mousson, J. B. Gouyon, F. Huet and C. Thauvin-Robinet (2010). "Renal insufficiency, a frequent complication with age in oral-facial-digital syndrome type I." Clin Genet **77**(3): 258-265.

Saeki, Y., T. Kudo, T. Sone, Y. Kikuchi, H. Yokosawa, A. Toh-e and K. Tanaka (2009). "Lysine 63-linked polyubiquitin chain may serve as a targeting signal for the 26S proteasome." EMBO J **28**(4): 359-371.

Sanchez, I. and B. D. Dynlacht (2016). "Cilium assembly and disassembly." Nat Cell Biol **18**(7): 711-717.

Sanders, A. A., E. de Vrieze, A. M. Alazami, F. Alzahrani, E. B. Malarkey, N. Sorusch, L. Tebbe, S. Kuhns, T. J. van Dam, A. Alhashem, B. Tabarki, Q. Lu, N. J. Lambacher, J. E. Kennedy, R. V. Bowie, L. Hetterschijt, S. van Beersum, J. van Reeuwijk, K. Boldt, H. Kremer, R. A. Kesterson, D. Monies, M. Abouelhoda, R. Roepman, M. H. Huynen, M. Ueffing, R. B. Russell, U. Wolfrum, B. K. Yoder, E. van Wijk, F. S. Alkuraya and O. E. Blacque (2015). "KIAA0556 is a novel ciliary basal body component mutated in Joubert syndrome." Genome Biol **16**: 293.

Santos, N. and J. F. Reiter (2014). "A central region of Gli2 regulates its localization to the primary cilium and transcriptional activity." J Cell Sci **127**(Pt 7): 1500-1510.

Sasai, N. and J. Briscoe (2012). "Primary cilia and graded Sonic Hedgehog signaling." Wiley Interdiscip Rev Dev Biol **1**(5): 753-772.

Sasaki, H., Y. Nishizaki, C. Hui, M. Nakafuku and H. Kondoh (1999). "Regulation of Gli2 and Gli3 activities by an amino-terminal repression domain: implication of Gli2 and Gli3 as primary mediators of Shh signaling." Development **126**(17): 3915-3924.

Satir, P. and S. T. Christensen (2007). "Overview of structure and function of mammalian cilia." Annu Rev Physiol **69**: 377-400.

Satir, P., L. B. Pedersen and S. T. Christensen (2010). "The primary cilium at a glance." J Cell Sci **123**(Pt 4): 499-503.

Schmidt, M. and D. Finley (2014). "Regulation of proteasome activity in health and disease." Biochim Biophys Acta **1843**(1): 13-25.

Scholey, J. M. (2008). "Intraflagellar transport motors in cilia: moving along the cell's antenna." J Cell Biol **180**(1): 23-29.

Shearer, R. F. and D. N. Saunders (2016). "Regulation of primary cilia formation by the ubiquitin-proteasome system." Biochem Soc Trans **44**(5): 1265-1271.

Simpson, F., M. C. Kerr and C. Wicking (2009). "Trafficking, development and hedgehog." Mech Dev **126**(5-6): 279-288.

Singla, V. and J. F. Reiter (2006). "The primary cilium as the cell's antenna: signaling at a sensory organelle." Science **313**(5787): 629-633.

Singla, V., M. Romaguera-Ros, J. M. Garcia-Verdugo and J. F. Reiter (2010). "Ofd1, a human disease gene, regulates the length and distal structure of centrioles." Dev Cell **18**(3): 410-424.

Smith, D. M., S. C. Chang, S. Park, D. Finley, Y. Cheng and A. L. Goldberg (2007). "Docking of the proteasomal ATPases' carboxyl termini in the 20S proteasome's alpha ring opens the gate for substrate entry." Mol Cell **27**(5): 731-744.

Smith, L. A., N. O. Bukanov, H. Husson, R. J. Russo, T. C. Barry, A. L. Taylor, D. R. Beier and O. Ibraghimov-Beskrovnaya (2006). "Development of polycystic kidney disease in juvenile cystic kidney mice: insights into pathogenesis, ciliary abnormalities, and common features with human disease." J Am Soc Nephrol **17**(10): 2821-2831.

Sohara, E., Y. Luo, J. Zhang, D. K. Manning, D. R. Beier and J. Zhou (2008). "Nek8 regulates the expression and localization of polycystin-1 and polycystin-2." J Am Soc Nephrol **19**(3): 469-476.

Sorokin, S. (1962). "Centrioles and the formation of rudimentary cilia by fibroblasts and smooth muscle cells." J Cell Biol **15**: 363-377.

Sorokin, S. P. (1968). "Centriole formation and ciliogenesis." Aspen Emphysema Conf **11**: 213-216.

Stannard, W. and C. O'Callaghan (2006). "Ciliary function and the role of cilia in clearance." J Aerosol Med **19**(1): 110-115.

Stayner, C., C. A. Poole, S. R. McGlashan, M. Pilanthananond, R. Brauning, D. Markie, B. Lett, L. Slobbe, A. Chae, A. C. Johnstone, C. G. Jensen, J. C. McEwan, K. Dittmer, K. Parker, A. Wiles, W. Blackburne, A. Leichter, M. Leask, A. Pinnapureddy, M. Jennings, J. A. Horsfield, R. J. Walker and M. R. Eccles (2017). "An ovine hepatorenal fibrocystic model of a Meckel-like syndrome associated with dysmorphic primary cilia and TMEM67 mutations." Sci Rep **7**(1): 1601.

Stokman, M., M. Lilien and N. Knoers (1993). Nephronophthisis. GeneReviews(R). R. A. Pagon, M. P. Adam, H. H. Ardinger et al. Seattle (WA).

Stoll, C. and P. Sauvage (2002). "Long-term follow-up of a girl with oro-facio-digital syndrome type I due to a mutation in the OFD 1 gene." Ann Genet **45**(2): 59-62.

Stone, M., R. Hartmann-Petersen, M. Seeger, D. Bech-Otschir, M. Wallace and C. Gordon (2004). "Uch2/Uch37 is the major deubiquitinating enzyme associated with the 26S proteasome in fission yeast." J Mol Biol **344**(3): 697-706.

Suraweera, A., C. Munch, A. Hanssum and A. Bertolotti (2012). "Failure of amino acid homeostasis causes cell death following proteasome inhibition." Mol Cell **48**(2): 242-253.

Swatek, K. N. and D. Komander (2016). "Ubiquitin modifications." Cell Res **26**(4): 399-422.

Sweeney, W. E. and E. D. Avner (1993). Polycystic Kidney Disease, Autosomal Recessive. GeneReviews(R). R. A. Pagon, M. P. Adam, H. H. Ardinger et al. Seattle (WA).

Tabler, J. M., T. G. Bolger, J. Wallingford and K. J. Liu (2014). "Hedgehog activity controls opening of the primary mouth." Dev Biol **396**(1): 1-7.

Tammachote, R., C. J. Hommerding, R. M. Sinders, C. A. Miller, P. G. Czarnecki, A. C. Leightner, J. L. Salisbury, C. J. Ward, V. E. Torres, V. H. Gattone, 2nd and P. C. Harris (2009). "Ciliary and centrosomal defects associated with mutation and depletion of the Meckel syndrome genes MKS1 and MKS3." Hum Mol Genet **18**(17): 3311-3323.

Tang, Z., M. G. Lin, T. R. Stowe, S. Chen, M. Zhu, T. Stearns, B. Franco and Q. Zhong (2013). "Autophagy promotes primary ciliogenesis by removing OFD1 from centriolar satellites." Nature **502**(7470): 254-257.

Tay, S. Y., P. W. Ingham and S. Roy (2005). "A homologue of the Drosophila kinesin-like protein Costal2 regulates Hedgehog signal transduction in the vertebrate embryo." Development **132**(4): 625-634.

Tempe, D., M. Casas, S. Karaz, M. F. Blanchet-Tournier and J. P. Concordet (2006). "Multisite protein kinase A and glycogen synthase kinase 3beta phosphorylation leads to Gli3 ubiquitination by SCFbetaTrCP." Mol Cell Biol **26**(11): 4316-4326.

Tenorio, J., P. Arias, V. Martinez-Glez, F. Santos, S. Garcia-Minaur, J. Nevado and P. Lapunzina (2014). "Simpson-Golabi-Behmel syndrome types I and II." Orphanet J Rare Dis **9**: 138.

Thauvin-Robinet, C., S. Thomas, M. Sinico, B. Aral, L. Burglen, N. Gigot, H. Dollfus, S. Rossignol, M. Raynaud, C. Philippe, C. Badens, R. Touraine, C. Gomes, B. Franco, E. Lopez, N. Elkhartoufi, L. Faivre, A. Munnich, N. Boddaert, L. Van Maldergem, F. Encha-Razavi, S. Lyonnet, M. Vekemans, E. Escudier and T. Attie-Bitach (2013). "OFD1 mutations in males: phenotypic spectrum and ciliary basal body docking impairment." Clin Genet **84**(1): 86-90.

Tian, Z., P. D'Arcy, X. Wang, A. Ray, Y. T. Tai, Y. Hu, R. D. Carrasco, P. Richardson, S. Linder, D. Chauhan and K. C. Anderson (2014). "A novel small molecule inhibitor of deubiquitylating enzyme USP14 and UCHL5 induces apoptosis in multiple myeloma and overcomes bortezomib resistance." Blood **123**(5): 706-716.

Tomko, R. J., Jr., M. Funakoshi, K. Schneider, J. Wang and M. Hochstrasser (2010). "Heterohexameric ring arrangement of the eukaryotic proteasomal ATPases: implications for proteasome structure and assembly." Mol Cell **38**(3): 393-403.

Toprak, O., A. Uzum, M. Cirit, E. Esi, A. Inci, R. Ersoy, M. Tanrisev, E. Ok and B. Franco (2006). "Oral-facial-digital syndrome type 1, Caroli's disease and cystic renal disease." Nephrol Dial Transplant **21**(6): 1705-1709.

Toriello, H. V. (2009). "Are the oral-facial-digital syndromes ciliopathies?" Am J Med Genet A **149A**(5): 1089-1095.

Toriello, H. V., B. Franco, A. L. Bruel and C. Thauvin-Robinet (1993). Oral-Facial-Digital Syndrome Type I. GeneReviews(R). R. A. Pagon, M. P. Adam, H. H. Ardinger et al. Seattle (WA).

Tran, P. V., C. J. Haycraft, T. Y. Besschetnova, A. Turbe-Doan, R. W. Stottmann, B. J. Herron, A. L. Chesebro, H. Qiu, P. J. Scherz, J. V. Shah, B. K. Yoder and D. R. Beier (2008). "THM1 negatively modulates mouse sonic hedgehog signal transduction and affects retrograde intraflagellar transport in cilia." Nat Genet **40**(4): 403-410.

Tran, P. V., G. C. Talbott, A. Turbe-Doan, D. T. Jacobs, M. P. Schonfeld, L. M. Silva, A. Chatterjee, M. Prysak, B. A. Allard and D. R. Beier (2014). "Downregulating hedgehog signaling reduces renal cystogenic potential of mouse models." J Am Soc Nephrol **25**(10): 2201-2212.

Tsurusaki, Y., T. Kosho, K. Hatasaki, Y. Narumi, K. Wakui, Y. Fukushima, H. Doi, H. Saitsu, N. Miyake and N. Matsumoto (2013). "Exome sequencing in a family with an X-linked lethal malformation syndrome: clinical consequences of hemizygous truncating OFD1 mutations in male patients." Clin Genet **83**(2): 135-144.

Tukachinsky, H., L. V. Lopez and A. Salic (2010). "A mechanism for vertebrate Hedgehog signaling: recruitment to cilia and dissociation of SuFu-Gli protein complexes." J Cell Biol **191**(2): 415-428.

Tunovic, S., K. W. Baranano, J. A. Barkovich, J. B. Strober, L. Jamal and A. M. Slavotinek (2015). "Novel KIF7 missense substitutions in two patients presenting with multiple malformations and features of acrocallosal syndrome." Am J Med Genet A **167A**(11): 2767-2776.

Urbe, S., H. Liu, S. D. Hayes, C. Heride, D. J. Rigden and M. J. Clague (2012). "Systematic survey of deubiquitinase localization identifies USP21 as a regulator of centrosome- and microtubule-associated functions." Mol Biol Cell **23**(6): 1095-1103.

Vaden, J. H., B. J. Bhattacharyya, P. C. Chen, J. A. Watson, A. G. Marshall, S. E. Phillips, J. A. Wilson, G. D. King, R. J. Miller and S. M. Wilson (2015). "Ubiquitin-specific protease 14 regulates c-Jun N-terminal kinase signaling at the neuromuscular junction." Mol Neurodegener **10**: 3.

van der Vaart, B., W. E. van Riel, H. Doodhi, J. T. Kevenaar, E. A. Katrukha, L. Gumy, B. P. Bouchet, I. Grigoriev, S. A. Spangler, K. L. Yu, P. S. Wulf, J. Wu, G. Lansbergen, E. Y. van Battum, R. J. Pasterkamp, Y. Mimori-Kiyosue, J. Demmers, N. Olieric, I. V. Maly, C. C. Hoogenraad and A. Akhmanova (2013). "CFEOM1-associated kinesin KIF21A is a cortical microtubule growth inhibitor." Dev Cell **27**(2): 145-160.

Varjosalo, M., S. P. Li and J. Taipale (2006). "Divergence of hedgehog signal transduction mechanism between Drosophila and mammals." Dev Cell **10**(2): 177-186.

Varshavsky, A. (2017). "The Ubiquitin System, Autophagy, and Regulated Protein Degradation." Annu Rev Biochem **86**: 123-128.

Verma, R., L. Aravind, R. Oania, W. H. McDonald, J. R. Yates, 3rd, E. V. Koonin and R. J. Deshaies (2002). "Role of Rpn11 metalloprotease in deubiquitination and degradation by the 26S proteasome." Science **298**(5593): 611-615.

Villumsen, B. H., J. R. Danielsen, L. Povlsen, K. B. Sylvestersen, A. Merdes, P. Beli, Y. G. Yang, C. Choudhary, M. L. Nielsen, N. Mailand and S. Bekker-Jensen (2013). "A new cellular stress response that triggers centriolar satellite reorganization and ciliogenesis." EMBO J **32**(23): 3029-3040.

Vora, S. M. and B. T. Phillips (2016). "The benefits of local depletion: The centrosome as a scaffold for ubiquitin-proteasome-mediated degradation." Cell Cycle **15**(16): 2124-2134.

Walsh, D. M., S. A. Shalev, M. A. Simpson, N. V. Morgan, Z. Gelman-Kohan, J. Chemke, R. C. Trembath and E. R. Maher (2013). "Acrocallosal syndrome: identification of a novel KIF7 mutation and evidence for oligogenic inheritance." Eur J Med Genet **56**(1): 39-42.

Wang, B., J. F. Fallon and P. A. Beachy (2000). "Hedgehog-regulated processing of Gli3 produces an anterior/posterior repressor gradient in the developing vertebrate limb." Cell **100**(4): 423-434.

Wang, B. and Y. Li (2006). "Evidence for the direct involvement of {beta}TrCP in Gli3 protein processing." Proc Natl Acad Sci U S A **103**(1): 33-38.

Wang, C., U. Ruther and B. Wang (2007). "The Shh-independent activator function of the full-length Gli3 protein and its role in vertebrate limb digit patterning." Dev Biol **305**(2): 460-469.

Wang, W., T. Wu and M. W. Kirschner (2014). "The master cell cycle regulator APC-Cdc20 regulates ciliary length and disassembly of the primary cilium." Elife **3**: e03083.

Wang, X., C. F. Chen, P. R. Baker, P. L. Chen, P. Kaiser and L. Huang (2007). "Mass spectrometric characterization of the affinity-purified human 26S proteasome complex." Biochemistry **46**(11): 3553-3565.

Washington Smoak, I., N. A. Byrd, R. Abu-Issa, M. M. Goddeeris, R. Anderson, J. Morris, K. Yamamura, J. Klingensmith and E. N. Meyers (2005). "Sonic hedgehog is required for cardiac outflow tract and neural crest cell development." Dev Biol **283**(2): 357-372.

Waters, A. M. and P. L. Beales (2011). "Ciliopathies: an expanding disease spectrum." Pediatr Nephrol **26**(7): 1039-1056.

Weatherbee, S. D., L. A. Niswander and K. V. Anderson (2009). "A mouse model for Meckel syndrome reveals Mks1 is required for ciliogenesis and Hedgehog signaling." Hum Mol Genet **18**(23): 4565-4575.

Webb, T. R., D. A. Parfitt, J. C. Gardner, A. Martinez, D. Bevilacqua, A. E. Davidson, I. Zito, D. L. Thiselton, J. H. Ressa, M. Apergi, N. Schwarz, N. Kanuga, M. Michaelides, M. E. Cheetham, M. B. Gorin and A. J. Hardcastle (2012). "Deep intronic mutation in OFD1, identified by targeted genomic next-generation sequencing, causes a severe form of X-linked retinitis pigmentosa (RP23)." Hum Mol Genet **21**(16): 3647-3654.

Weissman, A. M. (2001). "Themes and variations on ubiquitylation." Nat Rev Mol Cell Biol **2**(3): 169-178.

Wentzensen, I. M., J. J. Johnston, J. H. Patton, J. M. Graham, J. C. Sapp and L. G. Biesecker (2016). "Exome sequencing identifies a mutation in OFD1 in a male with Joubert syndrome, orofaciodigital spectrum anomalies and complex polydactyly." Hum Genome Var **3**: 15069.

Wilkinson, C. R., M. Seeger, R. Hartmann-Petersen, M. Stone, M. Wallace, C. Semple and C. Gordon (2001). "Proteins containing the UBA domain are able to bind to multi-ubiquitin chains." Nat Cell Biol **3**(10): 939-943.

Wilson, S. M., B. Bhattacharyya, R. A. Rachel, V. Coppola, L. Tessarollo, D. B. Householder, C. F. Fletcher, R. J. Miller, N. G. Copeland and N. A. Jenkins (2002). "Synaptic defects in ataxia mice result from a mutation in Usp14, encoding a ubiquitin-specific protease." Nat Genet **32**(3): 420-425.

Wong, S. Y. and J. F. Reiter (2008). "The primary cilium at the crossroads of mammalian hedgehog signaling." Curr Top Dev Biol **85**: 225-260.

Wyndham, A. M., R. T. Baker and G. Chelvanayagam (1999). "The Ubp6 family of deubiquitinating enzymes contains a ubiquitin-like domain: SUb." Protein Sci **8**(6): 1268-1275.

Xavier, G. M., M. Seppala, W. Barrell, A. A. Birjandi, F. Geoghegan and M. T. Cobourne (2016). "Hedgehog receptor function during craniofacial development." Dev Biol **415**(2): 198-215.

Xu, D., B. Shan, H. Sun, J. Xiao, K. Zhu, X. Xie, X. Li, W. Liang, X. Lu, L. Qian and J. Yuan (2016). "USP14 regulates autophagy by suppressing K63 ubiquitination of Beclin 1." Genes Dev **30**(15): 1718-1730.

Yamagishi, C., H. Yamagishi, J. Maeda, T. Tsuchihashi, K. Ivey, T. Hu and D. Srivastava (2006). "Sonic hedgehog is essential for first pharyngeal arch development." Pediatr Res **59**(3): 349-354.

Yang, Y., P. Guillot, Y. Boyd, M. F. Lyon and A. P. McMahon (1998). "Evidence that preaxial polydactyly in the Doublefoot mutant is due to ectopic Indian Hedgehog signaling." Development **125**(16): 3123-3132.

Yau, R. and M. Rape (2016). "The increasing complexity of the ubiquitin code." Nat Cell Biol **18**(6): 579-586.

Yuan, X., R. A. Serra and S. Yang (2015). "Function and regulation of primary cilia and intraflagellar transport proteins in the skeleton." Ann N Y Acad Sci **1335**: 78-99.

Zeng, H., J. Jia and A. Liu (2010). "Coordinated translocation of mammalian Gli proteins and suppressor of fused to the primary cilium." PLoS One **5**(12): e15900.

Zullo, A., D. Iaconis, A. Barra, A. Cantone, N. Messaddeq, G. Capasso, P. Dolle, P. Igarashi and B. Franco (2010). "Kidney-specific inactivation of Ofd1 leads to renal cystic disease associated with upregulation of the mTOR pathway." Hum Mol Genet **19**(14): 2792-2803.

Appendix

Ciliopathy proteins regulate paracrine signaling by modulating proteasomal degradation of mediators

Yangfan P. Liu,[1] I-Chun Tsai,[1] Manuela Morleo,[2] Edwin C. Oh,[1] Carmen C. Leitch,[3] Filomena Massa,[2] Byung-Hoon Lee,[4] David S. Parker,[1] Daniel Finley,[4] Norann A. Zaghloul,[3] Brunella Franco,[2,5] and Nicholas Katsanis[1]

[1]Center for Human Disease Modeling, Duke University, Durham, North Carolina, USA. [2]Telethon Institute of Genetics and Medicine, Naples, Italy. [3]Department of Medicine, Division of Endocrinology, Diabetes, and Nutrition, University of Maryland School of Medicine, Baltimore, Maryland, USA. [4]Department of Cell Biology, Harvard Medical School, Boston, Massachusetts, USA. [5]Department of Medical Translational Sciences, Federico II University, Naples, Italy.

Cilia are critical mediators of paracrine signaling; however, it is unknown whether proteins that contribute to ciliopathies converge on multiple paracrine pathways through a common mechanism. Here, we show that loss of cilopathy-associated proteins Bardet-Biedl syndrome 4 (BBS4) or oral-facial-digital syndrome 1 (OFD1) results in the accumulation of signaling mediators normally targeted for proteasomal degradation. In WT cells, several BBS proteins and OFD1 interacted with proteasomal subunits, and loss of either BBS4 or OFD1 led to depletion of multiple subunits from the centrosomal proteasome. Furthermore, overexpression of proteasomal regulatory components or treatment with proteasomal activators sulforaphane (SFN) and mevalonolactone (MVA) ameliorated signaling defects in cells lacking BBS1, BBS4, and OFD1, in morphant zebrafish embryos, and in induced neurons from *Ofd1*-deficient mice. Finally, we tested the hypothesis that other proteasome-dependent pathways not known to be associated with ciliopathies are defective in the absence of ciliopathy proteins. We found that loss of BBS1, BBS4, or OFD1 led to decreased NF-κB activity and concomitant IκBβ accumulation and that these defects were ameliorated with SFN treatment. Taken together, our data indicate that basal body proteasomal regulation governs paracrine signaling pathways and suggest that augmenting proteasomal function might benefit ciliopathy patients.

Introduction

In vertebrates, the cilium and the basal body are key components of paracrine signaling transduction. This has, in turn, suggested that phenotypes of ciliopathy patients might be attributed to defective paracrine signaling (1), including polydactyly due to defective sonic hedgehog (Shh) signaling (2) and renal cysts attributed to unbalanced Wnt signaling (3). Some data have raised the possibility that a fraction of these defects, especially Wnt, are driven by nonciliary functions of ciliary and basal body proteins (2, 4); other findings have indicated that the cilium/basal body Wnt roles are likely specific to discrete spatiotemporal contexts (5–9).

Although basal body and ciliary proteins are not signaling molecules per se, these structures are thought to operate as a hub for coordinating networks of signaling cascades. Components of various signaling pathways localize to basal body and cilium (10–13). Moreover, mutations in a single basal body or ciliary gene can lead to defects in more than one signaling pathway (11, 14), while loss-of-function mutations in signaling molecules such as the Shh regulator kinesin family member 7 (KIF7) (15, 16) and the Wnt/planar cell polarity (PCP) effector Fritz (17) cause ciliopathies in some families.

The increasing association of ciliary and basal body proteins with signaling defects led us to ask whether a common mechanism might account for the convergence of multiple pathways. One candidate, the ubiquitin-proteasome system (UPS), is attractive for three reasons. First, the basal body is known to be a proteolytic center (18–21). Second, we reported previously that disruption of some basal body proteins results in loss of proteasome-dependent degradation of β-catenin (5), a phenotype reproduced subsequently (22). Finally, we noted that, in addition to Wnt, proteasomal degradation is implicated in most paracrine signaling cascades known to be defective in basal body mutants. For example, in Notch-mediated lateral inhibition, a transmembrane ligand of the Delta-Serrate-LAG2 (DSL) family binds a transmembrane Notch receptor in the adjacent target cells (23). To reduce Notch signaling, DSL ligands are ubiquitinated, internalized, and degraded by the proteasome (24); similarly, the intracellular domain of the Notch receptor is degraded by the proteasome to reduce Notch signaling (25). Likewise, when Shh ligand is present, glioma-associated oncogenes 2 and 3 (GLI2/3) exist in their full-length activator forms, whereas they are truncated by proteasome-mediated proteolysis to their repressor forms when Shh is removed (26); both the activator and repressor forms of GLI2/3 are also degraded by the proteasome (27). Besides GLI2/3, suppressor of fused homolog (SUFU), a negative regulator of Shh signaling that physically localizes at the cilium, is also degraded in a proteasome-dependent manner (28).

Authorship note: Yangfan P. Liu, I-Chun Tsai, Manuela Morleo, and Edwin C. Oh contributed equally to this work.

Conflict of interest: The authors have declared that no conflict of interest exists.

Note regarding evaluation of this manuscript: Manuscripts authored by scientists associated with Duke University, The University of North Carolina at Chapel Hill, Duke-NUS, and the Sanford-Burnham Medical Research Institute are handled not by members of the editorial board but rather by the science editors, who consult with selected external editors and reviewers.

Citation for this article: *J Clin Invest.* 2014;124(5):2059–2070. doi:10.1172/JCI71898.

Given these observations, we wondered whether basal body and ciliary proteins might regulate multiple signaling pathways by controlling proteasome-mediated degradation of signaling mediators. We show that suppression of basal body–localized ciliopathy proteins led to defective proteasomal degradation of such mediators, which in turn caused dysfunction in three major cilia-associated signaling pathways (Shh, Wnt, and Notch) in vitro and in vivo. These observations are unlikely to reflect nonspecific cellular malaise; not only could the ciliopathy proteins tested here interact with specific regulatory subunits of the proteasome holoenzyme, but also depletion of each of Bardet-Biedl syndrome 4 (BBS4) and oral-facial-digital syndrome 1 (OFD1) selectively perturbed the subunit composition of the centrosomal proteasome. Further, signaling phenotypes due to depletion of BBS1, BBS4, and OFD1 could be rescued by activating proteasomal function. Finally, because the model predicts that other proteasome-dependent paracrine signaling pathways should also be defective in the absence of basal body proteins, we examined NF-κB signaling, a pathway that has not been linked previously to basal body (dys)function. Consistent with our prediction, loss of each of BBS1, BBS4, and OFD1 repressed NF-κB activity, which could be restored by activating the proteasome. Taken together, these findings suggest that proteasome-mediated basal body regulation might be a common mechanism for a multitude of signaling cascades and that proteasomal activation might be a potential treatment paradigm for ciliopathies.

Results

Accumulation of signaling mediators upon depletion of ciliopathy proteins. We and others have reported previously that perturbation of some ciliopathy proteins alters the stability of Wnt signaling mediators such as β-catenin and Dishevelled (5, 8, 21, 29, 30). To study the physiological relevance of these findings in vivo, we mated *Bbs4*$^{-/-}$ mice with a transgenic proteasome reporter mouse line expressing unstable ubiquitin–tagged GFP (31) to generate *Ub*^{G76V}*-Gfp Bbs4*$^{-/-}$ mice. As a hallmark of potential proteasomal dysfunction, we examined GFP levels in a broad range of tissues with known pathology in BBS and observed no aberrant GFP accumulation in the kidney and liver of *Ub*^{G76V}*-Gfp Bbs4*$^{-/-}$ mice (Figure 1A; full uncut gels are shown in the Supplemental Material.) and modest increases in components of the central nervous system (hippocampus, cortex, and cerebellum; Figure 1A). By contrast, we detected significant accumulation of GFP from P14 onward in the retinas of *Ub*^{G76V}*-Gfp Bbs4*$^{-/-}$ mice (Figure 1B). To identify which cell types were accounting for the GFP signal, we performed immunohistochemical analyses of retina from three *Ub*^{G76V}*-Gfp* WT and three *Ub*^{G76V}*-Gfp Bbs4*$^{-/-}$ mice (masked to the genotypes). Cryosections from *Ub*^{G76V}*-Gfp Bbs4*$^{-/-}$ mice revealed significant aggregation of GFP in the rod and cone photoreceptor layers consisting of the outer segment, inner segment, and outer nuclear layer (Figure 1C). This phenotype was restricted to photoreceptors (Figure 1C) and was unlikely to be secondary to retinal degeneration, as we observed no anatomical photoreceptor defects on P14, consistent with reported findings for other *Bbs* mouse mutants (29).

Given the specificity of GFP degradation defects in the photoreceptors of *Bbs4*$^{-/-}$ mice and previous data on the abnormal stability of β-catenin in BBS4-depleted cells (5), we next asked whether proteasomal dysfunction might be more broadly relevant to basal body–mediated paracrine signal regulation. If this is true, then: (a) other basal body proteins should have similar functions; and (b) other known basal body–mediated pathways should also be perturbed. To evaluate functional links between basal body proteins, we first conducted an in silico study to analyze a network of coexpressed basal body and ciliary genes through a publicly available online tool (http://netview.tigem.it), which reconstructs the regulatory interactions among genes from genome scale measurements of gene expression profiles (32). This analysis revealed a subset of centrosomal transcripts ($P = 3.5 \times 10^{-7}$) including *BBS1*, *BBS4*, and *OFD1* (Supplemental Figure 1; supplemental material available online with this article; doi:10.1172/JCI71898DS1). We thus considered the possibility that loss of OFD1 also leads to changes in the stability of signaling mediators.

We turned to an established cilium-dependent paracrine signaling pathway, Hedgehog signaling (Hh) (2), and developed an in vitro neural differentiation model, in which the embryonic WT murine stem cells (WTESs) and *Ofd1*-deficient murine embryonic stem cells (KOESs) were cultured to generate neural progenitors (Supplemental Figure 2), a model that recapitulates the multi-step process of neural development in embryos (33). KOESs are male murine cells containing a gene trap mutation in *Ofd1*. As *Ofd1* is located on the X chromosome, *Ofd1* KOESs are hemizygous for *Ofd1* and do not produce the protein (34). Comparing *Ofd1*^{WT} neurons derived from WTESs and *Ofd1*^{KO} neurons from KOESs, we found a significant increase in GLI2FL (full-length GLI2) and SUFU at the T8 time point in *Ofd1*-depleted neurons (Figure 2A). We also found increased levels of GLI2FL and SUFU in lysates from *Ofd1*$^{\Delta 4-5/+}$ heterozygous female mouse embryos (data not shown) and *Ofd1*$^{\Delta 4-5/y}$ hemizygous male mouse embryos (Supplemental Figure 3A) compared with levels observed in WT littermates (Figure 2B). In addition, GLI3FL (full-length GLI3) increased both in *Ofd1*^{KO} neurons (Figure 2A) and in *Ofd1*$^{\Delta 4-5/+}$ (data not shown) and *Ofd1*$^{\Delta 4-5/y}$ mutant embryos (Figure 2B), with a concomitant decrease in glioma-associated oncogene 3 repressor (GLI3R) levels (Figure 2, A and B, and Supplemental Figure 3, B and C).

Similar to Hh and Wnt signaling, Notch signaling is regulated through the cilium (13), and if the overarching hypothesis is correct, this pathway should also be perturbed in our mutants. As a first test, we cotransfected Flag-tagged Notch1 intracellular domain (NICD) into HEK-293-FT cells depleted of BBS4 by shRNA-mediated gene silencing (*pSuperBBS4*) (5). Immunoblot analysis of transfected cells revealed an elevation of NICD protein levels upon knockdown of *BBS4* (Figure 2C). Further, we asked whether loss of BBS4 modulates the protein levels of a DSL ligand, Jagged 1 (JAG1). We therefore assayed GFP-tagged JAG1 in BBS4-depleted and control cells. Similar to our findings with NICD, knockdown of *BBS4* also resulted in an elevation of GFP-JAG1 (Figure 2D).

Selective disruption of UPS caused by loss of ciliopathy proteins. Given our data on Wnt, Shh, and Notch and the fact that the processing of components from these paracrine signaling pathways is known to be mediated by the proteasome (11, 35), we asked whether proteasomal agonists could ameliorate the signaling phenotypes of basal body mutants.

The expression levels of three catalytic subunits of the proteasome, proteasome subunit β types 5, 6, and 7 (PSMB5, PSMB6, and PSMB7), as well as the corresponding peptidase activities, increase upon treatment with sulforaphane (36) [SFN; 1-isothiocyanato-4(R)-methylsulfinylbutane], an isothiocyanate extracted from cruciferous vegetables, rendering this compound an attractive initial substrate for our studies. We found that treatment with SFN rescued the accumulation of GLI2FL,

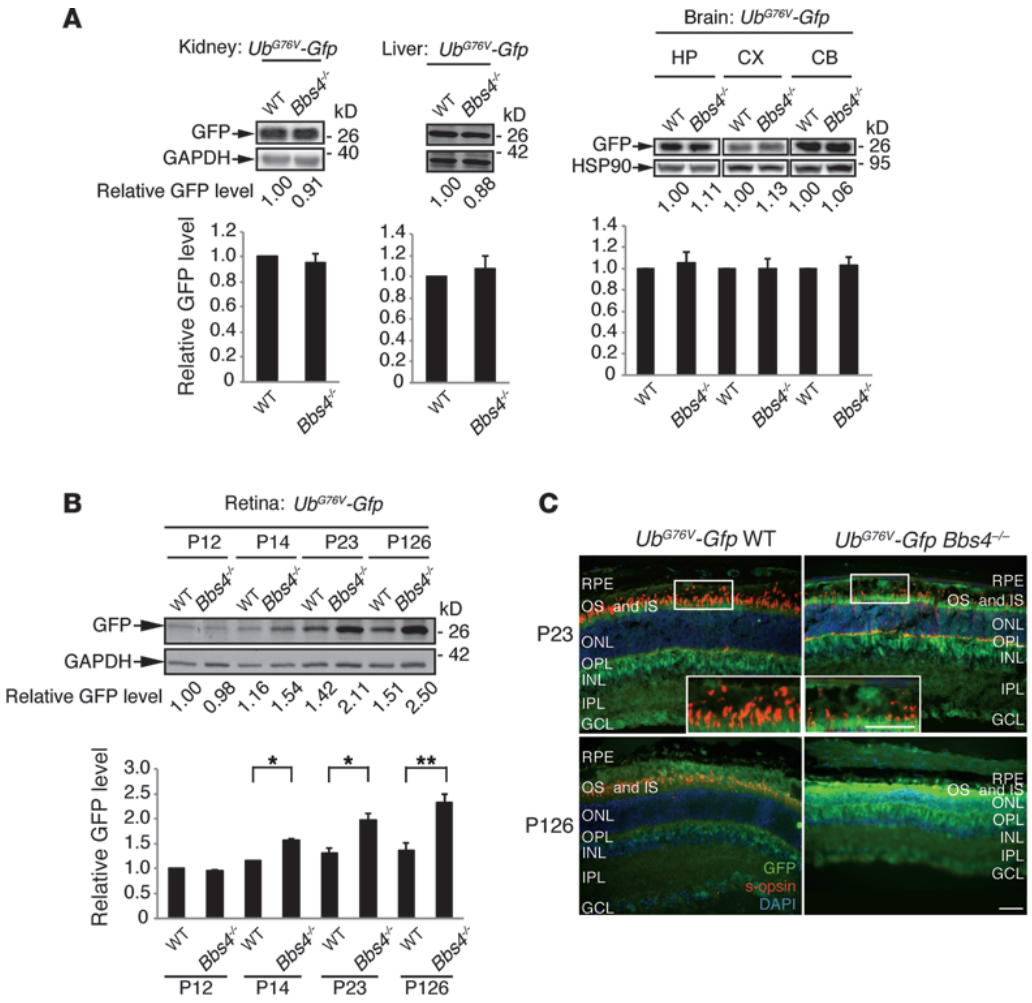

Figure 1

Accumulation of GFP in *Bbs4*$^{-/-}$ mice. (**A** and **B**) Immunoblotting with anti-GFP to examine the kidney (P80), liver (P144), several brain components (P80), and retina (P12–P126) (**B**) of *Ub*^{G76V}*-Gfp Bbs4*$^{-/-}$ mice, with *Ub*^{G76V}*-Gfp* WT littermates used as controls. Samples in each panel for the brain were run on the same gel but were noncontiguous. (**C**) Immunohistochemistry of retinal sections of P23 and P126 *Ub*^{G76V}*-Gfp* transgenic mice. Progressive retinal degeneration and GFP accumulation in photoreceptors (OS and IS, and ONL) were observed in *Bbs4*$^{-/-}$ mice, but not in WT littermates. OS was immunolabeled with anti–s-opsin; ONL and INL were labeled with DAPI staining. RPE, retinal pigment epithelium; OS, outer segment of the photoreceptors; IS, inner segment; ONL, outer nuclear layer; OPL, outer plexiform layer; INL, inner nuclear layer; IPL, inner plexiform layer; GCL, ganglion cell layer. White boxes delimit the enlarged images, showing OS and IS. HP, hippocampus; CX, cortex; CB, cerebellum. White boxes delimit the enlarged images, showing OS and IS. Scale bar: 25 μm in images and inserts. Bar graphs showing standard error of the mean are plotted adjacent to each blot. *$P < 0.05$; **$P < 0.01$.

GLI3FL, and SUFU in T8-derived *Ofd1*^{KO} neurons (Figure 3A). Consistent with the participation of the proteasome in both the processing and degradation of GLI2/3, treatment with SFN reduced GLI3R protein levels (Figure 3A and Supplemental Figure 3D). Moreover, SFN treatment of cells depleted of BBS4 also revealed a reduction in β-catenin protein levels relative to vehicle-treated cells (Figure 3B), suggesting that defects in proteasome-dependent processing and degradation of GLI2/3, SUFU, and β-catenin can be ameliorated.

Taken together, our data argue for a role of basal body proteins in regulating proteasome-mediated degradation and that we should observe a reciprocal signaling/proteasomal phenotype upon overexpressing our proteins of interest. We therefore overexpressed BBS4 in cells and observed a depletion of both NICD (Figure 3C and Supplemental Figure 3E) and JAG1 (Supplemental Figure 3F); further, we treated BBS4-overexpressing cells with two proteasome inhibitors, *N*-carbobenzoxyl-L-leucinyl-L-leucinyl-L-norleucinal (MG132) and lactacystin as well as DMSO vehicle as a control. While cells overexpressing BBS4 showed a 21%–50% reduction in total NICD levels (Figure 3C and Supplemental Figure 3E) and an approximately 50% ± 16% reduction in total JAG1 levels (Supplemental Figure 3F), treatment with MG132 and lactacystin restored NICD protein levels to 93% (Figure 3C) and 138% (Supplemental Figure 3E) of basal levels, respectively, and restored JAG1 levels to 99% ± 38% of basal levels (Supplemental Figure 3F), suggesting that BBS4 can facilitate the degradation of Notch signaling mediators in a proteasome-dependent manner.

Regulation of the proteasome complex by ciliopathy proteins. Although our observations in mouse mutants, zebrafish embryos (5), and cultured cells argue that the basal body proteins we studied are responsible for regulating the proteasome, the mechanism of that action is unclear, leaving the possibility that the observed phenotypes are surrogate effects of generalized cellular "malaise." We therefore explored the possibility of direct biochemical relationships between BBS1, BBS4, and OFD1 and the proteasome.

First, we conducted an unbiased mass spectrometry screen to identify putative OFD1-interacting proteins. This experiment uncovered a spectrum of proteasomal subunits including regulatory proteasome ATPase subunit 6 (RPT6), a finding confirmed by semiendogenous coimmunoprecipitation (Figure 4A). Independently, we tested for protein-protein interactions between multiple BBS proteins (BBS1, 2, 4, 5, 6, 7, 8, and 10) and several proteasomal subunits (proteasome subunit β type 1 subunit in the 20S particle [PSMB1], regulatory proteasome non-ATPase subunit

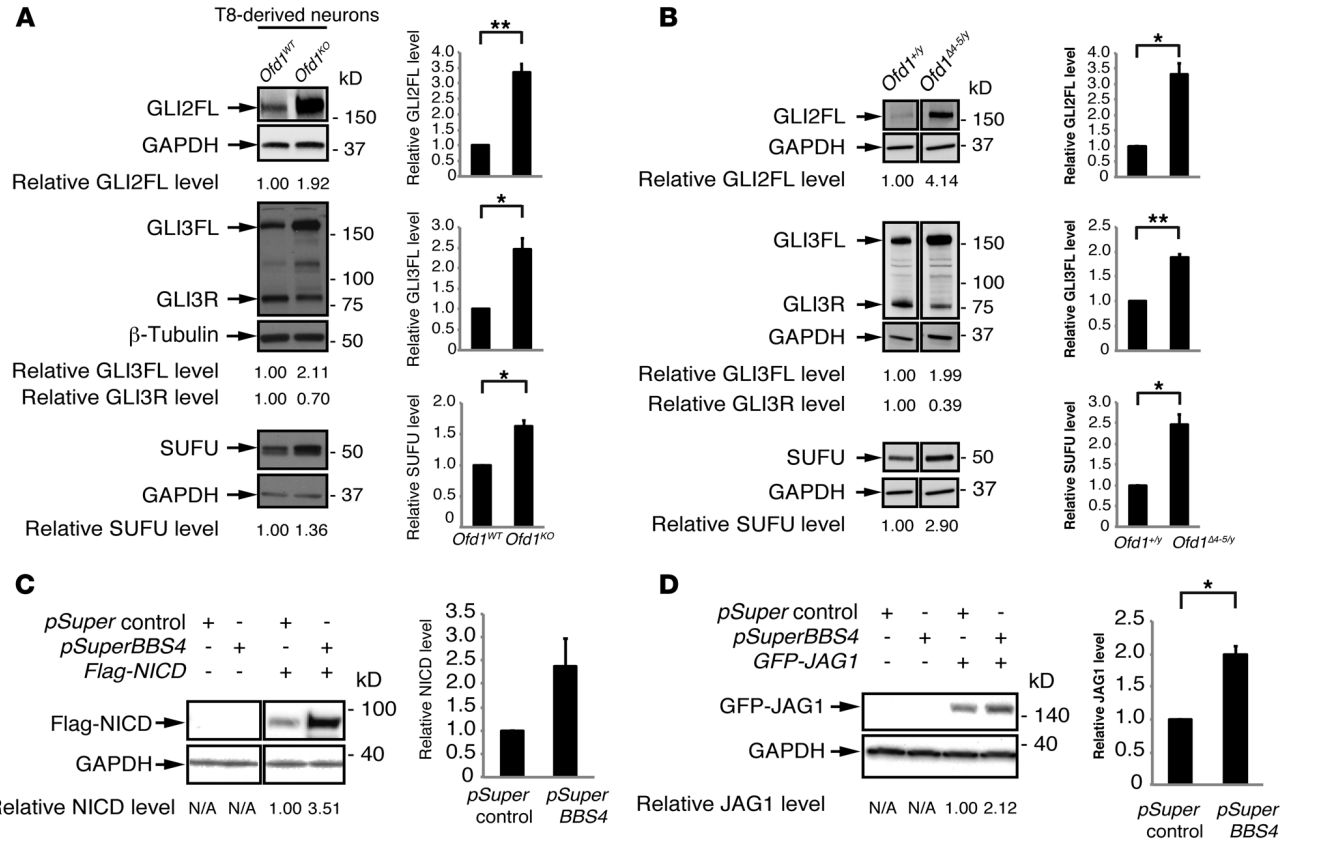

Figure 2

Accumulation of Shh and Notch signaling mediators upon depletion of ciliopathy proteins. (**A**) Accumulation of GLI2FL, GLI3FL, and SUFU as well as reduction of GLI3R in T8-derived *Ofd1*^{KO} neurons. (**B**) At E10.5, accumulation of GLI2FL, GLI3FL, and SUFU as well as reduction of GLI3R were detected in protein lysates from *Ofd1*$^{\Delta 4-5/y}$ mice, with *Ofd1*$^{+/y}$ mice used as controls. (**C**) Suppression of *BBS4* increases Flag-tagged NICD levels compared with those in *pSuper* controls. (**D**) Suppression of *BBS4* led to a 2-fold increase in GFP-tagged JAG1. The samples in each panel in **B** and **C** were run on the same gel but were noncontiguous. Bar graphs showing the SEM are plotted adjacent to each blot. **P* < 0.05; ***P* < 0.01.

10 [RPN10], regulatory proteasome non-ATPase subunit 13 [RPN13], RPT6, and non-19S regulatory subunit [PA28γ], selected based on antibodies available for subsequent experiments). Under stringent detergent conditions (1% Triton X-100), we confirmed the previously reported interaction between BBS4 and RPN10 (5) by semiendogenous coimmunoprecipitation (Figure 4A) and also observed a biochemical interaction of some BBS proteins (BBS1, BBS2, BBS4, BBS6, BBS7, and BBS8) with proteasomal components, while BBS5 and BBS10 did not interact with any tested proteasomal subunits (Supplemental Figure 4A). To test the physiological relevance of a BBS-proteasome interactome, we determined that BBS1 and RPN10 interacted at endogenous levels in protein lysates isolated from C57BL/6 mouse testes (Figure 4A).

To probe the relevance of these interactions, we asked whether loss of OFD1 or BBS4 alters the composition of the proteasome with respect to its subunits. Using a stable cell line expressing tagged regulatory proteasome non-ATPase subunit 11 (RPN11) (37), we suppressed OFD1, purified 26S proteasome complexes, and observed a robust reduction (60% ± 8%) of 26S-bound regulatory proteasome ATPase subunit 2 (RPT2) in OFD1-depleted cells in comparison with that in control, while total RPT2 protein abundance was not affected by OFD1 depletion (Figure 4B). We also assayed the fraction of 26S-bound RPN10 in BBS4-depleted cells and observed a modest but significant reduction (20% ± 3%) in RPN10 (Supplemental Figure 4B). Furthermore, we also tested the localization of RPN10 around the centrosome in HEK-293 cells depleted of BBS4 and OFD1 by quantifying the RPN10 signal that localized around centrosomal γ-tubulin; we did not observe appreciable changes in BBS4-depleted cells (data not shown), possibly because of a lack of spatial resolution. By contrast, we observed a 43% ± 2% reduction of pericentriolar RPN10 levels (normalized to cytoplasmic RPN10 levels) in OFD1-depleted cells (Figure 4C). Given these data, we tested whether loss of OFD1 or BBS4 altered the composition of RPN10, RPT2, and other proteasomal components by sedimentation. Based on the commercial availability of reliable antibodies against proteasomal subunits, we found that RPN10, RPN13, RPT2, and RPT6 were enriched in γ-tubulin–enriched fractions in control cells (Figure 4D and Supplemental Figure 4C). Depletion of OFD1 or BBS4, however, resulted in a shift in the peak expression of the proteasomal subunits (Figure 4D and Supplemental Figure 4C). Taken together, these data suggest that BBS proteins and OFD1 regulate the composition of the centrosomal proteasome, likely through direct biochemical interactions.

Activation of proteasomal components ameliorates signaling defects caused by loss of ciliopathy proteins that reside at the basal body. Our observations next led us to speculate that (a) if reduction of proteasomal

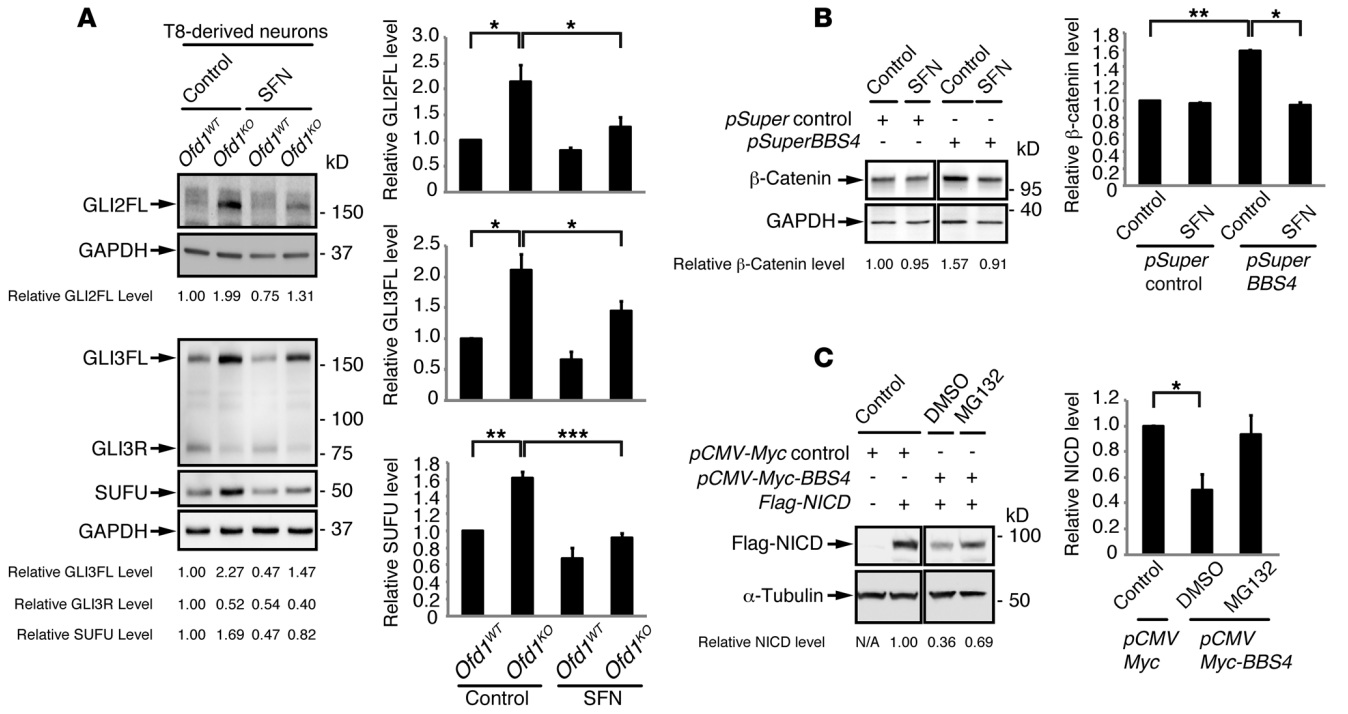

Figure 3

Disruption of proteasomal degradation caused by loss of ciliopathy proteins. (**A**) Treatment of proteasomal agonist SFN ameliorated the accumulation of GLI3FL, GLI2FL, and SUFU in T8-derived *Ofd1*^{KO} neurons. (**B**) Suppression of *BBS4* in HEK-293-FT cells led to a 1.57-fold increase in β-catenin protein levels that could be rescued by SFN. (**C**) Overexpression of *BBS4* reduced NICD levels. MG132 treatment restored Flag-NICD levels. Samples in each panel in **C** were run on the same gel but were noncontiguous. Bar graphs showing SEM are plotted adjacent to each blot. **P* < 0.05; ***P* < 0.01; ****P* < 0.001.

subunits in the centrosomal fraction of BBS4- or OFD1-depleted cells results in hampered degradation of signaling mediators, then increasing expression of the corresponding proteasomal subunits may ameliorate defective signaling phenotypes; and (b) activation of the proteasome might compensate for signaling defects.

We and others have reported previously that loss of ciliopathy proteins produces defects in convergent extension (CE) movements during gastrulation in zebrafish embryos (5, 29, 30). In addition to and independent of these phenotypes, we observed defects in the definition of somite boundaries in zebrafish embryos injected with morpholinos against *bbs* genes (*bbs* morphants [*bbs* MO]) (Supplemental Figure 5A and ref. 38). In vertebrates, somites develop as epithelial blocks at a temporal and spatial periodicity that is controlled, in part, by Notch signaling (39). Given the phenotypic overlap between *bbs* morphants and segmentation mutants (*mib*, *bea*, *des*, and *aei*) (39), as well as our biochemical Notch observations in BBS4-deficient cultured mammalian cells, we wondered whether dysfunction of these proteins might influence Notch signaling. Upon injection of the established *bbs4* morpholino (5, 38) into 1- to 8-cell-stage embryos, and scoring at the 9 ± 1 somite stage (9 ± 1 ss), 92% of embryos exhibited an expansion of the anteroposterior midline expression domain of *her4* (Supplemental Figure 5B), whose transcription is targeted directly by *notch1* activation (40). To differentiate between ectopic expression at developmental stages, when Notch signaling is already active, and the possibility that signaling is persistent throughout stages when it should be diminished, we performed an incremental developmental series of *her4* in situ hybridization over the first 5 days of development. Scoring WT embryos (staged by number of somites and, later, by the presence of anatomical features such as the swim bladder to ensure that embryos of the same age were compared across experiments), we observed that the expression of *her4* in neural structures of the head, including the developing forebrain, midbrain, hindbrain, and eye, was robust through 2.5 days post fertilization (dpf) and then began to wane. In *bbs4* morphants, we saw persistent *her4* expression through 5 dpf, especially in the eye (Supplemental Figure 5C).

Given the availability of experimentally tractable signaling phenotypes, we asked whether overexpression of proteasomal subunits that were seen to mislocalize in BBS4- and OFD1-depleted cells might rescue the *bbs4* and *ofd1* morphant phenotype. Upon blind scoring for the effects of coinjecting human *RPN10*, *RPN13*, or *RPT6* mRNA with the *bbs4* or *ofd1* morpholino, we measured substantial rescue of defective CE, somitic definition, and persistent *her4* expression (Figure 5A).

Next, as an independent test, we examined *bbs4* morphants coinjected with SFN, a known transcriptional activator of proteasomal subunits (36). Upon blind scoring at the 9 ± 1 ss, there was a significant reduction of *bbs4* morphants with CE and somitic defects ($P < 0.001$; Figure 5B). Moreover, coinjection of SFN with a *bbs4* morpholino ameliorated the ectopic expression of *her4* in neural structures at 4.5 dpf (Figure 5B). We also observed a similar rescue of *bbs1* and *ofd1* morphants, in which coinjection of SFN gave rise to the same robust rescue of defective CE phenotypes, somitic defects, and persistent *her4* expression as that observed in *bbs4* loss-of-function models (Figure 5, C and D).

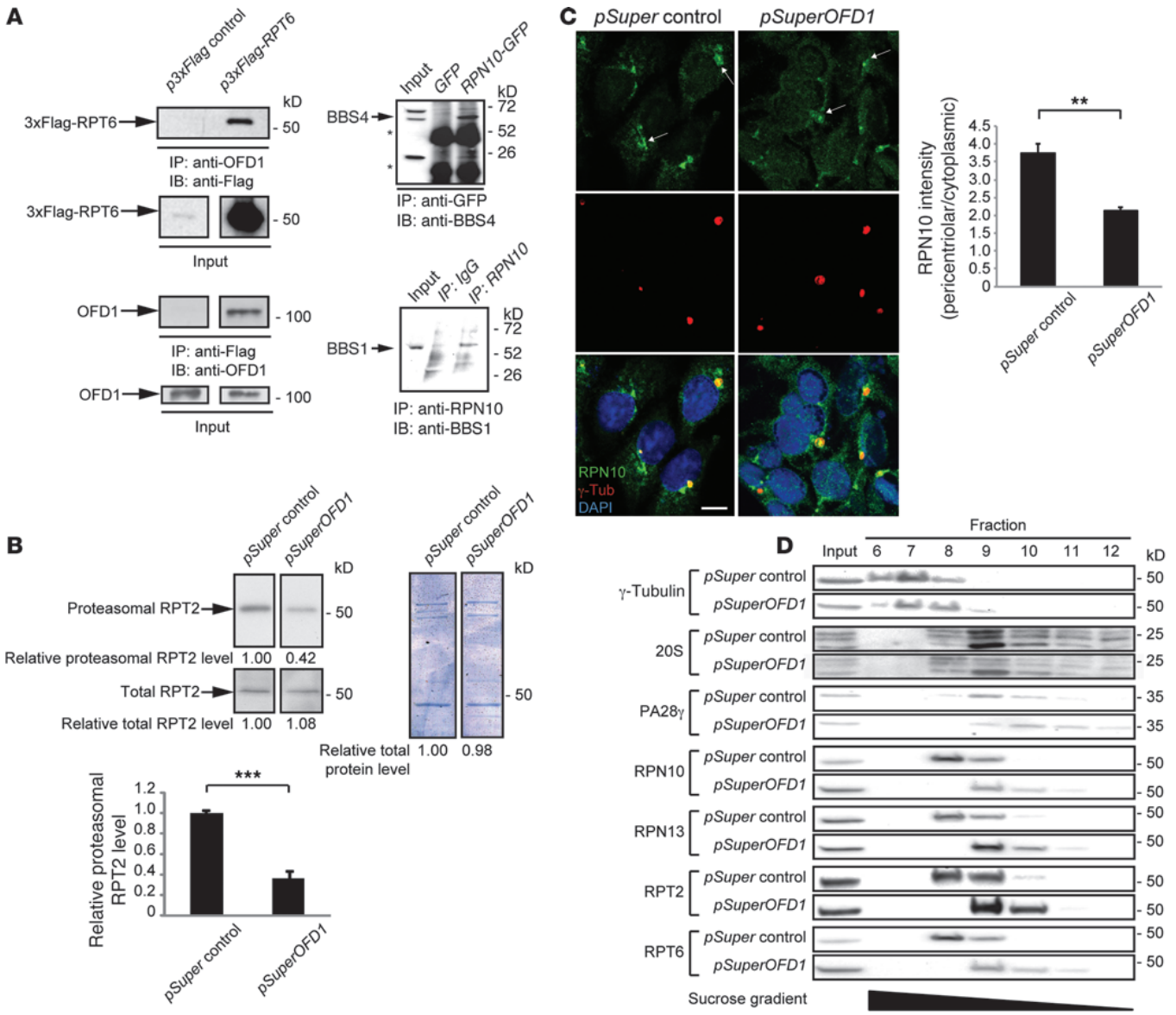

Figure 4

Ciliopathy proteins interact with proteasomal components and regulate proteasome composition. (**A**) Immunoblots show interaction between endogenous OFD1 and Flag-tagged RPT6 and endogenous BBS4 and GFP-tagged RPN10. An endogenous interaction was detected between BBS1 and RPN10 from protein lysate isolated from the testis of C57BL/6 mice. (**B**) Immunoblots show that suppression of OFD1 in HEK-293 cells reduced RPT2 protein levels in purified 26S proteasome. Densitometry measurements of proteasomal RPT2 protein levels were plotted ($n = 3$), and no significant difference in total RPT2 abundance was detected. Coomassie blue staining were carried out as a loading control and to measure the efficiency of the 26S proteasomal purification process. (**C**) Suppression of OFD1 in HEK-293 cells resulted in the reduction of pericentriolar RPN10 levels (normalized to cytoplasmic RPN10 levels) in OFD1-depleted cells. Scale bar: 10 μm. (**D**) HEK-293-FT cells transfected with *pSuper* control and *pSuperOFD1* were subjected to sucrose gradient centrifugation. Fractions (fractions 6–12 of 13 fractions) were then analyzed by immunoblotting with antibodies against γ-tubulin and proteasomal subunits. In control cells, the fractions enriched with all proteasome subunits partially overlapped with fractions enriched with γ-tubulin (fraction 8), and when OFD1 was depleted, peak levels of RPN10, RPN13, RPT2, and RPT6 shifted significantly and resulted in a decrease in the overlap between γ-tubulin–enriched fractions and 19S subunit–enriched fractions. $^{**}P < 0.01$; $^{***}P < 0.001$.

To substantiate the rescue effects of SFN, we used another proteasomal agonist, mevalonolactone [known as mevalonic acid lactone, mevalonate, and (±)-β-hydroxy-β-methyl-δ-valerolactone and abbreviated hereafter as MVA], to ask whether broad activation of the proteasome can alleviate basal body–dependent phenotypes. We coinjected MVA with the *bbs4* morpholino into zebrafish embryos, and upon blind scoring at 9 ± 1 ss, we found a reduction in *bbs4* morphant zebrafish with CE defects from 47.8% to 11.4% with MVA (Supplemental Figure 6). To investigate the persistence of Notch signaling in *bbs4* morphant zebrafish coinjected with MVA, we performed in situ hybridization for *her4*. Coinjection of MVA with a *bbs4* morpholino reduced *her4*

expression levels in neural structures, especially the retina, to those in WT zebrafish by 4.5 dpf (Supplemental Figure 6).

NF-κB signaling defects in basal body ciliopathy mutants can be rescued by activation of the proteasome. Our findings indicate that Wnt, Notch, and Shh phenotypes generated upon loss of three basal body proteins might converge at the point of proteasomal degradation. We therefore considered a model in which the basal body region serves as a broad regulator of paracrine signaling through proteasomal degradation. If this model is true, then (a) other paracrine pathways not implicated previously in ciliary/basal body biology, but known to be regulated by the proteasome, should exhibit signaling defects upon depletion of BBS proteins or OFD1; and (b) the model should also be able to predict the direction of the phenotype (suppressed or excessive signaling). To test this, we turned to NF-κB signaling, a pathway involved in inflammatory responses and lymphoid organogenesis with no known link to basal body (dys)function. In response to stimuli, IκBs are degraded by the proteasome, releasing NF-κB to translocate to the nucleus and activate the transcription of target genes (41).

We transfected HEK-293-FT cells with an NF-κB luciferase reporter plasmid containing three copies of the κB response elements of the murine MHC class I promoter (3X-κB-L). Cells stimulated by TNF-α and cotransfected with the *pSuperBBS4, pSuperBBS1*, and *pSuperOFD1* plasmids displayed a 55%, 53%, and 72% reduction in NF-κB activity, respectively, compared with that of control cells; incubation with SFN for 6 hours restored NF-κB activity (Figure 6, A–C). In cells with depleted basal body proteins, the direction of the NF-κB activity change (suppressive signaling) is opposite that of Wnt and Notch activity change (excessive signaling) (5, 22). This inverse relationship is consistent with our model, since the predicted basal body–regulated proteasomal degradation substrates are IκBs, which are negative regulators, while β-catenin and NICD are positive regulators. Also consistent with the luciferase assays, we observed accumulation of GFP-tagged IκBβ in *BBS4*-, *BBS1*-, or *OFD1*-suppressant cells, which can also be ameliorated by SFN treatment (Figure 6, D and E).

Finally, to probe the potential physiological relevance of the observed NF-κB data in vivo, we examined the expression and protein levels of the proteasomal substrate IκBβ in mice lacking *Ofd1*. Immunoblot analysis showed no differences in IκBβ protein levels on protein lysates from E10.5 $Ofd1^{\Delta 4-5/y}$ mutant embryos and controls (data not shown). Since loss of *Ofd1* in mice results in prenatal lethality, we generated and crossed *Ofd1*-floxed mice ($Ofd1^{fl}$) with a *CAG-Cre-ER*^{TM}–inducible general deletor line to examine IκBβ protein levels in postnatal *Ofd1* knockout mice. In $Ofd1^{fl/y}$ *CAG-Cre-ER*^{TM} ($Ofd1^{fl/y}$ *CKO*) mice, *Ofd1* inactivation was achieved at E18.5 by tamoxifen injection, and renal cysts were not observed at P8 (precystic stage). By P20, we observed a replacement of the renal parenchyma by cysts (cystic stage). Immunoblot analysis revealed an accumulation of IκBβ in protein lysates from kidney of $Ofd1^{fl/y}$ *CKO* male mice compared with controls; crucially, this phenotype was evident in both precystic and cystic stages (Figure 6F), suggesting that the accumulation of IκBβ is not a by-product of tissue disorganization and cystogenesis. At the precystic stage, mRNA levels of the IκBβ gene (*Nfkbib*) were lower in $Ofd1^{fl/y}$ *CKO* mice compared with mRNA levels in WT animals (Figure 6G), confirming that the accumulation of IκBβ is not due to increased mRNA transcription levels. *Nfkbib* mRNA levels were comparable between $Ofd1^{fl/y}$ *CKO* and controls at the cystic stage (Figure 6G).

Discussion

The study of ciliary and basal body proteins has highlighted a complex role for this cellular region in the regulation of signaling pathways. These observations have raised critical questions, including whether dedicated signaling transduction machinery aggregate around the cilium and basal body. Several transduction components have been localized to the basal body and/or the ciliary axoneme, including Smoothened, GLI proteins, SUFU, β-catenin, adenomatosis polyposis coli (APC), and Notch3 (8, 10, 11, 13, 29). At the same time, a model in which the cilium facilitates each pathway independently is difficult to reconcile with the fact that (a) with the possible exception of the PCP transducer Fritz (17) and the Shh motor KIF7 (15, 16), none of the other 60-plus genes and proteins mutated in human ciliopathies are components of a specific paracrine signaling pathway; (b) the phenotype of ciliopathy patients is a mixture of defects more consistent with a context-specific pathway dysfunction; and (c) animal models ablated for specific ciliary or basal body proteins exhibit multiple signaling defects (1).

Our data suggest a simpler model, in which at least some basal body proteins play a role in signal transduction regulation by exerting their primary effect not on a given pathway per se, but by regulating context-dependent proteolytic degradation. The alternative would be that the observed phenotypes are the nonspecific consequence of generalized cellular malaise and that the observed rescue effects were reflective of broad improvement in the ability of the cell to eliminate proteins targeted for degradation. Taken together, our experiments favor the former model. Cells and embryos suppressed or ablated for each of *BBS1*, *BBS4*, and *OFD1* had defects in proteasomal clearance of both reporter proteins and specific signaling components that included β-catenin, NICD, JAG1, GLI2, GLI3, SUFU, and IκBβ. It is also notable that the pronounced defects in proteasomal activity were concomitant with overt anatomical pathology in our murine models of disease, such as in the retina of *Bbs* mice and the cystic kidneys of conditional *Ofd1* animals, whereas no GFP accumulation was observed in *Bbs* mutant kidneys that, in our colony, never exhibited cyst formation.

We tested the robustness of the model in four ways: (a) by predicting that NF-κB signaling, which requires proteasomal degradation (41), but has no known ciliary link, would be defective in the absence of our proteins of interest; (b) by predicting the direction of the defect in NF-κB signaling; (c) by ameliorating the signaling defects for each tested pathway in vivo through the chemical upregulation of proteasomal components; and (d) by demonstrating that in the absence of some basal body proteins, the centrosomal proteasome is partially depleted of the various regulatory subunits whose overexpression also has an ameliorating defect in vivo.

Notably, we observed sucrose fraction sedimentation changes in multiple proteasomal subunits in the absence of OFD1 or BBS4, arguing that ciliopathy phenotypes are unlikely to be driven by specific defects in only one subunit, consistent with the observations that the mice haploinsufficient for the subunit RPN10 are phenotypically normal, at least by gross pathology, while homozygous $Rpn10^{-/-}$ mutants are embryonic lethal (42). An attractive mechanism is one in which basal body proteins regulate the composition of multiple subunits in the proteasome holoenzyme in a context-dependent manner. This is known to occur during cellular stress (43), and it is plausible that ciliary signaling can have a similar effect.

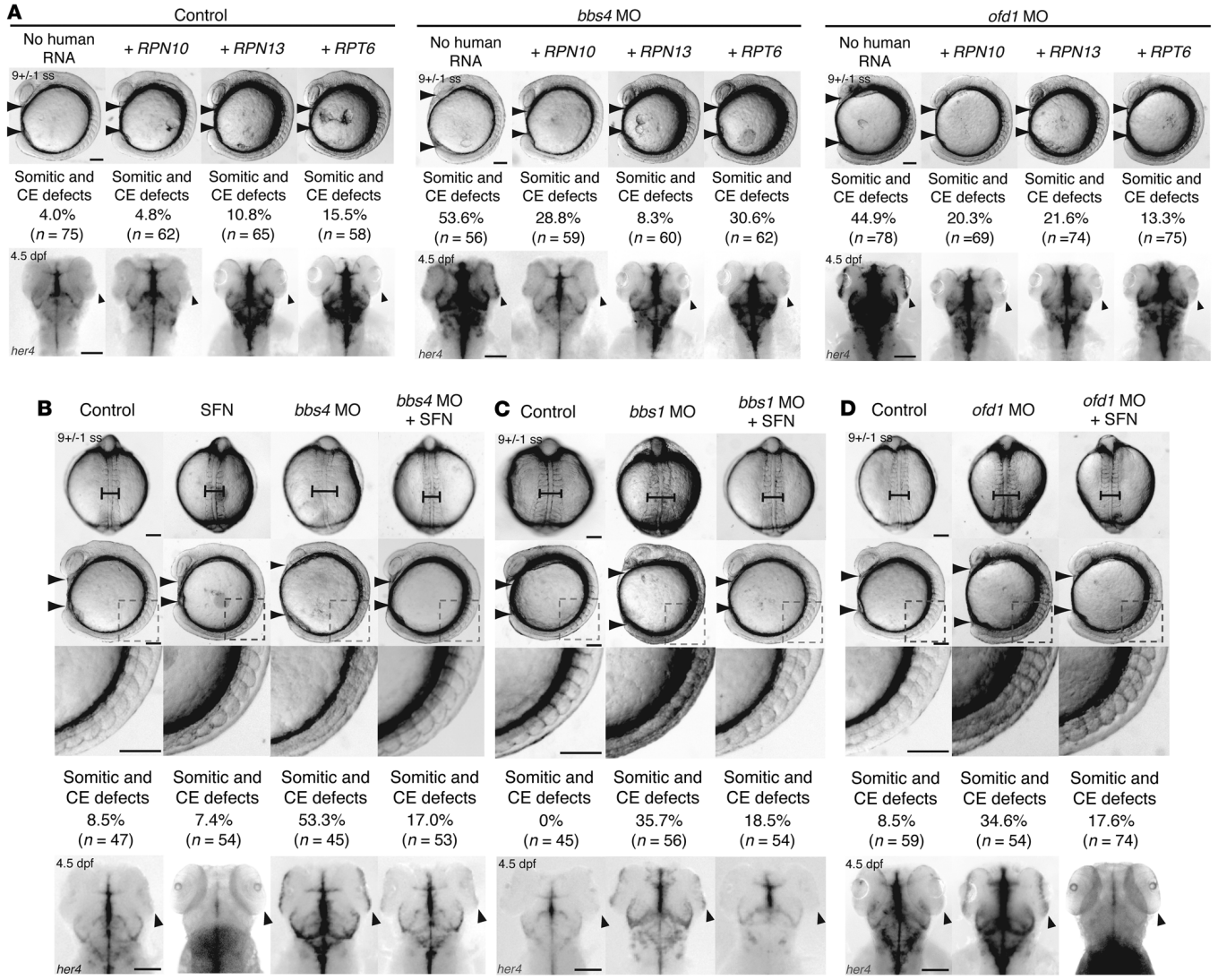

Figure 5

Activation of proteasome ameliorates signaling defects in *bbs* and *ofd1* morphant zebrafish embryos. (**A**) Coinjection of human *RPN10*, *RPN13*, and *RPT6* mRNA into *bbs4* and *ofd1* morphant zebrafish embryos rescued somitic and CE defects at the 9 ± 1 ss and ectopic expression of *her4* in the eye (arrowheads in lower row) at 4.5 dpf. CE defects were scored based on the body gap angle (arrowheads in upper row). Expression of *her4* was detected by whole-mount RNA in situ hybridization. (**B**, **C**, and **D**) Coinjection of SFN rescued somitic and CE defects as well as ectopic *her4* expression in *bbs4* (**B**), *bbs1* (**C**), and *ofd1* (**D**) morphant zebrafish embryos, while injection of SFN alone did not give rise to any obvious phenotype (**B**). As shown in the top row (dorsal view), the somites (bars) were longer in *bbs4* (**B**), *bbs1* (**C**), and *ofd1* (**D**) morphants and were shortened in morphant zebrafish embryos coinjected with SFN. In the second row (lateral view), the body gap angle (arrowheads) was greater in morphants and reduced in the presence of SFN. Dashed boxes delimit the enlarged images in the third row, showing the effects of SFN treatment on somite boundary definition defects. Percentage of embryos with somite boundary definition and CE defects and sample size (*n*) are noted below the images of each condition. Scale bars: 100 μm.

Moreover, it is likely that proteasomal dysfunction is only one contributor to the pathology of ciliopathies. The BBS proteins have been proposed to perforate vesicles and regulate vesicular transport, possibly into the ciliary axoneme, in a GTPase-dependent fashion (44), while BBS4 has also been reported to bind to EXOC7 (45). These data intimate additional layers of complexity, in which these proteins can either have both promoting and inhibitory functions with regard to proteasomal targeting or other subcellular surveying mechanisms, or might be themselves inhibited or activated by other ciliary and axonemal proteins in a spatiotemporal context. Emergent data suggest that the composition and function of primary cilia vary significantly across cell types (46). Such complexity might account for conflicting observations, in which each of the major signaling pathways mapped to date on this subcellular region have been shown to be activated, suppressed, or irrelevant in different tissues (4–6, 46, 47).

Finally, our findings indicate potential therapeutic applications. SFN has shown no toxic effects in humans and is currently being tested in several anticancer trials (48, 49). Should this compound show therapeutic benefit in rodent ciliopathy mod-

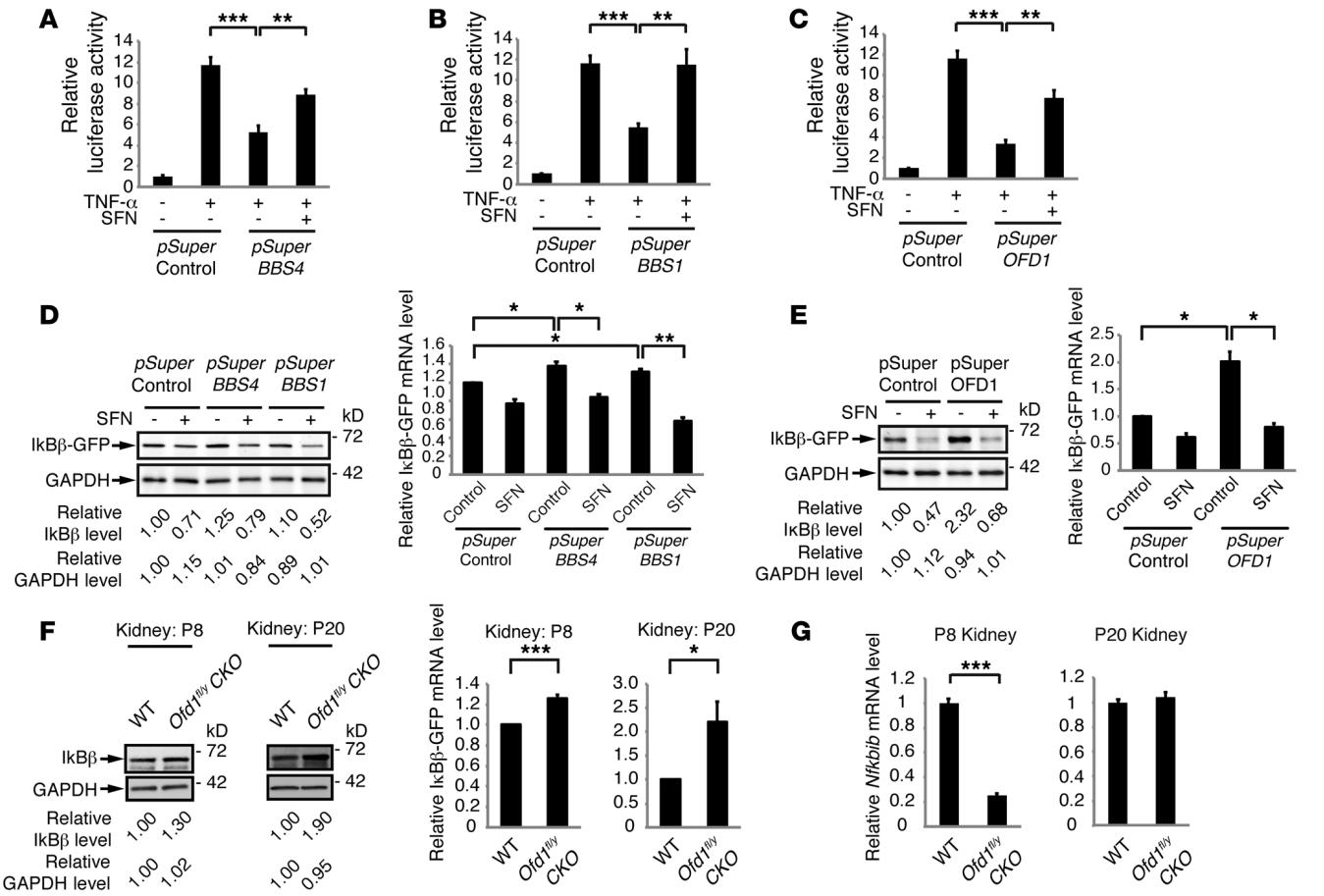

Figure 6

NF-κB signaling defects in BBS4-, BBS1-, and OFD1-depleted cells, and *Ofd1* conditional knockout mice. (**A**–**C**) Suppression of *BBS4* (**A**), *BBS1* (**B**), or *OFD1* (**C**) in HEK-293-FT cells led to decreased 3X-κB-L luciferase reporter responsiveness to a 12-hour TNF-α treatment. Incubation with SFN for 6 hours partially restored sensitivity to TNF-α stimulation ($n = 3$). (**D** and **E**) GFP-tagged IκBβ protein levels were higher in HEK-293-FT cells depleted of *BBS4*, *BBS1* (**D**), or *OFD1* (**E**) compared with those in control. SFN incubation rescued IκBβ-GFP accumulation. (**F**) Protein levels of IκBβ in kidney tissues isolated from *Ofd1*$^{fl/y}$ *CAG-Cre-ER*^{TM} (*Ofd1*$^{fl/y}$ *CKO*) mice at P8 (precystic stage) and P20 (cystic stage) were higher than the levels in kidney tissues from WT littermates. (**G**) mRNA levels of *IκBβ* (*Nfkbib*) in kidney tissues were lower in *Ofd1*$^{fl/y}$ *CKO* compared with mRNA levels in WT animals at P8 and were comparable between *Ofd1*$^{fl/y}$ *CAG-Cre-ER*^{TM} and controls at P20 ($n = 3$). Bar graphs showing SEM are plotted adjacent to each blot. *$P < 0.05$; **$P < 0.01$; ***$P < 0.001$.

els, it would be a candidate for clinical trials in some ciliopathy patients. More broadly, other SFN derivatives as well as unrelated proteasome agonists might also represent natural candidates. However, SFN is likely to confer a partial benefit that is possibly both genotype and subphenotype dependent. First, the observed rescue of embryos injected with the compound, although significant, was not complete. Second, SFN is unlikely to be of benefit to all pathway defects. The proteasome is known to degrade the negative regulator SUFU and both the activator and the repressor forms of GLI2/3; as such, it is likely that downstream Shh signaling defects will not be rescued. Likewise, long-term exposure to SFN repressed NF-κB activity (data not shown), suggesting that delivery, dosage, and duration of exposure might be critical. Finally, if basal body ciliopathy proteins participate in other cellular processes that regulate signaling, proteasomal modification will only be partially effective. Given our findings, however, a compound approach that includes targeting the proteasome may be of benefit.

Methods

Immunoblotting. Transfected cells and mouse tissues were lysed in modified RIPA buffer [150 mM sodium chloride, 50 mM Tris-HCl, pH7.4, 1% nonidet P-40, 0.1% sodium deoxycholate, 1 mM EDTA] with 1× proteasome inhibitor (Roche) and centrifuged at 4°C for 15 minutes. Protein concentration was measured by Lowry assay using the DC Protein Assay Kit (Bio-Rad) on a DU 530 Life Science UV/Vis Spectrophotometer (Beckman Coulter). Total protein in each sample was separated by SDS-PAGE on 4% to 15% Mini-PROTEAN TGX Precast Gel (Bio-Rad) with a Spectra Multicolor Broad Range Protein Ladder (Fermentas) and transferred to an Immun-Blot PVDF Membrane (Bio-Rad). The membrane was blocked with 5% nonfat milk or 5% BSA (Sigma-Aldrich) and probed with the following commercial primary antibodies: anti-GAPDH (ab9484 from Abcam or sc-32233 from Santa Cruz Biotechnology Inc.); anti-GFP (sc-8334; Santa Cruz Biotechnology Inc. or ab13970; Abcam); anti-HSP90 (sc-7947; Santa Cruz Biotechnology Inc.); anti-GLI2 (AF3635; R&D Systems); anti-GLI3 (AF3690; R&D Systems); anti-SUFU (sc-10934; Santa Cruz Biotechnology Inc.); anti-Flag (F7425; Sigma-Aldrich); anti-catenin (sc-7199; Santa Cruz

Biotechnology Inc.); anti–α-tubulin (T6199; Sigma-Aldrich); anti-NICD (ab8925; Abcam); anti-hsOFD1 (rabbit polyclonal antisera against human full-length OFD1 NM_003611); anti-mmOFD1 (rabbit polyclonal antisera against a portion of murine OFD1 NM_177429 aa 461-884); anti-BBS4 (AB15009; Millipore); anti-BBS1 (a166613; Abcam); anti–γ-tubulin (T7451; Sigma-Aldrich); anti-20S (NB600-1016; Novus); anti-PA28γ (NBP1-54587; Novus); anti-RPN10 (ab20239; Abcam); anti-RPN13 (H00011037-M01; Novus); anti-RPT2 (AP-107; Boston Biochem); anti-RPT6 (BML-PW9265; Enzo Life Sciences); anti-IκBβ (sc-9248; Santa Cruz Biotechnology Inc.); anti-Myc (m4439; Sigma-Aldrich); and anti-HA (ab16918; Abcam). Densitometric analysis was performed with Image Lab (Bio-Rad), Quantity One (Bio-Rad), or ImageJ 1.44p (NIH) software.

Immunohistochemistry. Mouse eyes were fixed in 4% PFA, followed by immersion in sucrose (10%, 20%, and 30%) in PBS. With the lens removed, eyecups were embedded in Optimal Cutting Temperature Compound (Sakura) and flash frozen. Cryosections were blocked with 10% FBS in PBS and probed with primary antibodies anti-GFP (ab13970; Abcam) and anti–S-opsin (a gift from Jeremy Nathans, Johns Hopkins University, Baltimore, Maryland, USA), followed by secondary antibodies Alexa Fluor 488 IgG (Invitrogen) and Alexa Fluor 594 IgG (Invitrogen). Nuclei were stained with DAPI (Roche). Images were captured with a Nikon Eclipse 90i microscope.

Bioinformatic analyses. We selected a subset of 271 transcripts that included: (a) transcripts mutated in human ciliopathies; (b) transcripts that, when mutated in animal models, give rise to ciliary dysfunction; (c) a group of transcripts found in at least three of the available datasets of ciliary proteins (50); and (d) a subset of transcripts recently shown to be modulators of ciliogenesis and cilium length (51). The publicly available online tool (http://netview.tigem.it) was used to analyze the regulatory interactions among genes from genome-scale measurements of gene expression profiles (microarrays) (32).

ES cell–derived in vitro neural differentiation. The *Ofd1*-deficient E14Tg2A.4 KOES line was obtained from BayGenomics. Both WT and *Ofd1* KOESs were maintained in an undifferentiated state by culture on a monolayer of mitomycin C–inactivated fibroblasts in the presence of leukemia-inhibiting factor (LIF). To induce neural differentiation, we followed previously described protocols (33). Briefly, 48 hours after ES cells were seeded on gelatin-coated plates, they were dissociated and plated on gelatin-coated plates at 1,000 cells/cm^2 on day 0 (T0). The culture medium for neuronal differentiation (serum-free KnockOut Serum Replacement–supplemented medium; Invitrogen) contained knockout DMEM supplemented with 15% KSR (Invitrogen), 2 mM L-glutamine, 100 U/ml penicillin-streptomycin, and 0.1 mM β-mercaptoethanol and was replaced daily during the differentiation process.

Cell culture, DNA transfection, and drug treatment. HEK-293 or HEK-293-FT cells and human dermal fibroblasts were grown in DMEM (Invitrogen) containing 10% FBS (Invitrogen) and 2 mM L-glutamine (Invitrogen), hTERT-RPE1 cells in DMEM and Ham's F-12 Nutrient 1:1 mixture (DMEM/F-12; Invitrogen) with 10% FBS and 2 mM L-glutamine. FuGene6 Transfection Reagent (Roche) was used for transfection of expression constructs (including the Notch1-NICD expression construct, a gift from Nicholas Gaiano, Johns Hopkins University, Baltimore, Maryland, USA), shRNA-expressing plasmids, and luciferase reporter plasmids; then cells were cultured for 72 hours. Drug treatment was carried out at a final concentration of 10 μM SFN (Sigma-Aldrich) for 6 to 24 hours, 30 μm *N*-carbobenzoxyl-L-leucinyl-L-leucinyl-L-norleucinal (MG132; Calbiochem) for 5 hours, 20 μM lactacystin (EMD Bioscience) for 5 hours, and 50 ng/ml TNF-α (Sigma-Aldrich) for 12 hours.

IP. For IP, approximately 1 mg of whole-cell, embryo, or tissue lysate was incubated with anti-OFD1, anti-Flag, or anti-GFP at 4°C overnight, followed by incubation with protein G–coupled agarose beads (Santa Cruz Biotechnology Inc.) at 4°C for 1 hour, or directly with anti-Flag M2 beads (A2220 Sigma-Aldrich). The beads were collected and washed with IP buffer (10% glycerol, 50 mM Tris-HCl [pH 7.5], 2.5 mM MgCl2, 1% NP40, and 200 mM NaCl). Proteins conjugated with the beads were then denatured and separated from the beads by boiling at 95°C to 100°C for 5 minutes before processing for immunoblotting.

Affinity purification of proteasome complex. The 26S proteasome complex was purified following a previously described protocol (52) with modifications. Briefly, HEK-293-FT cells expressing stable HTBH-tagged hRPN11 (a gift from Lan Huang, University of California, Irvine, California, USA) were transfected with either *pSuper* control plasmid or *pSuperBBS4* to knock down *BBS4* expression. Seventy-two hours after transfection, cells were lysed in buffer A (100 mM NaCl, 50 mM Tris-HCl [pH 7.5], 10% glycerol, 2 mM ATP, 1 mM DTT, and 5 mM $MgCl_2$) with 1× proteasome inhibitor (Roche). Lysates were centrifuged at 4°C for 15 minutes to remove cell debris. To purify proteasomes, an aliquot of the supernatant was incubated with streptavidin beads at 4°C overnight to precipitate HTBH-RPN11. The beads were then washed with buffer A three times, followed by one washing with TEB buffer (50 mM Tris-HCl, pH 7.5 and 10% glycerol). Finally, the beads were incubated in TEB buffer containing 1% TEV protease at 30°C for 1 hour, before SDS-PAGE and immunoblotting with anti-RPN10 (ab20239; Abcam).

Immunocytochemistry. HEK-293 cells cultured on coverslips were fixed in methanol, blocked in normal goat serum (1:10 in PBS containing 5% BSA), and then probed with anti-RPN10 and anti–γ-tubulin, followed by secondary antibodies Alexa Fluor 488 IgG and Alexa Fluor 568 IgG. Finally, nuclei were visualized with Hoechst 33258 (Sigma-Aldrich). Images were captured with a Zeiss LSM 710 confocal microscope and analyzed with ImageJ 1.44p software.

Sucrose gradient sedimentation. HEK-293-FT cells were transfected and treated with nocodazole (10 μg/ml) and cytochalasin B (5 μg/ml) for 1 hour at 72 hours after transfection. To collect cytoplasmic lysates, cells were harvested in lysis buffer (1 mM HEPES [pH 7.3], 0.5% NP-40, 0.5 mM $MgCl_2$, 0.1% β-ME, and 1× protease inhibitor), followed by centrifugation at 2,500 *g* for 10 minutes. After 10 mM HEPES and 5 U/ml DNase treatment for 30 minutes on ice, 1 ml of cytoplasmic lysates was layered on a discontinued sucrose gradient (70%, 50%, and 40% sucrose in the buffer containing 10 mM PIPES [pH 7.2], 0.1% NP-40, and 0.1% β-ME) and centrifuged for 1 hour at 195,000 *g*; 2% of lysates were kept before ultracentrifugation and served as an input. After ultracentrifugation, 13 fractions were collected and analyzed by immunoblotting.

Microinjection of morpholinos, mRNA, and sulforaphane. Morpholinos against *bbs1* (5′-CACACGTCCATCACTAACCAATAGC-3′), *bbs4* (5′-CCGTTCTCATAGCGTCGTCCGCCAT-3′), and *ofd1* (5′-ATCTTCTC-TACTGCAACACACATAC-3′) were purchased from Gene Tools, LLC. Human *RPN10*, *RPN13*, and *RPT6* mRNA were in vitro transcribed with an mMESSAGE mMACHINE SP6 Kit (Ambion). SFN was dissolved in DMSO (Sigma-Aldrich) at a stock concentration of 1 M and further diluted in water to 10 mM. The morpholino and mRNA or SFN were mixed, and a volume of 0.5 nl was microinjected.

Whole-mount RNA in situ hybridization. Zebrafish embryos were fixed overnight in 4% PFA at 4°C. Residual pigment was removed by bleaching with 3% H_2O_2/0.5% KOH. Whole-mount RNA in situ hybridization was performed with a digoxigenin-labeled anti-*her4* RNA probe (a gift from Tohru Ishitani, Kyush University, Fukuoka, Kyushu, Japan) synthesized by in vitro transcription (Roche), followed by immunological detection with Anti-Digoxigenin-AP, Fab Fragments (Roche) and nitro blue tetrazolium/5-bromo-4-chloro-3-indolyl-phosphate staining (Roche).

Luciferase reporter system assays. HEK-293-FT cells were seeded in 24-well plates at a density of 10^4 cells/well. After 24 hours, cells were transfected with expression constructs, short-hairpin plasmids, and a 3X-κB-L reporter (a gift from Tom Gilmore, Boston University, Boston, Massachusetts, USA) for NF-κB signaling. A pRL-SV40 plasmid expressing *Renilla* luciferase was used as an internal control. Seventy-two hours after transfection, cells were lysed with Passive Lysis Buffer (Promega). The luciferase activity of lysates was measured with the Dual Luciferase Reporter Assay System (Promega) on a FLUOstar Omega microplate reader (BMG LABTECH) and analyzed with MARS Data Analysis Software (BMG LABTECH).

Generation of Ofd1$^{fl/y}$ CAG-Cre-ER^{TM} mice by tamoxifen injections. *Ofd1$^{fl/+}$* females were crossed with *CAG-Cre-ER^{TM}* mice, a general deletor Cre line in which Cre-ER is ubiquitously expressed after tamoxifen injection. We treated pregnant mothers with a single i.p. injection of 100 μg tamoxifen/g of weight at E18.5. Tamoxifen (Sigma-Aldrich) was diluted in 10% ethanol and 90% sesame oil at a final concentration of 10 mg/ml. Quantification of *Ofd1* inactivation was assessed by quantitative RT-PCR (qRT-PCR) (data not shown).

Real-time qRT-PCR analyses. Total RNA was isolated with TRIzol (Invitrogen). The cDNA was synthesized from 5 μg of total RNA using SuperScript III (Invitrogen). qRT-PCR was performed with Power SYBR Green PCR Master Mix (Applied Biosystems) on a 7900HT Fast Real-Time PCR System (Applied Biosystems). The primers *Nfkbib* forward (5′-TTGGCTACGTCACTGAGGATG-3′) and *Nfkbib* reverse (5′-GCTCATGCTGATGAATCACAGC-3′) were used to test mRNA levels of *Nfkbib*, while the primers *ofd1* forward (5′-TGGCAGACCACTTACAAAGATG-3′) and *ofd1* reverse (AGACTGGATGAGGGGTTAATC-3′) were used to examine the conditional knockout efficiency, and the primers *gapdh* forward (5′-TCTTCTGGGTGGCAGTGAT-3′) and *gapdh* reverse (5′-TGCACCACCAACTGCTTAGC-3′) were used as internal controls. Real-time data were collected and analyzed with the Sequence Detection System software package, version 2.3 (Applied Biosystems).

Statistics. A one-tailed Student's *t* test was performed to compare the means of two populations. In the bar graphs, data represent the mean ± SEM of multiple repeats ($n \geq 3$). A χ^2 test was performed to compare two populations with several subgroups of different proportions. Statistical significance of differences between samples are indicated by $^*P < 0.05$, $^{**}P < 0.01$, and $^{***}P < 0.001$. A *P* value less than 0.05 was considered significant.

Study approval. Zebrafish and mouse studies were approved by the IACUC of Duke University (protocol A229-12-08 and A251-12-09) and by the IACUC of Cardarelli Hospital (Naples, Italy), to which the Telethon Institute of Genetics and Medicine (TIGEM) refers, and were authorized by the Italian Ministry of Health. The Cardarelli Hospital Ethics Committee (Naples, Italy) approved this study.

Acknowledgments

We thank Gopuraja Dharmalingam and the TIGEM Bioinformatic Core for the bioinformatic analysis, Nicholas Gaiano (Johns Hopkins University) for the Notch1-NICD expression constructs, Tom Gilmore (Boston University) for the 3X-κB-L reporter, Lan Huang (University of California, Irvine) for the HEK-293 cells stably expressing HTBH-hRPN11, Tohru Ishitani (Kyush University) for the *her4* probe plasmid, and Jeremy Nathans (Johns Hopkins University) for the anti–s-opsin antibody. This work was supported by grants from the NIH (NRSA fellowship F32DK094578, to I.-C. Tsai; R37GM04360, to D. Finley; K01DK092402, to N. A. Zaghloul; and R01HD04260, R01DK072301, and R01DK075972, to N. Katsanis), the Macular Vision Research Foundation and the Foundation for Fighting Blindness (to N. Katsanis), Telethon (TGM11CB3, to B. Franco), and the 7th Framework Large Integrated Project Syscilia (241955, to N. Katsanis and B. Franco). E.C. Oh is a NARSAD Young Investigator Award recipient. N. Katsanis is a Distinguished George W. Brumley Professor.

Received for publication July 1, 2013, and accepted in revised form February 6, 2014.

Address correspondence to: Brunella Franco, Telethon Institute of Genetics and Medicine, Via Pietro Castellino 111, 80131 Naples, Italy. Phone: 39.081.6132207; Fax: 39.081.5790919; E-mail: franco@tigem.it. Or to: Nicholas Katsanis, 466A Nanaline Duke Building, Box 3709, Duke University Medical Center, Durham, North Carolina 27710, USA. Phone: 919.613.4694; Fax: 919.684.1627; E-mail: katsanis@cellbio.duke.edu.

1. Hildebrandt F, Benzing T, Katsanis N. Ciliopathies. *N Engl J Med*. 2011;364(16):1533–1543.
2. Eggenschwiler JT, Anderson KV. Cilia and developmental signaling. *Annu Rev Cell Dev Biol*. 2007; 23:345–373.
3. Lancaster MA, Gleeson JG. Cystic kidney disease: the role of Wnt signaling. *Trends Mol Med*. 2010;16(8):349–360.
4. Ocbina PJ, Tuson M, Anderson KV. Primary cilia are not required for normal canonical Wnt signaling in the mouse embryo. *PLoS One*. 2009;4(8):e6839.
5. Gerdes JM, et al. Disruption of the basal body compromises proteasomal function and perturbs intracellular Wnt response. *Nat Genet*. 2007; 39(11):1350–1360.
6. Lancaster MA, Schroth J, Gleeson JG. Subcellular spatial regulation of canonical Wnt signalling at the primary cilium. *Nat Cell Biol*. 2011;13(6):700–707.
7. Simons M, et al. Inversin, the gene product mutated in nephronophthisis type II, functions as a molecular switch between Wnt signaling pathways. *Nat Genet*. 2005;37(5):537–543.
8. Corbit KC, et al. Kif3a constrains β-catenin-dependent Wnt signalling through dual ciliary and non-ciliary mechanisms. *Nat Cell Biol*. 2008; 10(1):70–76.
9. Oh EC, Katsanis N. Context-dependent regulation of Wnt signaling through the primary cilium. *J Am Soc Nephrol*. 2013;24(1):10–18.
10. Corbit KC, Aanstad P, Singla V, Norman AR, Stainier DY, Reiter JF. Vertebrate Smoothened functions at the primary cilium. *Nature*. 2005; 437(7061):1018–1021.
11. Haycraft CJ, Banizs B, Aydin-Son Y, Zhang Q, Michaud EJ, Yoder BK. Gli2 and Gli3 localize to cilia and require the intraflagellar transport protein polaris for processing and function. *PLoS Genet*. 2005;1(4):e53.
12. Schneider L, et al. PDGFRalphaalpha signaling is regulated through the primary cilium in fibroblasts. *Curr Biol*. 2005;15(20):1861–1866.
13. Ezratty EJ, Stokes N, Chai S, Shah AS, Williams SE, Fuchs E. A role for the primary cilium in Notch signaling and epidermal differentiation during skin development. *Cell*. 2011;145(7):1129–1141.
14. Cano DA, Murcia NS, Pazour GJ, Hebrok M. Orpk mouse model of polycystic kidney disease reveals essential role of primary cilia in pancreatic tissue organization. *Development*. 2004;131(14):3457–3467.
15. Dafinger C, et al. Mutations in KIF7 link Joubert syndrome with Sonic Hedgehog signaling and microtubule dynamics. *J Clin Invest*. 2011;121(7):2662–2667.
16. Putoux A, et al. KIF7 mutations cause fetal hydrolethalus and acrocallosal syndromes. *Nat Genet*. 2011; 43(6):601–606.
17. Kim SK, et al. Planar cell polarity acts through septins to control collective cell movement and ciliogenesis. *Science*. 2010;329(5997):1337–1340.
18. Wigley WC, et al. Dynamic association of proteasomal machinery with the centrosome. *J Cell Biol*. 1999;145(3):481–490.
19. Fabunmi RP, Wigley WC, Thomas PJ, DeMartino GN. Activity and regulation of the centrosome-associated proteasome. *J Biol Chem*. 2000; 275(1):409–413.
20. Li J, et al. USP33 regulates centrosome biogenesis via deubiquitination of the centriolar protein CP110. *Nature*. 2013;495(7440):255–259.
21. Mahuzier A, et al. Dishevelled stabilization by the ciliopathy protein Rpgrip1l is essential for planar cell polarity. *J Cell Biol*. 2012;198(5):927–940.
22. Itoh K, Jenny A, Mlodzik M, Sokol SY. Centrosomal localization of Diversin and its relevance to Wnt signaling. *J Cell Sci*. 2009; 122(pt 20):3791–3798.
23. Chitnis AB. The role of Notch in lateral inhibition and cell fate specification. *Mol Cell Neurosci*. 1995;6(6):311–321.
24. Lai EC, Deblandre GA, Kintner C, Rubin GM. Drosophila neuralized is a ubiquitin ligase that promotes the internalization and degradation of delta. *Dev Cell*. 2001;1(6):783–794.
25. Kopan R. All good things must come to an end: how is Notch signaling turned off? *Sci STKE*. 1999;1999(9):PE1.
26. Aza-Blanc P, Ramirez-Weber FA, Laget MP, Schwartz C, Kornberg TB. Proteolysis that is inhibited by hedgehog targets Cubitus interruptus protein to the nucleus and converts it to a repressor. *Cell*. 1997;89(7):1043–1053.

27. Pan Y, Bai CB, Joyner AL, Wang B. Sonic hedgehog signaling regulates Gli2 transcriptional activity by suppressing its processing and degradation. *Mol Cell Biol*. 2006;26(9):3365–3377.
28. Chen MH, et al. Cilium-independent regulation of Gli protein function by Sufu in Hedgehog signaling is evolutionarily conserved. *Genes Dev*. 2009;23(16):1910–1928.
29. Ross AJ, et al. Disruption of Bardet-Biedl syndrome ciliary proteins perturbs planar cell polarity in vertebrates. *Nat Genet*. 2005;37(10):1135–1140.
30. Ferrante MI, et al. Convergent extension movements and ciliary function are mediated by ofd1, a zebrafish orthologue of the human oral-facial-digital type 1 syndrome gene. *Hum Mol Genet*. 2009; 18(2):289–303.
31. Lindsten K, Menendez-Benito V, Masucci MG, Dantuma NP. A transgenic mouse model of the ubiquitin/proteasome system. *Nat Biotechnol*. 2003; 21(8):897–902.
32. Belcastro V, et al. Transcriptional gene network inference from a massive dataset elucidates transcriptome organization gene function. *Nucleic Acids Res*. 2011;39(20):8677–8688.
33. Fico A, Manganelli G, Simeone M, Guido S, Minchiotti G, Filosa S. High-throughput screening-compatible single-step protocol to differentiate embryonic stem cells in neurons. *Stem Cells Dev*. 2008;17(3):573–584.
34. Singla V, Romaguera-Ros M, Garcia-Verdugo JM, Reiter JF. Ofd1, a human disease gene, regulates the length and distal structure of centrioles. *Dev Cell*. 2010;18(3):410–424.
35. Pan Y, Wang B. A novel protein-processing domain in Gli2 and Gli3 differentially blocks complete protein degradation by the proteasome. *J Biol Chem*. 2007;282(15):10846–10852.
36. Kwak MK, Cho JM, Huang B, Shin S, Kensler TW. Role of increased expression of the proteasome in the protective effects of sulforaphane against hydrogen peroxide-mediated cytotoxicity in murine neuroblastoma cells. *Free Radic Biol Med*. 2007;43(5):809–817.
37. Lee BH, et al. Enhancement of proteasome activity by a small-molecule inhibitor of USP14. *Nature*. 2010;467(7312):179–184.
38. Zaghloul NA, et al. Functional analyses of variants reveal a significant role for dominant negative and common alleles in oligogenic Bardet-Biedl syndrome. *Proc Natl Acad Sci U S A*. 2010; 107(23):10602–10607.
39. Jiang YJ, Aerne BL, Smithers L, Haddon C, Ish-Horowicz D, Lewis J. Notch signalling and the synchronization of the somite segmentation clock. *Nature*. 2000;408(6811):475–479.
40. Takke C, Dornseifer P, v Weizsacker E, Campos-Ortega JA. her4, a zebrafish homologue of the Drosophila neurogenic gene E(spl), is a target of NOTCH signalling. *Development*. 1999; 126(9):1811–1821.
41. Shih VF, Tsui R, Caldwell A, Hoffmann A. A single NFκB system for both canonical and non-canonical signaling. *Cell Res*. 2011;21(1):86–102.
42. Hamazaki J, Sasaki K, Kawahara H, Hisanaga S, Tanaka K, Murata S. Rpn10-mediated degradation of ubiquitinated proteins is essential for mouse development. *Mol Cell Biol*. 2007;27(19):6629–6638.
43. Hanna J, Meides A, Zhang DP, Finley D. A ubiquitin stress response induces altered proteasome composition. *Cell*. 2007;129(4):747–759.
44. Jin H, et al. The conserved Bardet-Biedl syndrome proteins assemble a coat that traffics membrane proteins to cilia. *Cell*. 2010;141(7):1208–1219.
45. Oeffner F, Moch C, Neundorf A, Hofmann J, Koch M, Grzeschik KH. Novel interaction partners of Bardet-Biedl syndrome proteins. *Cell Motil Cytoskeleton*. 2008;65(2):143–155.
46. Garcia-Gonzalo FR, et al. A transition zone complex regulates mammalian ciliogenesis and ciliary membrane composition. *Nat Genet*. 2011;43(8):776–784.
47. Huang P, Schier AF. Dampened Hedgehog signaling but normal Wnt signaling in zebrafish without cilia. *Development*. 2009;136(18):3089–3098.
48. Egner PA, et al. Bioavailability of Sulforaphane from two broccoli sprout beverages: results of a short-term, cross-over clinical trial in Qidong, China. *Cancer Prev Res (Phila)*. 2011;4(3):384–395.
49. Shapiro TA, et al. Safety, tolerance, and metabolism of broccoli sprout glucosinolates and isothiocyanates: a clinical phase I study. *Nutr Cancer*. 2006;55(1):53–62.
50. Inglis PN, Boroevich KA, Leroux MR. Piecing together a ciliome. *Trends Genet*. 2006;22(9):491–500.
51. Kim J, et al. Functional genomic screen for modulators of ciliogenesis and cilium length. *Nature*. 2010;464(7291):1048–1051.
52. Wang X, Chen CF, Baker PR, Chen PL, Kaiser P, Huang L. Mass spectrometric characterization of the affinity-purified human 26S proteasome complex. *Biochemistry*. 2007;46(11):3553–3565.